THE BEHAVIOUR OF CURVED HYBRID GIRDERS

A thesis submitted in partial fulfilment of
the requirements for the degree of

MASTER OF SCIENCE

---

of

UNIVERSITY OF CAPE TOWN

Author: Kabani Matongo

Supervisor: Dr A. Masarira

December 2008

The financial assistance of the Department of Labour (DST) towards this research is hereby acknowledged. Opinions expressed and conclusions arrived at, are those of the author and are not necessarily to be attributed to the DST.

Declaration

I know the meaning of plagiarism and declare that all of the work in the document, save for that which is properly acknowledged is my own. This dissertation has not been submitted before for any degree or examination at any other University.

Signed by candidate

Signature Removed

Kabani Matongo
Decemeber 2008

Acknowledgements

I would like to extend my gratitude to the following:

- Dr Alvin Masarira for the research supervision,
- The NRF for the main scholarship,
- Prof Zingoni and the Civil Engineering department for the additional financial support,
- My collegues in the structural engineering and materials group most notably Bongani and Otieno for the encouragement and proof reading,
- Patrick Sibanda for all the latex hints and tricks,
- My family and friends: Masimba, Habeenzu, Mudenda and all the Kabanies for their support,
- The medical teams at Spencer Rd Clinic and UCT wellness for being there all the time for me,
- My beloved Mutinta and Nakwezi who bore the brunt of my absence

Abstract

Curved girders are used in bridges to fit predefined alignment. Hybrid girders are an innovative use of high strength steel enabling optimising moment capacity. Previous studies of curvature and hybrid girder effects have been disjointed, focusing on curved homogeneous girders and straight hybrid girders. There are no generally accepted curved girder equations and this has implications in the study of curved hybrid girders since the hybrid effects become apparent in the inelastic range. Furthermore, the range of radius to span ratio where available analytical procedures can be applied is not known.

A total of 48 girders are investigated, 12 of which are straight. The girders are all simply supported, un-braced and loaded at midspan. The load-deflection behaviour of curved hybrid girders is investigated. Stress plots of the girders are obtained at ultimate load. The radius to span ratio is varied from 5 to 50 for 5m span girders and from 5 to 30 for 8m span girders. Three steel grades are used to obtain hybrid girder configurations, with higher yield steel always used in the flanges. The web-flange yield steel combinations used are 350MPa/460MPa, 350MPa/690MPa and 460MPa/690MPa.

A finite element model using ADINA version 8.4 is used to investigate curved girder behaviour. The collapse analysis option is used to trace behaviour as the load is incremented automatically to a prescribed displacement. Available experimental data is used to check the validity of the modeling assumptions.

The presence of curvature radically modifies a girder's load pattern by causing additional lateral bending moments. Lateral bending moments reduce the vertical load carrying capacity of a girder and cause the flanges to be unequally stressed. For the girder and spans investigated, there is a reduction of 57% in ultimate load for radius to span ratio (R/L) of 5 compared to a straight girder of similar proportions and span. The effects of curvature reduce as R/L increases and this is observed in the 5m homogeneous girder with R/L of 50 which attained more than

91% of the straight girder load capacity. The 8m girder with R/L of 30 attained more than 83% of the equivalent straight load girder capacity.

The hybrid girders investigated had load-deflection curves close to corresponding homogeneous girders with flange steel grade, reaching more than 97% of the ultimate load capacity of reference homogeneous girders. The hybrid factors as proposed in the simplified design procedure are adequate and can be applied to analytical equations that predict curved homogeneous girder loads. The available analytical equations give conservative loads for both hybrid and homogeneous girders compared to the finite element method when R/L is 5 and are unconservative for higher rations.

Contents

List of Figures

List of Tables

Chapter 1

Introduction and literature review

1.1 Introduction

Plate girders have been used in bridges to replace trusses in order to achieve long spans. With considerable improvement in the practice of welding, plate girders are now welded as opposed to riveting and bolting. Plate girders differ from beams in that web buckling is more critical as opposed to web yielding. Several types of girders are utilised and are grouped as single web such as I girders or multi-web girders such as box girders. Alternatively the girders can be classified according to the material variations in the web and flange area. Thus homogeneous girders have the same material in both web and flange areas while hybrid girders have different steel grades in flanges and web. The word hybrid is thus used to denote girders with different steel grades while composite is used to refer to concrete-steel girders.

This study looks at horizontally curved hybrid girders with doubly symmetric cross section, here after simply referred to as hybrid curved girders. The horizontal curvature arises in highway bridge applications to fit predefined alignments for bridges, increase sight distance for drivers as well as allow high speed traffic to change direction (Hall, 1996).

Despite the increasing use of curved girders in bridges, their behaviour under different load conditions during and after construction and the reliability of analysis tools is still not fully understood (NCHRP-Report-563, 2006). Analytical studies on curved beams have been carried out by Timoshenko (1961); Vlasov (1961) and their formulations have been the starting point for many researchers. The curvature results in lateral moments in addition to the vertical moment experienced by straight girders.

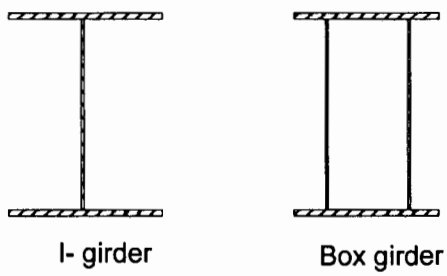

Figure 1.1: Single web and multiweb girder cross-section

Research on curved beams initially followed a rigorous theory of elasticity approach. Exact solutions have been formulated for solid sections as reported by Ugural and Fenster (1981). The most important departure from curved straight beams is the presence of radial stresses. The theory developed led to the following conclusions:

(i) if the depth of member is smaller relative to the radius of curvature then the initial curvature may be neglected.

(ii) the strain energy due to bending for a straight beam is a good approximation for the curved slender beams.

Other simplifications by Winkler resulted in formulae that are easier to use for rectangular sections. However, the formulae are not accurate for thin walled I sections because of the distortional effects of the stress variations in flanges and web. Tables of correction factors are used for the computation of stresses and strains for different loading cases of curved solid beams and hollow sections that do not fall in the class of thin walled sections. Modification factors have been proposed to correct the error occurring for thin walled beams.

Background research on plate girders was carried out by Basler(1961) whose study covered the aspects of shear, bending and combined shear and bending. Subsequent research on curved girders and hybrid girders was carried out rather disjointly.

Some of the early work in the area of curved girders was done under the Consortium University Research Team (CURT) project which developed analytical models and performed field tests. The results from the CURT project were included in the AASHTO Guide Specification that was published in 1976. The Guide Specifications that were developed in the US were disjointed and difficult to

follow (Hall, 1996). There are discontinuities between compressive strength formulations between compact and non compact sections and as the radius of curvature was increased to infinity, there is no convergence to the straight girder equations (Davidson *et al.*, 2000*b*). Other researchers such as Dabrowski presented equations for non uniform torsion of curved girders with non deformable asymmetrical cross section (Richard *et al.*, 1995). Approximate methods were developed including the V-load analysis for shears and moments. Corresponding work was done by the Hanshin Expressway Corporation where an interaction equation for limiting stresses in curved girders was proposed, culminating in the Hanshin Guide (Davidson *et al.*, 2000*b*; Hall, 1996)

Most of the research conducted especially in the US by CURT was on doubly symmetric I girders. The approach which will be reviewed in subsequent sections was for making adjustments to straight girder equations to predict curved girder behaviour. This approach has led to limited success in predicting curved girder behaviour and there is still no comprehensive theory explaining inelastic curved girder behaviour (Hall, 1996). More recent studies have addressed the behaviour of curved girders using Finite Element Models (Shanmugan *et al.*, 2003, 1995)

Hybrid steel girders have also been used in bridges (Veljkovic and Johansson, 2004; Haaijer, 1961). They result in savings in dead weight due to the optimisation of moment resistance properties. Hybrid girders are fabricated by welding different steel grades in the flanges and the web. In the elastic range the hybrid girder behaves just like a homogenous girders. However when the steel in the web yields, there is a slight reduction in stiffness. The flanges provide most of the moment carrying capacity and it is the yielding of steel in the flanges that reduce girder stiffness. Failure for straight hybrid girders is defined as the initial yielding of steel in the extreme flange fibres.

Some research on hybrid girders was done in in the 1960s most notably by Frost and Schilling (1964). These studies covered both experimental and theoretical aspects of hybrid girder design and formed the basis of the design procedures recommended by the ASCE-AASHO subcommittee on hybrid beams and girders. The deformation and stress patten where examined and stability issues were not examined as local and lateral buckling were excluded by careful proportioning of member sizes. A report by the subcommittee on hybrid beams and girders (ASCE-AASHO, 1968) noted that just like in homogeneous beams and girders, shear is significant in the web. While the web contributes little in bending resistance, web yielding may affect

the buckling of the compression flange of the girder. For hybrid girders, tension field action was ignored. Recent research has recommended a relaxation of this conservative assumption.

Hybrid girders can thus be designed in the same manner as homogeneous girders when their response is in the linear-elastic range. However, this does not fully utilise the full capacity of the higher grade steel in the flanges. The use of high strength steel in the flanges results in the web yielding first while the flanges remain elastic as the load is increased. Shear is normally carried by the web and thus there should be no significant difference with corresponding behaviour of homogenous girders. The effects of curvature and hybrid nature of the beams is thus presented in detail below.

1.2 Literature review

The study of hybrid girders closely follows the developments made in steel production science. As stated, hybrid girders make use of different grades of steel, the low strength steel in the web and a higher strength steel in the flanges. The placement of high strength steel in the flanges is because they are the primary moment resisting members. As high strength steel is often more expensive, the hybrid configuration provides an optimum solution by placing high strength steel where it is needed most. The web helps carry shear and also keep the distance between the flanges. A review of the use of steel and and types of steel is necessary if they are to be efficiently used in girders. The review is important also due to the limitations that design codes place on issues such as inelastic design and definitions of sections that can attain plastic moment capacity.

Advances in material science and analysis techniques have allowed innovative structural designs from the time iron became an affordable construction material. Different materials such as cast iron, wrought iron and steel have all been used in construction over the past 200 years. The main difference in chemical composition of these materials is the percentage of carbon in the iron. In steel the carbon is less than 2%. There are typically four groups of steel used for structural purposes with progressive increase in strength; carbon steels, high-strength low alloy (HSLA) steels, heat treated carbon and HSLA steels and heat-treated alloy steels. For classification of steel, regulatory bodies identify 'minimum' yield strength, chemical composition and heat treatment. Yield stressed are in the range

205-290MPa for carbon steels, 290-450MPa for HSLA steels, 315-515MPa for heat treated carbon and HSLA steels and 620-690MPa for heat treated alloy steels (Paik and Thayamballi, 2003). The ultimate tensile yield stresses are the in range 380-620MPa for carbon steels, 415-550MPa for HSLA steels, 450-790MPa for heat treated and HSLA steels and 760-895MPa for heat treated alloy steels (Paik and Thayamballi, 2003).

There are significant differences in the stress-strain curves for the different steels. Generally, mild steels exhibit a linear response up to the yield stress. This is followed by a yield plateau where strain increases at an almost constant load, after which strain hardening takes place. An example of such a steel is the A36 steel. The ability to undergo large strains after attaining yield stress is the basis for plastic design. In general, high strength steels tend not to have this yield plateau thus exhibiting poor ductility. This is the main reason for the LRFD not permitting plastic design or inelastic analysis for such steels (Salmon and Johnson, 1996).

Steel with tensile strength of 600MPa was used in bridge construction in the 1960s in Japan. Steel with strength 800MPa was used in mid 1960s in bridges such as Hanawa Overpass Bridge and Minato Ohashi Bridge. In the US, HSLA structural steels were developed in the 1960s and A514 steel was introduced (Bjorhivde, 2004). This A514 steel did not have sufficient ductility resulting in brittle fracture of tension flange of test specimen. 800MPa yield strength steels with better weldability were introduced in 1992 in Japan and a new grade A992 structural steel was introduced in the US in 1998. This A992 steel has better weldability, ductility and has a minimum yield strength of 350MPa.

High strength steels suffer from poor weldability and ductility though this is fast changing due to advances in steel production techniques. There has been a significant growth in the use of high strength steel particularly with the emergence of a class of steel referred to as High Performance Steel (HPS). This is partly due to technological innovations in steel production such as the Thermo-Mechanical Control Process (TMCP) that controls rolling and cooling process producing steel with fine microstructure (Gunther, 2005). These steels have superior properties such as higher ductility, weldability, fracture toughness and better weathering properties apart from the high strength. In the US, the development of bridge HPS only started in 1992. The Figure 1.2 shows the number of bridges constructed in the US using HPS up to 2004. There has been an increase in the use of HPS over the period shown.

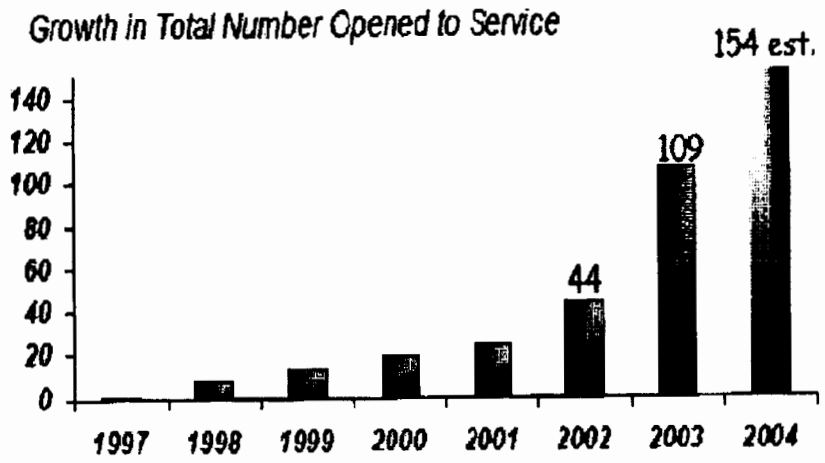

Figure 1.2: HPS Bridges in service in U.S (Gunther, 2005)

The general costs involved in using HPS can vary depending on complexity of structure and location. The cost of materials can often be a small component of the structure. Table 1.1 shows cost comparison based on experience in the US. Other costs include erection and fabrication costs. The comparison is on unit cost of material, fabricated members and in-place cost. TMCP technology has resulted in a slight cost reduction as reflected by Table 1.1 for HPS70W and HPS70 TMCP.

Table 1.1: Cost comparison of steel grades (Gunther, 2005)

	Material ($ per kg)	**Fabricated** ($ per kg)	**In-Place** ($ per kg)
Grade 50W	0.77-0.93	1.21-1.37	2.20-2.76
HPS 50W	0.93-1.10	1.39-1.57	2.54-3.09
HPS 70W	1.06-1.32	1.65-1.83	2.60-3.31
HPS 70W TMCP	0.99-1.27	1.54-1.72	2.54-3.20

The areas regarding use of HPS in bridges that were highlighted for research included deflection criteria, ductility, flexural capacity in negative regions, limitation on tension field action in hybrid girders, toughness, fatigue and fracture (Azizinamini *et al.*, 2004). The advantages of using HPS have been well documented (Gunther, 2005; Miki *et al.*, 2002). High yield strength means that fewer girders can be used to carry load and longer spans can be obtained for bridge applications. Alternatively, shallower girders can be used where clearance height is of concern. Good weathering properties mean the steel can be exposed to

the atmosphere without having to paint it, thus reducing life-cycle costs. However, there are restrictions placed by design codes on the use of high strength steel, particularly on the definition of compact sections (Wollman, 2004). These restrictions limit the full utilisation of HPS strength. Inelastic analysis and moment redistribution are not allowed for steels with a yield strength greater than 490 MPa. Such limits are based on the general reduced ductility that was observed in high strength steels whose stress-strain curve generally has no well defined yield plateau. The South African code SANS10162:1-2005 does allow the use of steel within the following limitations:

(i) the specified yield stress shall not exceed 700MPa.

(ii) ratio of the minimum tensile strength to specified yield stress shall be at least 1.2:1.

(iii) the elongation (on a gauge length of 5.56 $\sqrt{A_0}$ mm) shall be at least 15%, where A_0 is the original area of the cross section in square millimetres

A compact section with adequate bracing is expected to develop full plastic moment and meet the ductility criteria to allow for both plastic design and inelastic moment redistribution. However, previous AASHTO(1998, 2002) have restrictions placed on the definition of a compact section by giving a limit on steel yield strength. Thus the requirement for a section to be compact is among others that the steel used should have a yield stress less than 490MPa (Wollman, 2004). It is evident that the full benefits for HPS can be realised if design codes allow plastic design as well as inelastic analysis. This has greater implications for hybrid girders as they rely on the optimum use of high strength steel in regions of high moments. The limitations have been the subject of study. The studies mainly followed the pattern where girders both homogeneous and hybrid are designed while ignoring the restriction placed on steel strength. The objective of these studies was to check if such girders could have enough flexural ductility in terms of rotational capacity to allow plastic moment capacity to be attained.

Sufficient ductility is necessary for a section to develop plastic moment capacity. Brittle fracture should not occur so that plastic hinges can develop. Examples of steels with desirable characteristics with regard to weldability and ductility are given in the ASCE (1971) as ASTM A36, A441 and A572. In general, such steels have adequate plastic yield plateau and show strain hardening. This allows plastic hinge formation and maintenance of the plastic capacity until the collapse mechanism is

fully developed. Ductility can be defined as the amount of permanent strain before fracture. For flexural members, ductility is measured in terms of rotational capacity R, given below (ASCE, 1971) and the other variables in the definition are shown in Figure 1.3:

$$R = \left\{ \frac{\theta_u}{\theta_p} - 1 \right\} \tag{1.1}$$

where θ_u is the rotation when moment capacity drops below M_p during unloading and θ_p is the theoretical plastic rotation at which plastic moment is achieved based on elastic beam stiffness.

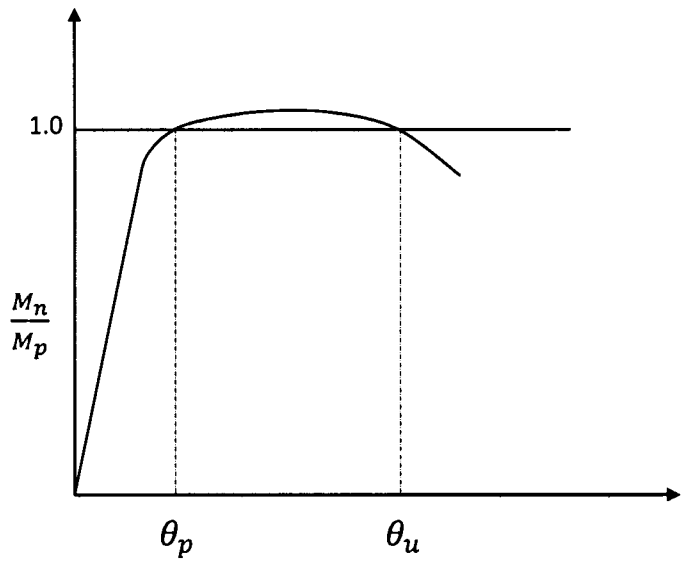

Figure 1.3: Moment-rotation curve illustration moment ductility parameters

Another useful measure is the total inelastic rotation of a girder (Sause and Fahnestock, 2001):

$$\theta_{inel} = 2\left(\theta - \frac{M}{M_p}\theta_p\right) \tag{1.2}$$

where θ is the rotation at one end of a girder during loading history, M is the moment during loading history and M_p is the plastic moment capacity. Another ductility measure is the total rotation $\theta_{inel,u}$ through which M_p is sustained:

$$\theta_{inel,u} = 2(\theta_u - \theta_p) = 2R\theta_p \tag{1.3}$$

The above ductility measures are critical as a compact section is expected to have rotational capacity R of at least 3. Ductility allows local yielding in regions of high

stresses to occur and thus allow for moment redistribution. Schilling (1988) has proposed 0.015 - 0.02rad for plastic rotation for bridge girders. For a section to attain plastic moment capacity, sufficient rotation must occur for hinge formation. Thus the ability of girders made of different HPS exceeding 490MPa has been the subject of study by many researchers.

Frost and Schilling (1964) conducted experimental and analytical studies of three girders simply supported, two of them hybrid. Steel used had yield strength of 689.5MPa for flanges while webs had yield strength of 227.5 MPa and 344.7 MPa. For straight hybrid girders design, the yield moment M_y is defined as the moment when the flange starts yielding. Such girders can still attain plastic moment capacity but more severe provisions should be followed to allow enough rotation and to prevent local and global instability. The load deflection curves for three girders, two of which are hybrid is presented in Figure 1.4.

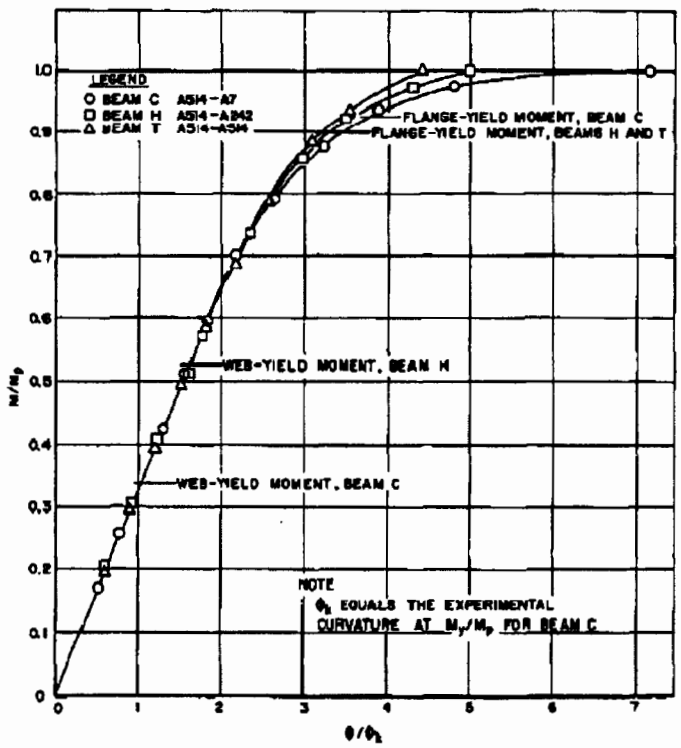

Figure 1.4: Experimental bending behaviour curves for hybrid beams (ASCE-AASHO, 1968)

At lower loads all the girders behave elastically, thus there is no distinction between hybrid and homogeneous girders. With increasing load, the webs yield while the flanges remain elastic. As the web moment resisting contribution is small, only

minor differences occur in the different girders. Increasing the load further results in flange yielding. A comparison of the girder load-deflection curves showed that they were close for both hybrid and homogeneous girders. However, in the inelastic range the girder with the lowest yield ratio of web to flange steel had less stiffness and experienced larger deflections at plastic moment. Thus the deflections are more for the hybrid girders compared to the homogeneous girder.

Earls (1999) studied the inelastic failure of beams made of HSLA80 using finite element analysis. This steel has no well defined yield plateau and no substantial strain hardening modulus. In the study, the flange slenderness and brace spacing were varied. Geometric imperfections were included in the model. Two inelastic buckling modes were studies. An interaction between local and global buckling was observed. The rotational capacity and development of plastic mechanism was influenced by the inelastic buckling modes that developed. The inelastic buckling modes that developed either increased or reduced rotational capacity. By adjusting the brace locations, unfavourable modes that lead to a reduction in rotation capacity are eliminated.

Sause and Fahnestock (2001) conducted both experimental and finite element studies to assess the ductility of girders made from HPS-100W which has a minimum yield stress of 690MPa. The girders were designed following AASHTO(1998) but neglecting the restriction on the steel yield strength. The girders were loaded in three point bending to simulate negative bending on piers. The results showed that compact girders were able to reach plastic moment capacity. However the required rotation of 3 was not reached. The inelastic rotation was within the range given by Schilling (1988) for bridges. It was further concluded after analysis of previous results on conventional steel grades that compact girders with web slenderness near the compact limit did not always have a rotational capacity of 3. Thus girders made from HPS-100W with similar normalised slenderness were not expected to have rotation capacity of 3. The conclusions were based only on two test girders and thus more research was recommended. While the girders under study were homogeneous, it was to test the assertion that HPS-100W could not develop enough ductility to enable attainment of plastic moment capacity.

Studies were conducted by Barth *et al.* (2007) of girders designed to AASHTO (2001, 2003). The studies using finite element analysis were based on a hypothetical hybrid girder with 690MPa flange and 480MPa web. The parameters

varied were web slenderness, lateral brace spacing, flange slenderness and percentage of web in compression. With such variations in slenderness from compact to non compact, it was observed that all the girders reached or exceeded the capacities given in AASHTO(2001, 2003). The results show that the restrictions placed on steel strength regarding moment capacity are not necessary. Furthermore, a design optimisation of hybrid and homogeneous girders for a selected bridge showed that hybrid girders are effective for greater span to depth ratios resulting in significant weight reduction. The studies above show that adequate flexural ductility can be attained for beams made from HPS (Gunther, 2005)

Moment rotation capacities of hybrid girders were studied by Ito *et al.* (2005). The studies focused on the plastic rotation necessary for inelastic design. A concept of effective plastic moment M_{pe}, was proposed to allow slender sections be designed by inelastic analysis. By definition a rotation of 0.063rad is required to reach M_{pe}. Six hybrid and homogenous girders designed to AASHTO(1998) compactness criteria were fabricated and tested and the results compared with those proposed by White and Barth (1998). It was observed that the curves proposed by White and Barth (1998) are conservative for hybrid girders. It was also shown that hybrid girders can develop sufficient inelastic rotation and the difference in the curves for the hybrid and homogeneous girders was more significant for slender webs (Ito *et al.*, 2005). Further, the girders with low web to flange steel yield ratio had higher rotation capacities than those with higher steel yield ratios. It must be observed that the definition of M_{pe} ensures the attainment of 0.062rad for inelastic rotation. This is much higher than the 0.015 - 0.02rad given by Schilling (1988) for bridge girders.

Shear resistance in I-girders is provided by the web while flexural resistance is mainly provided by the flanges. Due to the use of lower strength steel in the web, hybrid girders have a smaller ratio of shear to flexural resistance compared to homogeneous girders (ASCE-AASHO, 1968). The shear resistance of a hybrid girder is equal to that of a homogeneous girder made of web steel. The response of a hybrid girders under patch loading on tension and compression flanges has been investigated by Schilling (1967). It was shown that crippling loads equal to or greater than yield load can be applied to tension or compression web even when longitudinal stresses are close to flange yield stress. Furthermore, it was observed that the reduction in moment capacity due to crippling loads was small enough to be neglected in design.

For continuous plate girders with compact sections in negative flexure, the maximum

moment is limited to yield moment M_y rather than plastic moment M_p. Furthermore inelastic analysis and design is not allowed for HPS with strengths equal to or exceeding 490MPa. Research by Azizinamini *et al.* (2004); Sause and Fahnestock (2001) has shown that compact HPS 70W (485MPa) and HPS 100W (690MPa) plate girders can develop plastic moment capacity. However the rotational ductility in these regions does not meet the required 3. HPS 100W had a maximum inelastic rotation of 0.019rad.

The behaviour of a curved beam or girder is significantly different from the straight one because of the curvature effects. Yang and Kuo (1987) have pointed out that unlike in a straight beam, the stresses are coupled and also there are radial stresses. Further, the curvature effects and hybrid effect have been largely studied rather disjointly. There exist different curved beam formulations and these are briefly discussed. Two approaches are used to derive beam equations and these are equilibrium and energy methods. Early beam theories by Vlasov (1961) and Timoshenko (1961) followed the equilibrium method. The main drawback of this approach is the high likelihood of terms being omitted when deriving governing equations. More recent theories by Yoo (1982); Yang and Kuo (1987) have followed the energy approach.

Theoretical studies on curved beams have been done by different researchers (Kang and Yoo, 1994*a*,*b*; Yang and Kuo, 1986; Papangelis and Trahair, 1987; Yang and Kuo, 1987; Yoo, 1982; Vlasov, 1961; Timoshenko, 1961). Exact solutions for curved beams of rectangular and circular cross section have been derived and approximate theories such as Winkler's theory can be used to give radial and tangential stresses (Ugural and Fenster, 1981). For such sections it has been noted that plane sections of a curved beam subjected to pure bending remain plane subsequent to bending. This assumption neglects the warping effects and results in error when applied to I, T or thin-curved beams. It is important to note that the condition of cross sections being undistorted is the cornerstone of the theories that have been presented. A study by Kang and Yoo (1994*a*) reviewed the theories on curved beams and the following reasons are given for the disparities in predicted results:

(i) There are differences in methods of formulation. The equilibrium and energy methods have been used to derive beam equations. The equilibrium method suffers a drawback in that it is easy to omit terms in the formulation.

(ii) There are misinterpretations of assumptions regarding fundamental thin walled section behaviour. While the assumptions adopted are the same, the

mathematical meaning of the assumptions appears to differ among researchers. A good example is that of vanishing shears which Yang and Kuo (1987) interpreted as allowing radial stresses while Kang and Yoo (1994*a*) disagree with such an interpretation.

(iii) there are different degrees of approximation of curvature effect in derivation. This source of error as pointed out by Kang and Yoo (1994*a*) increases as subtended angle increases.

Timoshenko (1961) derived the differential equations of curved beam based on equilibrium but the effects of warping were ignored in the formulation. These equations were also established by Boussinesq (Timoshenko, 1961). Closed form solutions for rings and arches have been derived and these have proved to be useful in comparing the different formulations for curved beams. The theory has been found to be accurate for solid sections. However, the solutions are expected to be in error in thin walled members where warping is significant. Further, the derivation was not consistent because of the straight beam analogy used to derive curved beam equations.

Vlasov (1961) presented the general theory of thin-walled beams and this was the starting point for many researchers investigating curved girder behaviour. The curved girders under consideration fall under the category of thin-walled beams. These are defined loosely as structures made of thin plates joined along their edges such that their cross sections satisfy the following criteria:

$$\frac{\delta}{d} \leq 0.1$$

$$\frac{d}{l} \leq 0.1$$

where δ is the plate or shell thickness, d is a characteristic dimension of the cross section such as width or height and l is the length.

Such structural members are widely used in construction and include plate girders, box girders and purlins. In the present, the plate girders under consideration posses little torsional rigidity. The important difference with solid beams is that shear stresses and strains become relatively large. The general elementary flexure theory is based on the Bernoulli hypothesis that plane sections remain plane over the entire section after bending. In thin walled sections, warping can occur and if restrained then warping stresses result. The Bernoulli hypothesis is thus restrictive and is

replaced by the general law of sectorial areas. The general theory is based on the following assumptions which have been used by subsequent theories:

(i) Shear strains due to change of normal stresses are negligible

(ii) Deformations are small with respect to dimensions of cross section

(iii) Shear stresses in the middle surface vanish

The generalised equations for a straight beam are developed from the above assumptions. Vlasov (1961) derived the differential equations for curved beam based on the straight beam equation. The generalised strains for a straight beam were replaced with strains for curved beam in the straight beam equation. It has been argued by Yang and Kuo (1986); Yoo and Heins (1972) that such an approach is not consistent. The approach assumes that the curved girder equation is analogous to the straight girder equation and there is no proof to support this assumption. The generalised curved beam equations by Vlasov (1961) have been the starting point for investigations on curved girders by other researchers such as Yoo (1982); Yoo and Heins (1972).

A different approach was also taken up by Yoo (1982) who used the energy equation for a straight beam as a starting point. The concept of minimum potential energy was used to derive the elastic flexural-torsional load for in plane and out-of-plane buckling modes. The generalised strains for a curved beam were substituted in the straight beam energy equation. A comparison of the closed form solutions with those of Vlasov (1961); Timoshenko (1961) show vast differences. The direct substitution of curvature terms into the straight beam equation by Vlasov has been pointed out by Yoo (1982) to be an error and to account for the large differences in the comparison of the closed form solutions. Likewise, Yoo (1982) substituted the curvature terms into the straight beam energy equation. This approach is without proof and has been pointed out by other researchers such as Rajasekaran and Ramm (1982) and Yang and Kuo (1986) because it is not a consistent approach. Yang and Kuo (1986) have argued that such a representation of curved beam by straight beam amounts to neglecting both the jacobian in the volume integral and the radial stresses in the virtual work equation.

Curved beam theories that try to remedy the deficiencies of consistency and whose derivation is based on minimum energy principles have been proposed by Kang and Yoo (1994*a*); Papangelis and Trahair (1987); Yang and Kuo (1986); Rajasekaran and

Ramm (1982). The formulation by Yang and Kuo (1987, 1986) gives a curved girder equation derived from first principles with the virtual work equation as a starting point. The key thing to note is the inclusion of radial stresses in the formulation.

A comparison for the case of a curved beam under pure bending show that results for Yang and Kuo (1986) are close to those for Timoshenko (1961); Vlasov (1961). The presence of radial stresses in the formulation by Yang and Kuo (1987) has been pointed out as a discrepancy in the equations by Kang and Yoo (1994*b*). The basic assumption in thin walled beams is that cross-sections don't distort and this can not allow radial stresses to occur. While this assumption is used, it is important to note that the radial stresses occur in finite element studies of curved girders (Davidson and Yoo, 1996). Such stresses have been shown to be tensile on the inner flange with respect to the centre of curvature and compressive on the outer half of the flange. A finite difference approach by Culver and Frampton (1970) has shown the existence of such radial stresses in curved beams. While the vanishing shear assumption is interpreted differently by Kang and Yoo (1994*a*) and Yang and Kuo (1986), it is accepted that in beams with severe curvature such as hooks, the radial stresses exist.

Kang and Yoo (1994*a*) presented a theory that uses the virtual work theorem and minimisation of potential energy. The minimisation energy procedure was chosen for reasons earlier stated and is recommended for general derivation of beam equations (Murray and Rajasekaran, 1975) Further, the derivation was consistent derivation as opposed to the earlier theory by Yoo (1982). Curvature terms were approximated systematically based on a binomial expansion theory. The predicted in-plane and out-of-plane buckling loads were compared with theories by Yang and Kuo (1987); Rajasekaran and Ramm (1982); Yoo (1982); Vlasov (1961); Timoshenko (1961). For in plane buckling, the theory gives considerably lower loads as subtended angle is increased while for out-of-plane buckling the theories give rather close results.

Yoo and Heins (1972) have also considered the plastic behaviour of horizontally curved girders. The starting point of the analysis are the curved beam equations derived by Vlasov (1961) and finite difference techniques to analyse curved girders with different boundary conditions such as pinned-pinned, pinned-fixed and fixed-fixed. The argument regarding the consistency of Vlasov's derivation has already been highlighted.

Curved girders under gravity loads have to sustain lateral and vertical moments (Schilling, 1996). The vertical moments cause strains that vary through the depth

of the girder while the lateral moments cause strains that vary across the flange width. To explain the load carrying capacity of a curved girder, the concept of a reduced flange width is introduced. It is assumed that a part of the flanges is used for the lateral moment resistance and the remainder resists the applied vertical moment. This concept has been used by Schilling (1996) to derive the interaction equations. A curved girder's capacity to sustain a load is reduced by the presence of the lateral moment.

Fukumoto and Nishida (1981) conducted both experimental and analytical studies on curved girders to determine their ultimate strength. The studies focused on the effect of curvature and included analytical studies using matrix transfer method followed by experimental work in which six simply supported beams and loaded at midspan. The six beams had varying curvatures and two spans were chosen. There was a reduction in ultimate strength with increasing curvature. Fukumoto and Nishida (1981) developed a quartic equation for predicting the strength of curved girders. In developing the approximate equation, the second order elastic curve for beam is equated to the second order rigid plastic curve, the intersection being the desired solution. The equation is solved by iteration and has four roots. Its main drawback is that it is not easy to use by designers.

Richard *et al.* (1995) used the analytical approach proposed by Fukumoto and Nishida and modified the equation while taking into account the higher order terms to derive an ultimate load equation. The stability equations formulated by Yang and Kuo (1986) were used to derive an ultimate load equation and compared to the transfer matrix used by Fukumoto and Nishida (1981). The equation which is similar in structure to Fukumoto's equation is also a quartic equation and has more terms. It was derived to be more accurate over a greater range of curvatures, however the results of this study show otherwise. The equation gives generally higher ultimate strength than that presented by Fukumoto and Nishida (1981) and this is shown in the Figure 1.5. It too suffers the drawback of being cumbersome to use for design as such equations are solved by iteration.

Pi and Bradford (2001) have urged that equations presented by Richard *et al.* (1995); Fukumoto and Nishida (1981) ignore the effects of torsion. These effects of torsion are significant at higher included angles. In the interaction equations, it is argued that there is no justification for maintaining plastic capacity M_P as the reference moment and this too can be pointed out for equations presented by Richard *et al.* (1995); Fukumoto and Nishida (1981). Not all beams can attain plastic moment and

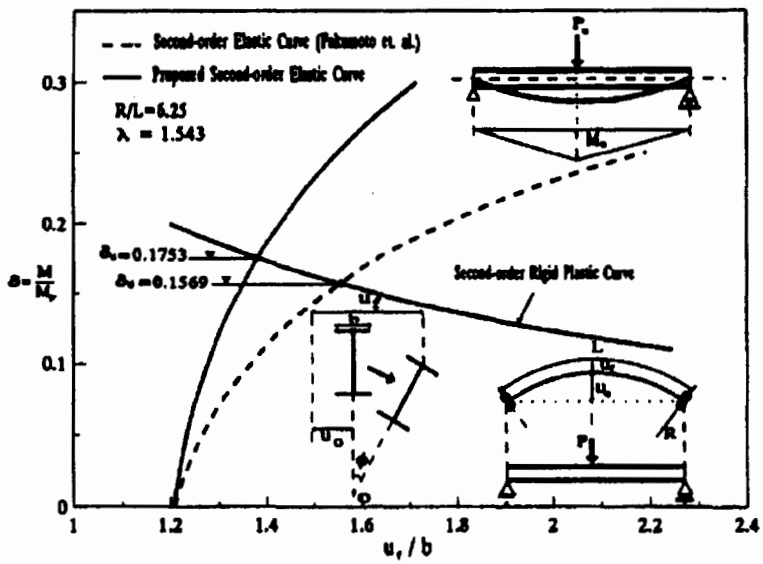

Figure 1.5: Comparison of Fukumoto and Nishida (1981) and Shanmugan *et al.* (2003) equations

thus it is not a good reference. The plastic moment capacity used in equations by Richard *et al.* (1995); Fukumoto and Nishida (1981) ignores the moment resisting contribution of the web. The omission of web contribution term mean that curved hybrid and homogeneous girders will have the same capacity. However, this is not explicitly stated in the application of the equations.

Shanmugan *et al.* (2003) conducted experiments on laterally supported curved girders in which the curvature and slenderness were varied. The girders were simply supported and also loaded at midspan. Bearing stiffeners were provided in areas of load application and support. Finite element models were also created in ABAQUS. The finite element model gave ultimate load values close to experimental results for all the girders. It was observed that ultimate strength reduces with increase in curvature. When the beam span is kept constant, it is observed as expected that at a lower subtended angle the girder behaves almost as a straight girder. The failure mode was also observed as web slenderness was increased. At $\frac{d}{t} = 288$, the failure is similar to straight girders with significant tension field action. Parametric studies on girders with maximum span to curvature ratios (L/R) of 0.1 and varying web slenderness were performed and it was shown that in this range of curvatures, the curves are close to straight girder. Generally there is a reduction in ultimate strength with increasing slenderness.

Interaction equations have been used to predict the behaviour of curved girders. The common equation is the circular interaction equation:

$$\left(\frac{M}{M_p}\right)^2 + \left(\frac{T}{T_p}\right)^2 = 1 \tag{1.4}$$

where M_p is major axis full plastic moment of the cross section, M is the major axis bending moment, T_p is full plastic torque of the cross section and T is the torsion. The circular interaction equation has been used by Yoo and Heins (1972) to study the plastic behaviour of curved girders. Pi and Bradford (2001) have pointed out the drawbacks associated with the circular interaction equation. The reference T_p can not be defined accurately for nonuniform torsion of a curved girder and the use of M_p as a reference is not justified in situations where lateral buckling occurs. The circular interaction equation further ignores the effects of secondary torsion and the minor axis bending. These effects become significant in curved beams as deformations increase. Thus the circular interaction equation tends to overestimate the interaction strength. Pi and Bradford (2001) have proposed an alternative interaction equation based on finite element studies:

$$\left(\frac{M_u}{M_{bx}}\right)^{\gamma_x} + \left(\frac{T_u}{T_p}\right)^{\gamma_s} = 1 \tag{1.5}$$

where M_u and T_u are the maximum nominal in-plane bending moment and torque determined from first order analysis, M_{bx} is the nominal member capacity of the corresponding straight beam with same length and same boundary conditions; γ_x=2.0 and γ_s=1.0 for continously braced curved beams; γ_x=1.5 and γ_s=1.0 for centrally braced curved beams; γ_x=1.0; and γ_s=1.0 for un-braced beams.

Schilling (1996) derived a set of interaction equations relating the vertical and lateral moments. For a compact section the relationship is based on full section becoming plastic under combined vertical and lateral moments. For compact flange section, the average stress is less than the yield stress though some sections of the flange are permitted to yield. For the non compact section, the whole section remains elastic. The equations by Schilling (1996) do not make use of the un-braced length directly. This has been pointed out by Yoo and Davidson (1997) as a weakness in using the equations as a design tool. Yoo and Davidson (1997) have presented an alternative set of equations with include un-braced length as parameter.

The Hanshin Expressway Corporation Guidelines developed an interaction equation between vertical and lateral bending stresses (Hall, 1996). The lateral and bending

moments are to be computed using the V-load method and the interaction equation is given below:

$$\frac{f_a}{(F_{ba})_c} + \frac{f_w}{F_{bao}} \leq 1.0 \tag{1.6}$$

where f_a is the normal flexural stress, F_{bac} is the critical normal bending stress, f_w is the lateral bending stress and F_{bao} is the yield stress. The ratio of un-braced length to radius is limited to 0.2. Davidson *et al.* (1999) investigated the effects of curvature and slenderness on membrane stresses. As the curvature and slenderness are increased, the membrane stress distribution becomes nonlinear through the section depth. Thus in a curved girder the flanges have to carry more load. The phenomenon described by Davidson *et al.* (2000*b*) has the same effect as the load shedding observed in straight girders and the distinction between the two is unclear. The lateral deflection of the curved panel also causes plate bending stresses in the web panel.

Hall did an analytical study of curved girders and compared the results generated from the various equations given by Fukumoto, Nikai and AASHTO Bridge Design Specification (Hall, 1996). The AASHTO strength equations presented were a modification of the lateral torsional equations given in the specification (Hall, 1996; Jung and W.White, 2006). It was seen that the different equations produced qualitatively similar plots and tended to significantly underestimates test specimen strength.

The notion of section class is still relevant when considering girder behaviour. Section classifications of compact and non-compact that are used for straight girders can still be used. Thus compact sections with appropriate bracing can reach the plastic moment capacity and the non compact sections reach yield moment. Schilling (1996) suggested an additional section class called compact flange. Such a section satisfies the compression flange slenderness and bracing of a compact section and the web slenderness of a non compact section. This allows a larger lateral moment to be carries for a given vertical moment.

In a girder, the web carries the shear as well as keep the the flanges apart and thus provide the lever arm. Although plates have been shown to posses significant post buckling strength reserve, the onset of elastic buckling has been used in formulating strength equations. The buckling modes important in a girder are listed below and these are illustrated in Figure 1.6:

(i) web buckling due to bending in the web plane,

(ii) buckling of compression flange in vertical direction,

(iii) buckling due to shear

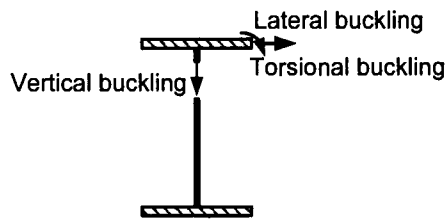

Figure 1.6: Possible buckling modes of I-Girder sectionSalmon and Johnson (1996)

Basler and Thurlimann (1961) observed that the transition between pre buckling and post buckling in webs is not accompanied by increased deflections. Thus it can not be used as a limit for bending strength. This observation holds for hybrid beams that web buckling due to bending or shear does not cause failure (ASCE-AASHO, 1968). The strength is determined by the failure of compression flange. Compression flange buckling is treated by equating the critical buckling stress to the transverse component of flange force. The slenderness limits are thus imposed on the web to prevent vertical flange.

The major factors affecting buckling of compression flange have been identified as warping stress gradient and torsional restraint by web. Research has been done to determine the local buckling behaviour of curved girders (Culver and Frampton, 1970) using finite difference methods. The effects of flange-web rigidity and radial stress on the plate buckling factor k and general local buckling behaviour were investigated. Unlike the straight girders, the stress situation in curved flanges is also affected by radial stresses. The radial stresses are tensile on outer half of flange and compressive on the inner half. Because of the stress differences in these sections of the flange, buckling occurs in the compressive half of the flange first. Culver and Frampton (1970) showed that when the flange-web junction is assumed fixed, the outer flange half buckles first and if the flange-web junction is simply supported then the inner half buckles first. The relevant buckling coefficients k for different panel aspect ratios and curvatures were obtained.

More recent studies by Davidson and Yoo (1996) using finite element analysis have generally confirmed the Culver and Frampton (1970) findings. While Culver and Frampton (1970) attributed the observed behaviour to geometry, Davidson and

Yoo (1996) have shown that the buckling behaviour can occur in a straight flange with stress gradient. Further, the modeling of boundary conditions in the finite difference technique was shown to be opposite to the effects observed in the finite element model. The web has the effect of pushing the flanges in the radial direction causing radial compressive stresses on outer half and tensile stresses on the inner half of the flange. Davidson and Yoo (1996) performed parametric studies in which boundary conditions, curvature, web thickness and length were varied. A simple equation based on these studies has been presented equations that expresses the buckling stress of the curved flange in relation to the straight one:

$$(\sigma_{st})_{cv} = (\sigma_{cr})_{st}\psi_{cv} \tag{1.7}$$

where

$$\psi_{cv} = \left(1.05 - \frac{l_{br}^2}{4Rb_f}\right)$$

is the stress reduction factor,
σ_{cv} is the curved girder stress,
σ_{cr} is the elastic critical stress for straight girder,
l_{br} is the cross-frame bracing spacing,
R is the radius of curvature at web line and b_f is the flange width.

Alternatively limits are imposed on flange slenderness to prevent buckling:

$$\left(\frac{b}{t}\right)_{cv} \leq \left(\frac{b}{t}\right)_{st} \sqrt{\psi} \tag{1.8}$$

where b and t are the flange width and thickness respectively, ψ_{cv} is a reduction factor that is applied to the straight girder equation. While the curvature affects local buckling behaviour of a curved flange, the suggested correction parameter only increases the straight girder slenderness by 2%. Limits on slenderness are also imposed by the Japanese Guidelines to prevent local buckling (Davidson and Yoo, 1996). The limit increases the curved compression flange thickness over the straight girder by 30%.

Abdel-Sayed (1973) investigated the bifurcation behaviour of curved web panels under shear and combined shear and bending. The elastic critical load of the curved panels were greater than corresponding flat panels. The model used did not include flange-web and lateral torsional rigidity. Davidson *et al.* (2000*a*) investigated curved web panels using finite element analysis. The results showed that curvature results in an increase in the elastic critical loads. Further, when

pure bending was dominant, no bifurcation was observed while when pure shear dominates bifurcation was observed near the elastic critical load.

Bifurcation buckling of cylindrically curved web does not occur under shear due to the out of plane bending actions resulting from curvature. A curved web behaves like a column with initial deformation. Lee and Yoo (1998) have shown through numerical models that curvature increases the linear buckling strength of a web panel though no design equations were presented. The finite displacement behaviour under pure shear showed a bifurcation type behaviour at or near the elastic buckling stress.

Several equations for critical elastic moment of curved girder have been put forward from each of the different curved beam theories. The equation presented in the Guide (Galambos, 1998) is that derived by Nishida given below:

$$M_{cr} \approx \sqrt{\left(1 - \frac{L^2}{\pi^2 R^2}\right) \frac{\pi^2 E I_y}{L^2} \left(GJ + \frac{\pi^2 E C_w}{L^2}\right)} \tag{1.9}$$

where I_y, J and C_w are minor axis moment of inertia, St.-Venant torsion constant and warping constant. The equation 1.9 above shows that there is a reduction in critical moment with increasing curvature. It is noted that there is no universal agreement on the bifurcation stability equations of curved girders.

The issue of bracing in curved girders is treated differently because unlike in straight girders, the bracing and cross frames are primary load carrying members. The braces perform two functions; to prevent the buckling and to limit the lateral flange bending. The limits imposed on the brace spacing are thus to satisfy the above mentioned functions. While other factors such as vertical bending and deflection are considered, the critical parameter in cross frame spacing has been shown to be the warping stresses. Davidson *et al.* (1996) investigated the issue of cross-frame spacing using finite element models. The parameters varies included girder depth, span length, number of girders, girder spacing and flange width. The results obtained were fitted into an equation using regression to obtain a spacing length. Yoo and Littrell presented a formula to satisfy these conditions and it is this formulary presented in the Guide (Galambos, 1998). However, the modeling was not adequate, no proper mesh refinement was done and only effects of span and radius of curvature were considered, thus making the limits unconservative (Davidson *et al.*, 1996).

The behaviour of curved girders under shear has been investigated by several researchers (Jung and W.White, 2006; Lee and Yoo, 1998; Abdel-Sayed, 1973).

Shear strength can be limited by plate buckling or yielding. However, the yield condition can only occur in compact webs. The critical stress in a plate is given by:

$$\tau_{cr} = \frac{\pi^2 E k_v}{12(1-\nu^2)} \left(\frac{t}{b}\right)^2 \tag{1.10}$$

were t is the plate thickness and b is plate height and k is the shear coefficient.

Early theories on web shear assumed that the web was simply supported (Basler and Thurlimann, 1961). Basler model assumes simple support flange-web boundary condition and provides a lower bound for web shear resistance. However, finite element analysis studies by Lee and Yoo (1999*a*) have shown that the boundary conditions are more towards the fixed condition, making the simply supported assumption conservative. The boundary condition is dependant on flange rigidity. Lee and Yoo (1999*a*) suggested the use of shear buckling coefficient for flange-web thickness ratio $t_f/t_w \geq 2.0$ given below:

$$k = k_{ss} + 0.8(k_{sf} - k_{ss}) \tag{1.11}$$

where k_{ss} is the shear buckling coefficient for rectangular plates simply supported on all four edges and k_{sf} is the coefficient for rectangular plates with two opposite sides simply supported and fixed respectively. Hybrid girders under combined bending and shear behave differently from homogeneous girders. This is because web yielding due to bending reduces web stiffness. Due to insufficient data on hybrid girder shear behaviour, the ASCE-AASHO (1968) suggested a conservative shear design procedure that neglects tension field action. Studies using finite element models by Shanmugan *et al.* (2003) investigated curved girders using finite element models and tension field action is indeed present in slender curved members.

The buckling strength of curved web panels has been shown to be greater than that for a corresponding straight web (Lee and Yoo, 1999*b*; Abdel-Sayed, 1973). Abdel-Sayed (1973) did an analytical study of curved panels under combined shear and bending. Shear buckling coefficients for curved panels were obtained and it was shown through a plot that for a given panel aspect ratio, the buckling coefficients are greater than those for a straight panel. Lee and Yoo (1999*b*) have shown that the ultimate shear strength for a panel reduces with increasing curvature. Defining a curvature parameter $c = \frac{a^3}{8Rt_w}$ where R is the radius of curvature, a is the panel arc length and t_w is the web thickness, Lee and Yoo (1999*b*) showed that for $c \leq 1.0$ the ultimate strength of a curved panel is not significantly different from a straight one. It was shown further that curved panels can develop significant post buckling

strength. This post buckling strength reserve for curved webs is ignored in AASHTO Guide Specifications (1993) (Lee and Yoo, 1999*b*).

For vertical flange buckling the LRFD (Salmon and Johnson, 1996) gives the limit for a straight girder web:

$$\frac{h}{t_w} = \frac{96500}{\sqrt{F_{yf}}(F_{yf} + 114)} \tag{1.12}$$

where h is the web height, t_w is the web thickness and F_{yf} is the flange stress.

Shear buckling reduces the distance between flanges reducing this reduces load carrying capacity. Carskaddan (1968) recommends treating the shear buckling strength to be the ultimate strength for un-stiffened hybrid girders. However, plates posses significant post buckling reserve strength and this would be conservative. The design practice is to impose limits on the slenderness ratios so as to preclude local buckling.

Early studies by Japanese researchers on local flange buckling showed that curvature effects can be neglected within certain curvature limits (Davidson and Yoo, 1996). These limits are given as $\frac{b}{R_w} \ll 0.05$ where b is the compression flange half width and R_w is the radius of curvature of the web line.

Curved I-girders have been modelled using finite element methods. The finite element method has the advantage of accurately represent the capacities due to local flange buckling and lateral torsional buckling, both in terms of the resistance of the cross-section and in terms of the deflected shape (NCHRP-Report-563, 2006).

The studies of curved girders have covered a wide range of cases from modeling composite girder bridges, the study of girders with openings and the shear lag in curved girders. In general, commercially available software packages such as ABAQUS have been used. Richard *et al.* (1995) used a variation of both linear triangular elements and bilinear quadrilateral elements to study the effects of radius of curvature to span effects and residual stresses on the ultimate load carrying capacity. Linear triangular elements were used. These triangular elements provide efficiency in computational time though they yield less accurate results when coarse meshes are used and also lock out shear. Quadrilateral elements allow shear deformation. The material was modelled as non linear using an incremental plastic theory and assuming the material is elastic-plastic with strain hardening rate dependent.

These studies have shown that the ultimate strength of thin walled girders is dependent on factors such as type of loading, span length, curvature, initial residual stresses and boundary conditions. Richard *et al.* (1995) investigated the second order in-elastic effects of curved beams using finite element analysis. Mixed element models were used. This was compared with experimental results obtained by Fukumoto and Nishida (1981) and analytical results obtained from the differential equations of equilibrium derived by Yang and Kuo (1987). Simply supported curved beams and beams with intermediate supports were studied. The results obtained in simply supported case showed that the ultimate strength of beams with smaller curvature was always higher than the beams with larger curvature. The equation was found to be more conservative than the ABAQUS model up to a maximum of 35% in some cases.

Chung and Sotelino (2006) used models with either shell elements or a combination of shell and beam elements. When using a mixed model, the shell elements were placed at the centroid of girder flanges while beam elements were placed at the girder web. Rigid links were applied through constraints in degree of freedom to model composite action. A comparison of these model with experimental results revealed maximum error of 6%. It was found when modeling in ABAQUS that overlapping flange elements with web elements by sharing the same node resulted in significant modeling errors because of the incorrect moment of inertia about the primary bending axis.

An experimental and analytical study on curved girders was conducted by Zureick *et al.* (2000). Three curved girders held together by cross frames were assembled. The finite element model utilising four types of elements in ABAQUS was developed. As with other researchers shell and beam elements were used in addition to unidirectional gap and super elements. S4R elements in ABAQUS were used to represent girder web, flange and stiffener plates. This element can model thin or thick shells, finite membrane strains and large strains. Zureick *et al.* (2000) conducted further experiments investigating post buckling shear response of I-girders. The results from these experiments were analysed by Jung and W.White (2006) in finite element models. The objectives of the study was to present finite element analysis results based on the experiments of Zureick and parametric variations. A displacement based bilinear quadrilateral shell element with reduced integration was used in the model. The strength of the girders in experiments were between 89% to 97% of the finite element analysis.

A comprehensive treatment of finite element analysis involving arbitrary curved beams is given by Saje *et al.* (1998). The formulation is based on Reissner non linear beam theory. Large displacements and rotations were allowed and an arbitrary curved beam considered. A range of techniques including use of strain elements, hybrid and mixed element formulations were applied. The formulation results in a model where only the rotation function need to be interpolated. Internal forces are calculated with the same accuracy as displacements and rotations. Further, unknown variables correspond to the fixed in space coordinate system structure thus there is no need for local to global coordinate transformation. The later results in increased computational efficiency.

1.3 Research motivation

The review shows some of the work going on in the area of both hybrid and curved girder research. Efforts have been undertaken to derive curved beam equations but no generally agreed formulation exists. The approach to simplify equations from strength of materials-small deflection theory considerations have resulted in equations that either break down when the curvatures are large or equations that are cumbersome to use by designers. For hybrid girders, research has shown that they behave almost like homogeneous girders. However efficient design of hybrid girders is curtailed by the restrictions on high performance steels that have yield strength greater than 490MPa. For such steels, inelastic moment redistribution and hence plastic design are not permitted. Hybrid curved girders have not been covered and are the focus of this study.

In the absence of curved girder equations, research on inelastic curved girder behaviour is hampered. Numerical techniques such as finite element analysis remain the main investigative tool to develop semi-empirical design guides. With increasing computational power, finite element models have been employed in the study of the behaviour of both curved and hybrid girders and valuable recommendations based on these studies have been presented. As in the case of other techniques, the reliability and validity of finite element analysis for curved girder studies has been highlighted as an area that needs research NCHRP-Report-563 (2006). The report points out other areas of research which include the yield criterion, the validity of analysis tools, the development of interaction equations and extreme event dynamic behaviour of curved girders.

1.3.1 Problem definition

Curved bridges are often the best alternative to straight girders when predefined road or railway alignments or presence of buildings place constraints on design. This happens in urban environments and even remote locations. Horizontally curved girders experience lateral moments when subjected to gravity loads and this alters their load resistance capacity. Hybrid girders arise due to the need of building structures that are less imposing on the environment or the need to reduce overall dead weight in long span bridges. Such girders utilising high strength steel offer economy. The different steel combinations in hybrid girders coupled with the presence of curvature complicates the analysis of curved hybrid girders.

1.3.2 Research aims

The following areas investigated in this study:

(i) The effect of varying curvature on the girder load-deflection behaviour
Girder behaviour changes as horizontal curvature is introduced. This is because a curved girder caries both lateral and vertical moments. The load carrying capacity as curvature is changed is examined for selected span lengths.

(ii) Stress-strain variation in the girder
The stress-strain variations both through girder depth and across the flanges are investigated. The stress distribution has a bearing on plastic hinge formation and affects areas prone to local buckling. The stress-strain profile for a curved girder is different from that of a straight girder due to the presence of lateral moments. The stress variation is also of interest because of the different steel grades used in flange and web.

(iii) Effect of varying steel grades in girder
The hybrid effects are studied by varying steel grade in web and flange. For hybrid girders optimised to carry moments, the web yields because it has steel with low yield strength. In the inelastic range, the modulus of the web reduces after yielding and this results in slight stiffness reduction for hybrid girders. The load-deflection response of the curved hybrid girder is thus of interest after the web has yielded.

(iv) The accuracy of available ultimate load equations
The behaviour of curved girders is still an area of investigation and no generally

agreed equations exist for curved girders. The effectiveness of available design procedures and accuracy of available ultimate load equations is examined and compared to finite element analysis results.

1.3.3 Scope of research

This study is limited to the following:

(i) Hybrid girders that are optimised for moment capacity. Such girders have high yield strength steel in the flanges and low yield strength steel in the web.

(ii) A cross section of 812 × 300 (8,16) is used for the investigation. The effects of local buckling as slenderness ratios are varied are not investigated.

(iii) Two spans of 5m and 8m are used for the investigation.

(iv) Three steel grades with yield strength of 350MPa, 460MPa and 690MPa are used for the investigation.

(v) Computational modeling is used for the investigation. Laboratory experiments are not done, however, the experimental data available from literature is used to verify the model.

1.3.4 Research limitations

The resources in both time and money did not allow for any scaled laboratory model test. The lack of experimental tests lead to great reliance on the two readily available experimental data sets for calibration. The experimental data used for calibration was on curved homogeneous girders, data on hybrid curved girders was available for model verifications.

The finite element method has been shown from the literature review to give results close to experiments for the curvature ratios adopted in this study. However, the reliability and range of applicability of the finite element method to curved girder problems is still an area of investigation and this has been highlighted in NCHRP-Report-563 (2006).

The effect of curvature on girder behaviour is investigated. In this respect, the girder arc length and span are not significant parameters. The major parameter used is curvature ratio and this is varied to within limits given in the literature

review. Thus only two spans are used and in this study, the arch length to radius of curvature ratio is used to compare the girder results.

The study is limited to three steel grades and this is purely due to the limitation on available data which included one mild steel grade and two high strength steel grades.

The curvature modifies the lateral and stress pattern in the girder. The investigation focuses only on the curvature and hybrid effect on ultimate load of a girder and therefore local buckling is not investigated. In this regard, only one girder cross-section is used.

Chapter 2

Theory

2.1 Introduction

This chapter presents an overview of the principles that govern hybrid girders, curved girders and the expected behaviour of curved hybrid girders. The theory governing straight girder behaviour is given first. Later, the areas of departure from this straight girder behaviour are shown through the consideration of hybrid and curvature effects. Design equations, interaction equations and modifications to slenderness limits are also presented.

Plate girders are large flexural members fabricated from plates. In recent years, there has been a shift from bolts and rivets when fabrication girders. Welds are now extensively used and they are a more aesthetically pleasant form of connection. Girders are optimised to carry large flexural loads over long spans that can not be carried by available hot rolled members. The applications of plate girders is in highway bridges and buildings with large open spaces. Unlike hot rolled sections, girders offer greater flexibility to the designer in proportioning members and also in material selection. Girders do behave differently from other flexural members such as hot rolled beams. This is mainly because girders are deep and thus the web tends to experience web buckling. The web stress relationship also deviates from the linear beam theory through the depth.

Hybrid girders have been studied extensively and the review shows that the studies did not cover the combined hybrid-curvature effects. This is the area of investigation in the current study. Hybrid girders have already been defined as girders with different steel grades in flanges and the web. The present study investigates hybrid girders with higher steel grade in the flange and lower grade steel in the web. The

development and availability of high strength steel and the need for economy are the primary reasons for considering hybrid girders in design. The research on hybrid girders has largely been on rotational ductility to assess the attainment of plastic capacity and moment redistribution especially in areas of negative flexure (Barth *et al.*, 2007; Ito *et al.*, 2005; Azizinamini *et al.*, 2004; Miki *et al.*, 2002; Sause and Fahnestock, 2001). The research has resulted in revision of design code requirements regarding use of HPS from a steel yield limit of 345MPa to 490MPa for plastic design and moment redistribution.

Numerous theories of curved beam have also been put forward (Yang and Kuo, 1986; Yoo, 1982; Fukumoto and Nishida, 1981; Vacharajittiphan and Trahair, 1975; Vlasov, 1961; Timoshenko, 1961). A comparison of closed form solutions for elastic critical moment obtained show the wide differences in predictions of critical loads. The differences are due to assumptions regarding warping, differences in the formulations of the theories, approximation procedures for curvature terms and interpretation of vanishing shear assumption in thin walled members. There is no accepted set of equations for the general case of thin walled curved beams. The absence of such equations has reduced progress in the study of inelastic behaviour of curved girders.

Despite the absence of generally accepted curved beam equations, research has progressed and equations for ultimate strength have been put forward together with semi-empirical interaction equations. Numerical techniques such as finite element analysis have also been used to study curved girder behaviour. Design guidance is provided that gives some rules on the design of curved hybrid girders (ASCE, 1977). There are two design guides that cover curved girders; Hanshin Guide and AASHTO Guide Specifications. What is presented here are the guidelines adopted in the AASHTO Guide together with background literature. This is largely because of no access to the Japanese codes or literature on curved girder research in Japan.

When designing hybrid girders, the approach is to consider a homogeneous girder and then apply hybrid reduction factors (Salmon and Johnson, 1996). For curved girders, the curvature can be ignored for small curvatures. The ASCE (1977) gives guidelines for general flexural behaviour of both curved homogeneous and curved hybrid girder design. It is thus important as a starting point to outline the general flexure theory for straight homogeneous girders and highlight areas of departure as hybrid and curvature effects are introduced.

2.2 Plate Girder behaviour

Plate girders are welded plate assemblies and the present study only considers I-girders. The process of manufacture which involves welding different plates also introduces residual stresses that can be significant. Imperfections are also introduced in manufacturing and assembly process and these have an influence on both buckling behaviour and yield pattern.

The general experimental and theoretical basis for girder design was done by Basler and Thurlimann (1961). Background work on diagonal-tension theory for shear capacity had already been presented by Wagner. The main difference between beams and girders is the web behaviour which in most cases is non-compact. Modifications have been suggested to the theory by Basler in recent years, however due to the simplicity and relative accuracy, its equations or their modification appear in many codes including the SAN 10162.

The bending resistance contribution from the web in a girder is rather small. Only a small strip of the compression part of the web estimated to have a depth of $30t_w$ and the tension part are considered for flexural resistance (Basler and Thurlimann, 1961). Even under combined bending and shear, it has been observed that shear buckling of the web can not be used as a limit for load carrying capacity. Ultimate moment considerations are thus based on local compression flange buckling, vertical buckling of flange into web and lateral torsional buckling of the girder.

2.2.1 Buckling

A beam or girder can fail by yielding or buckling when subjected to moments. The instability situation is especially significant when thin walled members such as girders are loaded. This instability can be due to lateral torsional buckling or buckling of compression flange into the web. The elastic stability of beams has been investigated by many authors such as Trahair and Bradford (1988), Vlasov (1961) and Timoshenko (1961). For a simply supported doubly symmetric section under uniform bending in the web plane, the governing differential equations are given below (Tall, 1974):

$$EI_y \frac{d^4y}{dz^4} + M\frac{d^2\phi}{dz^2} = 0 \tag{2.1}$$

$$EC_w \frac{d^4\phi}{dz^4} - GK_T \frac{d^2\phi}{dz^2} + M\frac{d^2u}{dz^2} = 0 \tag{2.2}$$

where I_y is the moment of inertia about y-axis, u is the displacement in the x-axis, ϕ is the angle of twist, C_w is the warping torsional constant, G is the shear modulus, K_T is the St Venant torsional constant.

The solution to the above equations is given below:

$$M_{cr} = \frac{\pi}{L}\sqrt{EGI_y\left(\frac{EC_w}{GJ}\frac{\pi^2}{L^2}+1\right)} \tag{2.3}$$

where J and C_w are torsional and warping constants.

The above case is the simplest and many practical cases can be dealt with by starting with equation 2.3 and applying modifications. The modifications come in form of a factor that is given for particular cases depending on loading and boundary conditions.

Plate girders are made by welding different plates together and thus the behaviour of plates gives some idea on how the assembly behaves. The plate elements of a girder can reach instability through the following:

(i) Elastic bend-buckling strength

(ii) Elastic shear-buckling strength

(iii) vertical flange buckling

When transverse loads are applied to a plate, the critical stress is reached and this is given in the equation below:

$$\sigma_{cr} = \frac{\pi^2 Ek}{12(1-\nu^2)}\left(\frac{t}{b}\right)^2 \tag{2.4}$$

where k is the plate buckling coefficient, t is the plate thickness and b is the plate width.

The equation 2.4 holds for plates subjected to shearing forces and compression forces. However, the buckling coefficient is calculated differently for these cases. When calculating the critical stress for plate assemblies, the restraint offered by the joints can be significant. For a long plate subjected to bending k depend on the plate support conditions and for simple supports $k = 23.9$ while for fixed supports $k = 39.6$. Clearly the two values represent the lower bound and upperbound for all girder configurations. It is common to proportion girders such that the flange

offers some restraint to web bend buckling. The AISC procedure assumes the fixity condition to be 80% toward the the fixed condition (Salmon and Johnson, 1996)

A similar procedure to determine critical shear stress is used. The buckling stress is given by the equation similar to equation 2.4 and the buckling coefficients presented (Trahair and Bradford, 1988)

$$\tau_{cr} = \frac{\pi^2 E k_v}{12(1-\nu^2)} \left(\frac{t}{b}\right)^2$$

where for $\frac{h}{L} \leq 1$

$$k_v = 4.0 + \frac{5.34}{\left(\frac{h}{L}\right)^2} \tag{2.5}$$

and for $\frac{h}{L} \geq 1$

$$k_v = \frac{4.0}{\left(\frac{h}{L}\right)^2} + 5.34 \tag{2.6}$$

h and L are the plate height and width respectively.

Lee *et al.* (1996) has shown that the web-flange boundary condition is dependant on the thickness ratios of flange and web. After conducting numerical investigations on the boundary conditions and the following equations were proposed for the shear coefficients, where t_f is the flange thickness and t_w is the web thickness:

For $\frac{1}{2} < \frac{t_f}{t_w} < 2$

$$k = k_{ss} + \frac{4}{5}(k_{sf} - k_{ss}) \left[1 - \frac{2}{3}\left(2 - \frac{t_f}{t_w}\right)\right] \tag{2.7}$$

For $\frac{t_f}{t_w} > 2$

$$k = k_{ss} + \frac{4}{5}(k_{sf} - k_{ss}) \tag{2.8}$$

Note: k_{ss} is given by the shear coefficients given earlier as k_v. The case where two opposite edges of a plate are simply supported and fixed respectively is also presented below: For $\frac{h}{L} < 1$

$$k_{sf} = \frac{5.34}{(h/L)^2} + \frac{2.31}{(h/L} - 3.44 + 8.39(h/L)$$

For $\frac{h}{L} \geq 1$

$$k_{sf} = 8.98 + \frac{5.61}{(h/L)^2} - \frac{1.99}{(h/L)^2}$$

The equations for k_{sf} presented above are similar with the equations for short plate with clamped edges given in the (Galambos, 1998).

Basler and Thurlimann (1961) proposed the following limits for web slenderness:

$$\frac{h}{t} \leq \sqrt{\frac{\pi^2 E}{24(1-\nu^2)} \frac{A_w}{A_f} \frac{1}{\sigma_f \epsilon_f}}$$

where $\frac{A_w}{A_f}$ is the ratio of web to flange area, ϵ_f and σ_f are the strain and stress in flange respectively. In general the ratio $\frac{A_w}{A_f}$ is 0.5.

Analytical studies on both stiffened and un stiffened plates have been done and these provide an insight into plate girder behaviour. Local and global buckling modes can be significant in affecting failure mode. In design practice the buckling types above are treated separately even though there can be interaction between lateral, torsional and local buckling. This is a simplification to obtain closed form solutions for the lateral and torsional buckling. Local buckling is prevented by careful choice for plate slenderness parameter. Section classification is used a way to determine the extent to which local buckling affects the section capacity to develop the design moment. Different design guides give limits and below are extracts from some of the standards. Though expressed differently, there is a connection between the local buckling limits and the material yield stress. Numerical studies such as finite element analysis are used to investigate the lateral, torsional and local buckling interaction and this is used in the current study.

The SANS 10162 gives the limits for flexural members presented in Table 2.1. The classes are as follows:

(i) class 1 sections will permit attainment of the plastic moment and subsequent redistribution of the bending moment;

(ii) class 2 sections will permit attainment of the plastic moment but need not allow for subsequent moment redistribution;

(iii) class 3 sections will permit attainment of the yield moment; and

(iv) class 4 sections will generally have local buckling of elements in compression as the limit state of structural resistance.

Table 2.1: SANS10162 Section classification

Element in compression	Section classification		
	Class 1	Class 2	Class 3
I or T-section flange	$\frac{b}{t} \leq \frac{145}{\sqrt{F_y}}$	$\frac{b}{t} \leq \frac{170}{\sqrt{F_y}}$	$\frac{b}{t} \leq \frac{200}{\sqrt{F_y}}$
Web	$\frac{h_w}{t_w} \leq \frac{1100}{F_y}$	$\frac{h_w}{t_w} \leq \frac{1700}{F_y}$	$\frac{h_w}{t_w} \leq \frac{1900}{F_y}$

where h_w and t_w refer to web height and thickness respectively and F_y is the steel yield stress.

The Euro code 3 follows a similar procedure, the classes are just as defined in above for SANS61-1 (EN1993-1-1). The limits are given in the Table 2.2:

Table 2.2: EN3-1-1 Section classification

Element	Class 1	Class 2	Class 3
Internal compression part	$\frac{c}{t} \leq 72\varepsilon$	$\frac{c}{t} \leq 83\varepsilon$	$\frac{c}{t} \leq 124\varepsilon$
Outstand flanges	$\frac{c}{t} \leq 9\varepsilon$	$\frac{c}{t} \leq 10\varepsilon$	$\frac{c}{t} \leq 14\varepsilon$

where $\varepsilon = \sqrt{235/f_y}$ and $f_y \leq 460\text{MPa}$

2.2.2 Bending

The stress distribution in a girder differs slightly from that of a beam. The compression web carries less load than that predicted by beam theory. Some of the compressive force is redistributed to the compression flange. The compression resistance of the web in the compression part is ignored except for a small section next to the flange. The strength of the compression flange largely determines the moment capacity of a girder. The compression flange can fail by lateral, torsional and vertical buckling. These aspects have already been reviewed in section before.

Having proportioned a girder not to fail though local buckling, the bending strength is determined. In SANS 10162 the factored moment resistance for class 1 or 2 doubly symmetric sections for is given as follows:

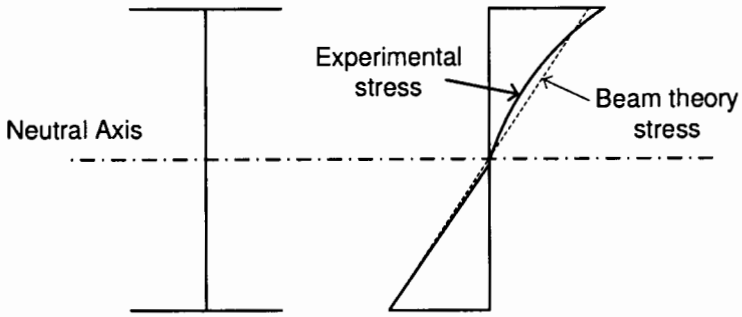

Figure 2.1: Girder stress

(i) when $M_{cr} > 0.67M_p$

$$M_r = 1.15\phi M_p \left(1 - \frac{0.28M_p}{M_{cr}}\right) \text{ but not greater than } \phi M_p$$

(ii) when $M_{cr} \leq 0.67M_p$

$$M_r = \phi M_{cr}$$

where: M_{cr} is elastic buckling moment given in equation 2.3,
M_p is the plastic moment resistance capacity given as $M_p = \phi Z_p f_y$,
For class 3 or 4 sections, M_P is replaced with M_y given as $M_y = \phi Z_e f_y$,
Z_p and Z_p are plastic section modulus and elastic section modulus respectively and f_y is the steel yield strength.

For a web exceeding class 3, the moment resistance from above is modified and M_r is limited to M_r' as follows:

$$M_r = M_y \left[1 - 0.0005\frac{A_w}{A_f}\left(\frac{h_w}{t_w} - \frac{1900}{\sqrt{M_u/\phi Z_e}}\right)\right] \tag{2.9}$$

where $A_w = h_w t_w$ is the web area
A_f is the flange area
M_u is the actual moment in girder under ultimate load.

2.3 Hybrid girders

The theoretical behaviour of straight hybrid beams was outlined by Frost and Schilling (1964) and the relevant equations are simply repeated here. In the

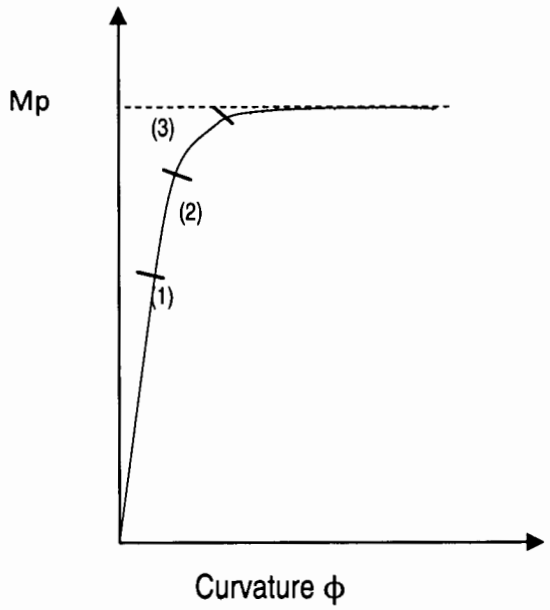

Figure 2.2: Moment deflection for hybrid girder

flexural behaviour of hybrid girders, it is important to define yield. This is because in hybrid beams, the web is designed intentionally of lower yield steel as compared to the flanges. In line with moment capacity definitions for homogeneous girders, a plastic moment capacity can be expected if buckling is prevented and enough rotational ductility is mobilised. At plastic moment, the whole section is considered to be yielded. Though infinite rotation is required for whole section to yield; such a mathematical abstraction is very useful as strain hardening and inelastic behaviour allow this capacity to be reached without the centre of the web yielding.

The concept of plastic section is useful, but severe restrictions on the slenderness limits and bracing requirements are necessary to attain it. Another important point is the initial yield at the extreme fibres of the flange or simply referred as flange yield. In this case, sections of the web yield before the extreme fibres of the flanges yield. The girder is expected to have load deformation behaviour shown in the Figure 2.2. The first stage consists of elastic deformations and there is no difference with homogeneous girder. The behaviour exhibited in the elastic range is the same for both straight and curved girders in that hybrid and homogeneous girders show no difference. This is followed by the yielding of the web and later the flange yields.

Some insight can be gained in the flexural behaviour of a straight hybrid girder using

Bernoulli-Euler theory. For this to apply, a straight girder adequately braced and proportioned such that local buckling does not occur is considered. For a straight beam under pure bending, the strains are proportional to the distance from the neutral axis. The general differential equation together with flexure formula are given below:

$$M = EI\kappa \tag{2.10}$$

where M is the moment and κ is the curvature term and

$$\sigma = -\frac{My}{I} \tag{2.11}$$

where y is the distance from neutral axis.

For simplicity, a perfectly elastic plastic material is considered with yield stress of σ_y. For small loads the stresses are determined from Hooke's law using equation 2.11 and remain within the elastic range. In this zone, the load deflection curve is linear. When the load is increased, the web yield is reached and this results in the extreme fibres of the web undergoing plastic deformation.

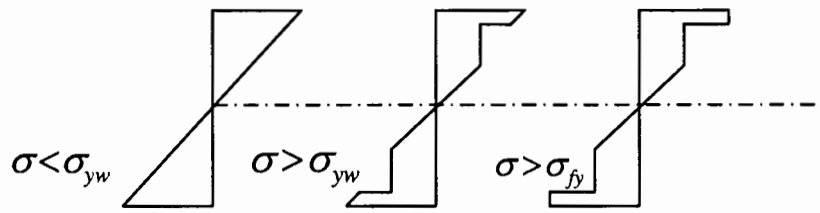

Figure 2.3: Hybrid girder stress distribution

As the load is increased, the linear variation of strain is maintained but the stresses in the web reach yield value. For the consideration of moment capacity, the web contribution is small and thus the changes in the load deflection curve resulting from web yielding are small. In this range of loading, the moment capacity is given below:

$$M = EI_f\phi + Z_w f_{yw} - \frac{f_{yw}^3}{3E^2\phi^2} \tag{2.12}$$

When the load is increased further, the depth of the yield zone for the web increases and the strains in the extreme fibres of the flanges begin to yield. This results in significant increase in deflection for a given load due to the loss of stiffness. This

is expected as the flanges are primarily the moment carrying components. The moment capacity is given:

$$M = Z_f f_{yf} + Z_w f_{yw} - \left(\frac{f_{yw}^3 t + f_{yf}^3 b}{3E^2\phi^2} \right) + \frac{c^2 b}{12} (3f_{yf} - E\phi c) \tag{2.13}$$

Finally with increasing load, the remaining elastic zones of the web yield the moment is given as:

$$M = Z_f f_{yf} + Z_w f_{yw} - \frac{f_{yw}^3}{3E^2\phi^2} \tag{2.14}$$

In line with the concepts of yield moment and plastic moment for homogeneous girders, the following are calculated from the expressions (Frost and Schilling, 1964): Plastic moment:

$$M = Z_f f_{yf} + Z_w f_{yw} \tag{2.15}$$

Flange yield moment:

$$M = \frac{2I_f}{d} f_{yt} + Z_w f_{yw} - \frac{td^2}{12} \left(\frac{f_{yw}^3}{f_{yf}^2} \right) \tag{2.16}$$

It has been recommended that the design of hybrid girders be based on moment causing initial flange yield (Frost and Schilling, 1964). Plastic moment capacity requires more bracing and more deflections to be reached and thus is considered not a practical limit. Due to initial yielding of the web and the differences in steel yield strength of the web and flange, other considerations such as deflection limits have to be assessed. When a moment larger than twice the yield moment is applied to the girder, inelastic action occurs under unloading. Frost and Schilling (1964) recommended that the ratio of yield strength of the flange and web steel is kept less than two. This restriction is also imposed by the Euro codes 3-1-5 (Veljkovic and Johansson, 2004). The limitation on the steel strength ratio is more stringent in AASHTO (2007) in that the lower yield still must be the greater of 250MPa and 70% of the higher steel flange AASHTO (2007).

2.3.1 AASHTO LRFD Approach

A first principles approach to design of hybrid girders is useful in appreciating the yield pattern involved. However, design guides such as the AASHTO (2007) follow a different approach as recommended by ASCE (1977). The nominal moment strength

is calculated by assuming a homogeneous girder made of flange steel and a reduction factor is applied to account for hybrid effects (Salmon and Johnson, 1996; ASCE, 1977; Frost and Schilling, 1964). The reduction factor gives the ratio of the flange yield moment of a hybrid section to that of a homogeneous section consisting of flange steel. It is suggested here that as a consequence of the above simplification, the section classification of a hybrid girder proceed as done in a homogeneous girder. The equation for moment capacity of a hybrid girder is presented as a modification of a homogeneous section is given below:

$$M_n = S_x F_{cr} R_{PG} R_e \tag{2.17}$$

where R_e is the reduction factor accounting for web yielding prior to initial flange yield, R_{PG} is the reduction due to web bend buckling.

AASHTO (2007) gives the hybrid reduction factor R_h which is applied to equivalent homogeneous beam. This factor first proposed by ASCE (1977) is given as follows:

$$R_h = \frac{12 + \beta(3\rho - \rho^3)}{12 + 2\beta} \tag{2.18}$$

where:
$\beta = \dfrac{2D_n t_n}{A_{fn}}$, ρ is the smaller of $\dfrac{F_{yw}}{f_n}$ and 1.0,
A_{fn} is the sum of the flange area and the area of any cover plates on the side of the neutral axis corresponding to D_n (mm^2),
D_n is the distance from neutral axis to the inside face of the flange on the side of the neutral axis where yielding occurs first,
f_n is the largest of the specified minimum yield strengths of each component included in calculation of A_{fn}. The factor R_h is always close to unity (AASHTO, 2007).

Restrictions are placed on the ratio of yield strengths by the AASHTO (2007). The web steel should be the larger of 250MPa and 70% of the higher strength flange steel. In general the difference between the steel should be one grade up. This condition will clearly not be upheld in the present study first because it is the general behaviour of hybrid girders that is of interest and second because of the restriction placed due to the available steel stress-strain data for the study.

Since the web yields first, the support offered by the web to the flange is of interest. The yielding of the web in the compression zone of the girder does not compromise its ability to prevent flange vertical buckling. Also the lateral torsional buckling is only sightly affected by web yielding.

2.3.2 EN3-1-1 Approach

The relevant code EN 3 does not make reference to design of hybrid girders. However, a design procedure based on modifications of EN 3 has been put forward by Veljkovic and Johansson (2004) and this is summarised in sections that follow.

Section classification

The section classification is done as given in section 5.5 of EN3-1-1. The web is classified using the flange steel strength and this is considered conservative. The above procedure implies that there should be no distinction in classification of both homogeneous and hybrid girders. There is a limit of 460 MPa for the steel used.

Bending moment

In general, a girder has the same amount of steel in the web as in the two flanges combined. The lever arm for the web steel is less and the web contributes less than 25% of the bending resistance in a homogeneous girder. The code allows the design to be based only on flange class if the web is assumed not to contribute to the bending resistance. Depending on class, the bending resistance is given below:

(i) Cross-section 1 and 2: The contributions of the web and flange are simply added up and the moment resistance is given below;

$$M_{Rk} = f_{yf} A_f (h_w + t_f) + f_{yw} A_w h_w / 4 \tag{2.19}$$

where f_{yf} and f_{yw} refers to the yield stresses for flange and web steel respectively; t_f is flange thickness, h_w and A_w refer to web height and area respectively.

(ii) Cross-section classes 3 and 4: The flanges should be class 3 or lower. The effective cross-section of web is determined by the yield strength of the compression flange. The approximate formula for the bending resistance is given below:

$$M_{Rk} = f_{yf}(W_{eff} - \Delta W) \tag{2.20}$$

where

$$W_{eff} = W\left[1 - 0.1\frac{A_w}{A_f}\left(1 - 124\varepsilon\frac{t_w}{h_w}\right)\right]$$

when h_w/t_w 124ε

$$\varepsilon = \sqrt{235/f_{yf}}$$

$$\Delta W = h_w A_w \left(1 - \frac{fyw}{f_{yf}}\right)^2 \frac{2 + \frac{f_{yw}}{f_{yf}}}{12}$$

The interaction between shear and bending is ignored for class 1 and 2 while the rules for interaction are applied for class 3 and 4.

The yield strength ratio for the flange and web is limited to 2. Within this limit, the reduction of stiffness due to web yielding is considered small. Larger strains and thus deflections are required for high strength steel to reach yield. Serviceability requirements have to be reviewed to enable efficient use of such steels. In comparison, the EN3 approach is less flexible compared to AASHTO approach when applied to curved girders. The approach is along the first principles and is not easily modified to give results for curved girders. The AASHTO design approach suggests that cross-section class can be based on homogeneous girder and this is taken up by EN3-1.

2.4 Curved girders

Curvature in girders results in lateral moments in addition to vertical moments. The lateral moments causes stresses that vary linearly across the flange while the vertical moments cause stresses that vary through the web depth. This significantly changes the load resistance pattern of these girders.

The presence of a lateral moment has the effect of reducing the vertical bending resistance of a girder. This can best be explained using the concept of a reduced flange section presented by Schilling (1996). In this concept, a portion of the flanges is assumed to resist lateral moments and the remaining section resists the vertical moments. It therefore follows from the above and has been shown by experiment that a curved girder will have less flexural capacity as compared to a straight girder of similar proportions under similar loading and boundary conditions (Shanmugan *et al.*, 2003; Richard *et al.*, 1995; Fukumoto and Nishida, 1981).

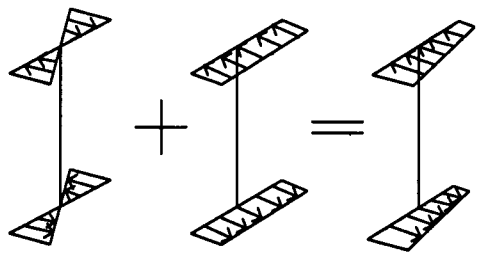

Figure 2.4: Warping and vertical bending stresses

2.4.1 Curved girder equations

From the literature review it is noted that two approaches have been used to derive curved beam equations. The approaches are the equilibrium method used by Timoshenko (1961) and Vlasov (1961) and the other approach being the energy method which has generally been embraced by more recent researchers including Kang and Yoo (1994*a*); Yang and Kuo (1987); Yoo (1982)

Vlasov Equations

Vlasov presented a theory of thin walled members that was not restricted to the Navier hypothesis of plane sections (Vlasov, 1961). This restrictive hypothesis is replaced by the notion of sectorial areas. The Vlasov equations have been the starting point of other researchers such as (Heins, 1975; Yoo and Heins, 1972) and the concise form given here is taken from Heins (1975).

Consider an element subjected to six external loads shown in Figure 2.5: three distributed loads q_x, q_y and q_z all acting in the respective axes of the element and three distributed torques m_x, m_y and m_z acting in respective girder axes.

Resisting internal forces are generated as a result of the external forces. These are shearing forces Q_x and Q_y; normal force N_z; bending moments M_x and M_y and torsional moment T. The force increments are shown over a length dz. The basic equilibrium equations have to be satisfied.

From Figure 2.6, the forces in X direction are summed below:

$$\frac{\partial Q_x}{\partial z} + \frac{N_z}{R} + q_x = 0 \tag{2.21}$$

Forces in Y direction:

$$\frac{\partial Q_y}{\partial z} + q_y = 0 \tag{2.22}$$

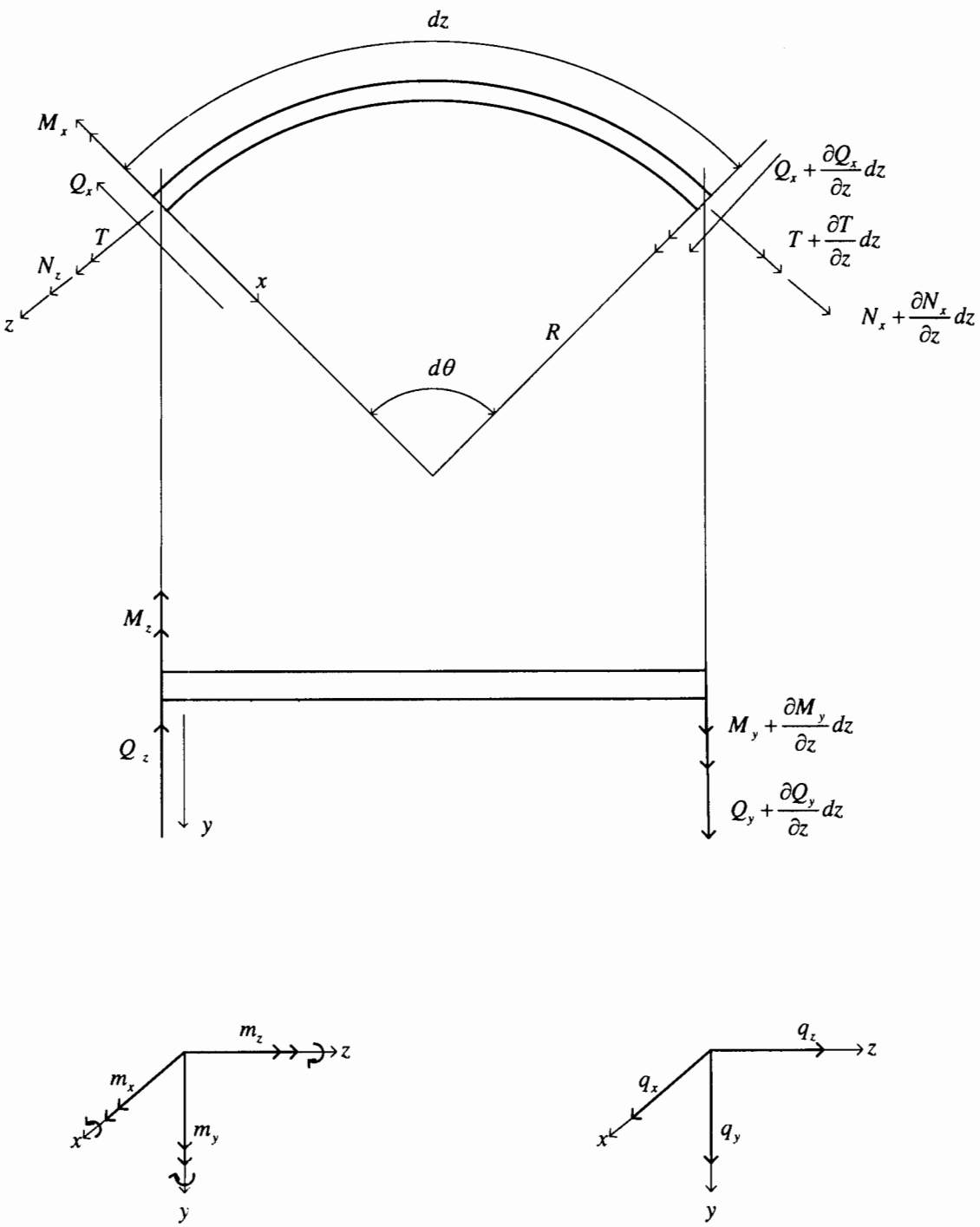

Figure 2.5: Forces on a curved girder element (Heins, 1975)

Forces in Z direction:

$$\frac{\partial N_z}{\partial z} - \frac{Q_x}{R} + q_z = 0 \tag{2.23}$$

Moments about X-axis:

$$\frac{\partial M_x}{\partial z} + \frac{T}{R} - Q_y + m_x = 0 \tag{2.24}$$

Moments about Y-axis:

$$\frac{\partial M_y}{\partial z} + m_y + Q_x = 0 \tag{2.25}$$

Moments about Z-axis:

$$\frac{\partial T}{\partial z} + \frac{M_x}{R} + m_x = 0 \tag{2.26}$$

The above six equations are reduced to only three equations. The shears are eliminated from the equations by first differentiating equation 2.24 with respect to z and differentiating equation 2.25 twice with respect to z:

$$\frac{\partial^2 Q_x}{\partial z^2} = -\frac{\partial N_z}{\partial z}\frac{1}{R} - \frac{\partial q_x}{\partial z} \tag{2.27}$$

$$\frac{\partial^3 M_y}{\partial z^3} + \frac{\partial^2 m_y}{\partial z^2} + \frac{\partial^2 Q_x}{\partial z^2} = 0 \tag{2.28}$$

Substituting equation 2.27 into equation 2.28:

$$\frac{\partial^3 M_y}{\partial z^3} + \frac{\partial^2 m_y}{\partial z^2} - \frac{\partial N_z}{\partial z}\frac{1}{R} - \frac{\partial q_x}{\partial z} = 0 \tag{2.29}$$

Now equation 2.25 is rewritten in terms of Q_x and the resulting equation substituted in equation 2.23

$$Q_x = -\frac{\partial M_y}{\partial z} - m_y$$

Thus

$$\frac{\partial N_z}{\partial z} = \frac{1}{R}\left(-\frac{\partial M_y}{\partial z} - m_y\right) - q_z = 0 \tag{2.30}$$

Substituting equation 2.30 into equation 2.29:

$$\frac{\partial^3 M_y}{\partial z^3} + \frac{1}{R^2}\frac{\partial M_y}{\partial z} = \frac{\partial q_x}{\partial z} - \frac{q_z}{R} - \frac{\partial^2 m_y}{\partial z^2} - \frac{m_y}{R^2} \tag{2.31}$$

The partial derivative of 2.24 with respect to z is taken and the result is substituted in 2.22 to give:

$$\frac{\partial^2 M_x}{\partial z^2} + \frac{1}{R}\frac{\partial T}{\partial z} = -q_y - \frac{\partial m_x}{\partial z} \tag{2.32}$$

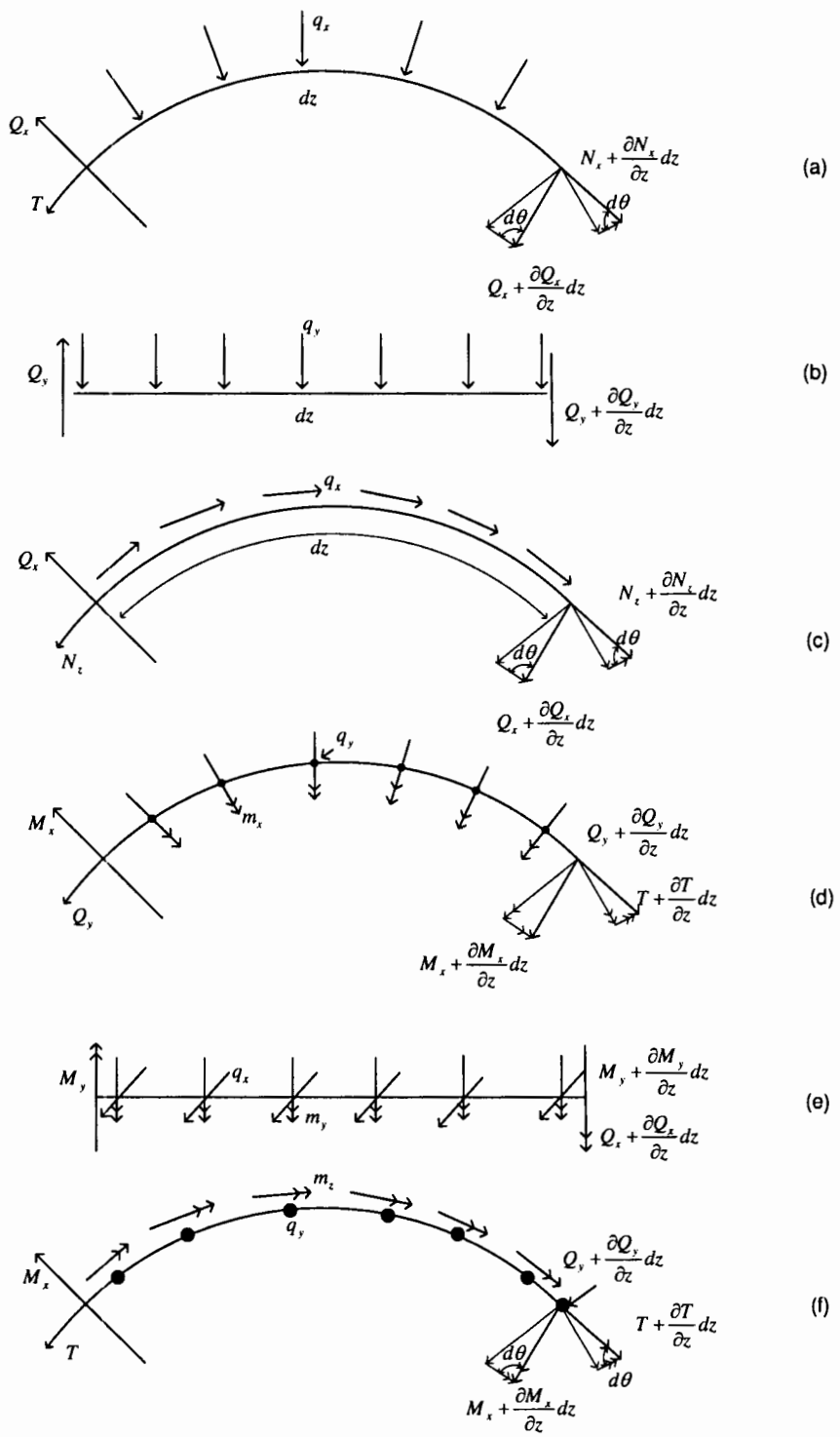

Figure 2.6: Equilibrium of forces on curved girder element (Heins, 1975)

Lastly, the equation 2.26 is restated:

$$\frac{\partial T}{\partial z} + \frac{M_x}{R} + m_x = 0$$

The force-deformation equations are also given and the general deformations are presented where $\psi(z)$ is longitudinal deformation, $\xi(z)$ is transverse deformation, $\eta(z)$ is vertical deformation and $\phi(z)$ is rotation

The longitudinal strain for a curved element is given as:

$$\varepsilon_z = \frac{d\psi}{dz} - \frac{\xi}{R} \tag{2.33}$$

The curvatures due to moments are given:

$$K_y = \frac{\xi}{R^2} + \frac{d^2\xi}{dz^2} \tag{2.34}$$

$$K_x = \frac{d^2\eta}{dz^2} - \frac{\phi}{R} \tag{2.35}$$

Twist per unit length:

$$\tau = \frac{d\phi}{dz} + \frac{1}{R}\frac{d\eta}{dz} \tag{2.36}$$

The forces are given below; assuming complete elasticity;

$$N_z = EA\varepsilon_z$$

Substituting equation 2.33:

$$N_z = EA\left(\frac{d\psi}{dz} - \frac{\xi 1}{R}\right) \tag{2.37}$$

$$M_y = -EI_yK_y$$

Substituting equation 2.34:

$$M_y = EI_y\left(\frac{d^2\xi}{dz^2} + \frac{\xi}{R^2}\right) \tag{2.38}$$

$$M_x = -EI_xK_x$$

Substituting 2.34:

$$M_x = -EI_x\left(\frac{d^2\eta}{dz^2} - \frac{\phi}{R}\right) \tag{2.39}$$

Torsional equation for a straight girder:

$$T = -EI_w \frac{d^2\tau}{dz^2} + GK_T\tau$$

Substituting 2.36

$$T = -EI_w \left(\frac{d^3\phi}{dz^3} + \frac{1}{R}\frac{d^3\eta}{dz^3}\right) + GK_T \left(\frac{d\phi}{dz} + \frac{1}{R}\frac{d\eta}{dz}\right) \tag{2.40}$$

The general equilibrium equations for a curved are given (Vlasov, 1961):

$$EI_y \left[\xi^v + \frac{2}{R^2}\xi''' + \frac{1}{R^4}\xi'\right] = \frac{\partial q_x}{\partial z} - \frac{q_z}{R} - \frac{\partial^2 m_y}{\partial z^2} + \frac{m_y}{R^2} \tag{2.41}$$

$$\left[\frac{EI_w}{R^2} + EI_x\right]\eta^{iv} - \left[\frac{GK_T}{R^2}\right]\eta'' + \left[\frac{EI_w}{R}\right]\phi^{iv} - \left[\frac{EI_x + GK_T}{R}\right]\phi'' = q_y + \frac{\partial m_x}{\partial z} \tag{2.42}$$

$$\left[\frac{EI_w}{R}\right]\eta^{iv} - \left[\frac{EI_x + GK_T}{R}\right]\eta'' + [EI_w]\phi^{iv} - [GK_T]\phi'' + \left[\frac{EI_x}{R^2}\right]\phi = m_z \tag{2.43}$$

The above equations have been solved using finite difference technique by Yoo and Heins (1972) and used to study the plastic behaviour of curved homogeneous beams.

Yoo and Kang Equations

More recent formulations have followed the energy approach. The weakness of the equilibrium method is that terms can easily be missed in the derivation. The derivation is rather long and details are left to the paper by Kang and Yoo (1994*a*,*b*).

At the heart of the energy method is the principle of virtual work. Beam equation formulation procedures based on this principle have been proposed by Murray and Rajasekaran (1975). The application of energy principles to curved beams has been varied especially the interpretation of the governing assumptions given below:

(i) Cross-sections retain their original shapes

(ii) The displacements are finite.

(iii) The shear strains due to change of normal stresses, such as bending and warping are negligibly small

(iv) The shear strains along the middle surface of the thin-walled cross section are negligibly small

(v) the radius of curvature is sufficiently large so that the primary bending normal stress distribution remains linear across the cross section

The total potential energy is the sum of strain energy and loss of potential energy due to applied loads:

$$\Pi = U + V \tag{2.44}$$

where U is the strain energy and V is the loss of potential energy.

For elastic body, strain energy is given below:

$$U = \int_V \frac{1}{2} \tau_{ij} \varepsilon_{ij} dV \tag{2.45}$$

where ε_{ij} is the Green strain tensor and τij is the second Piola Kirchoff stress tensor.

The loss of potential energy due to the applied loads is given below:

$$V = \int_s T_i u_i ds \tag{2.46}$$

where T_i are the components of the traction vector on the boundary surface S and u_i are those of the displacement vector. A variation of the energy equation is taken and set to zero:

$$\delta\Pi = \delta U + \delta V = 0 \tag{2.47}$$

The constitutive relations are used:

$$\sigma_z = E\varepsilon_z$$

$$\tau_{xz} = G\gamma xz$$

$$\tau_{yz} = G\gamma yz$$

where σ_z, τ_{xz} and τ_{yz} are normal stress in z direction, shear stress in x and y direction, E is Young's modulus and G is modulus of rigidity.

The variation of energy equation is developed by specialising stresses and displacements associated with thin-walled curved beams. The general strains used in Kang and Yoo (1994*a*) derivation and higher powers of the derivative of the

longitudinal displacement w are neglected because longitudinal displacements are small in comparison to lateral displacements u and v. The details of variational calculus involved in derivation are omitted here and only the stability equations derived are stated. The many energy theory approaches differ in the treatment of curvature terms and interpretation of the vanishing shear at the mid-surface.

2.4.2 Preliminary design

The guidelines on preliminary member sizing are based on experience gained in curved girder construction, analytical and numerical studies as well as the need to prevent instability. It is recommended that flange width be greater than 15% of web depth and that flange thickness be greater than 1.5 times web thickness (Linzell *et al.*, 2004). When classifying sections for straight girders, one is only concerned with the compact and non-compact classes. An additional section class has been proposed by Schilling (1996); Yoo and Davidson (1997) as a result of the presence of flange lateral bending. This class referred as compact flange has a flange meeting the compact flange criterion and a non compact web. It has the advantage of being able to carry higher vertical moments for a given lateral moment.

The presence of a stress gradient across compression flange width results in the two flange halves being differently stressed. Thus unlike in straight girders, one half of the flange will buckle first. To prevent local buckling, it is necessary to put limits on slenderness limits. The critical buckling stress for a plate is given by the well known equation below:

$$\sigma_{cr} = \frac{\pi^2 E k}{12(1-\nu^2)} \left(\frac{t}{b}\right)^2 \tag{2.48}$$

where k is the plate buckling coefficient, t is the plate thickness and b is the plate width. Davidson *et al.* (2000*a*) conducted numerical studies on curved flanges and showed that the stress can be related to that of a straight girder through the use of reduction factors;

$$(\sigma_{cr})_{sv} = (\sigma_{cr})_{st}\psi_{cv} \tag{2.49}$$

where ψ is the strength reduction factor given by

$$\psi_{cv} = 1.05 - \frac{l_{br}^2}{4Rb_f} \tag{2.50}$$

Defining slenderness as:

$$\frac{(\sigma_{cr})_{cv}}{\sigma_y} = \frac{1}{\lambda^2} \tag{2.51}$$

Rearranging terms and letting $\frac{1}{\lambda^2} \leq 1.0$; the slenderness is obtained:

$$\left(\frac{b}{t}\right)_{cv} \leq \left(\frac{b}{t}\right)_{st}\sqrt{\psi} \tag{2.52}$$

where the prefix *st* refers to straight girder and *cv* refers to curved girder . It is worth observing that the equation above will increase the slenderness by a maximum of 2.5% and thus is not that significantly different from straight girder slenderness limit. This negligible modification has been pointed out by Davidson *et al.* (2000*a*). ASCE (1977) gives limits within which the effects of curvature can be ignored, however the resulting nonuniform torsion must be calculated. The compression flange slenderness is given below in AASHTO LRFD (Wollman, 2004):

$$\frac{b_f}{2t_f} = 0.38\sqrt{\frac{E}{F_{yc}}} \tag{2.53}$$

where F_{yc} is the compression flange yield stress.

Japanese researchers have proposed the slenderness for the flange given below (Galambos, 1998):

$$\frac{b}{t} \leq 0.312\sqrt{\frac{E}{F_y}} \tag{2.54}$$

where b is the half flange width, F_y is the flange yield stress and E is modulus of elasticity.

The ASCE (1977) gives the straight girder flange limits to be used for curved flanges. This was based on the fact that for the practical range, the effects of curvature on local buckling are not significant. The 2003 Guide specifications limit the non compact flange slenderness as given below (Linzell *et al.*, 2004):

$$\frac{b_f}{t_f} \leq 1.02\sqrt{\frac{E}{f_b + f_l}} \leq 23 \tag{2.55}$$

where b_f is the flange width (in), t_f is the flange thickness (in), E is the modulus of elasticity (ksi), f_b is the largest factored vertical factored bending stress(ksi) and f_l is the corresponding factored lateral load.

For un stiffened web, the limits are given below: For $R \leq 213$m

$$\frac{h_w}{t_w} \leq 100 \tag{2.56}$$

For $R \geq 213$ m

$$\frac{h_w}{t_w} \leq 100 + 0.125\,(R - 213) \leq 150 \tag{2.57}$$

where h_w and t_w are the web height and thickness.

Different theories have been put forward to explain the behaviour of curved girders. There are no generally accepted set of equations for curved girder behaviour. Curvature and warping affect the behaviour of curved girders though at low curvatures, the effects are negligible. The equation presented by Galambos (1998) is that presented by Nishida given earlier equation 1.9:

$$M_{cr} \approx \sqrt{\left(1 - \frac{L^2}{\pi^2 R^2}\right) \frac{\pi^2 E I_y}{L^2} \left(GJ + \frac{\pi^2 E C_w}{L^2}\right)} \tag{2.58}$$

where I_y, J and C_w are minor axis moment of inertia, St.-Venant torsion constant and warping constant. Equation 2.58 shows that just like in columns with initial curvature, there is a reduction in the buckling load of the curved girder over the straight girder.

For a girder to reach design moment, it must be prevented from instability failure through local or global buckling and issue of bracing in curved girders is critical. Bracing and cross frames are primary load carrying members in curved girders unlike straight girders. Thus it is recommended that an analysis of curved girders be done on the whole structure. While bracing in straight girders is primarily to limit buckling, in curved girders there is the added function of limiting lateral bending moments. With this in view, the brace spacing formulations are given to limit the ratio of lateral to bending moment f_l/f_v. It is recommended that the ratio of bending to warping stresses be less than 0.3. Davidson *et al.* (1996) presented the formulae below that can be used:

$$S_{max} = L\left[-In\left(\frac{Rb_f}{2000L^2}\right)\right]^{-1.52} \tag{2.59}$$

where S_{max} is the maximum cross-frame spacing, L(m) is the span length between vertical supports, R(m) is the radius of curvature, b_f is the flange width. The equation is derived on a warping to bending ratio of 0.25.

Alternatively, a formula is presented where the ratio can be specified and the required spacing calculated:

$$S = \left(\frac{5}{3} F_{ws} R b_f\right)^{1/2} \tag{2.60}$$

where F_{ws} is the warping to bending ratio, all other variables defined as before.

Due to the lateral moment, there are torsional effects and the interaction with the vertical moment is of interest. It has been pointed out in the previous chapter that the circular interaction equation used by Yoo and Davidson (1997) is not accurate. The difficulty lies in the definition of the reference full plastic torque for curved beams and the lack of justification in the continued use of reference plastic moment since not all beams attain it. Pi and Bradford (2001) conducted finite element studies on curved beams and the following interaction equation is suggested:

$$\left(\frac{M_u}{M_{bx}}\right)^2 + \left(\frac{T_u}{T_p}\right)^2 \leq 1 \tag{2.61}$$

where M_u and T_u maximum nominal in-plane bending moment and torque determined by first-order elastic analysis;

γ_x=2.0; γ_s=1.0; for continously curved beams

γ_x=1.5; γ_s=1.0; for centrally braced curved beams

γ_x=1.0; γ_s=1.0; for un braced curved beams

M_{bx} is the nominal member moment capacity of corresponding straight member with same length and boundary conditions.

The torque is given as:

$$T_p = M_{up} + Mwp \tag{2.62}$$

where M_{up} is the full uniform plastic torque given below:

$$M_{up} = \frac{\sigma_y}{\sqrt{3}}\left[bt_f^2\left(1 - \frac{t_f}{3b}\right) + (h - 2t_f)\frac{t_w^2}{2} + \frac{t_w^3}{6}\right] \tag{2.63}$$

M_{wp} is the full plastic warping torque of the corresponding straight beam given as:

$$M_{wp} = \frac{2M_{fp}h}{S} \tag{2.64}$$

and the flange moment M_{fp} is given by:

$$M_{fp} = \frac{1}{4}b^2 t_y \sigma_y \tag{2.65}$$

The above set of interaction equations provide a lower bound for the cases studied Pi and Bradford (2001)

Ultimate strength of curved girders have been studied by different researchers. Experimental and analytical investigations were conducted by Fukumoto and

Nishida (1981); Richard *et al.* (1995); Shanmugan *et al.* (2003). Analytical studies have the drawback stated earlier since there is no system of generally accepted equations. The general feature is the agreement in all the theories that curvature does reduce ultimate moment capacity. From literature, two equations for ultimate load have been put forward. Fukumoto and Nishida (1981) derived equations based on transfer matrix method. The equation derived by Fukumoto and Nishida (1981) is given below and it is relatively simpler than that presented by Richard *et al.* (1995):

$$\lambda^4\delta^4 - \left(\left[\left(1+\frac{p_e(d-t_{cf})}{2M_p}\right)\left(\frac{L^2}{2Rb_{cf}}\right)\lambda^4+1\right]\right)\delta^2 - \left(\frac{L^2}{2Rb_{cf}}\right)\delta+1 = 0 \quad (2.66)$$

where $\lambda = \sqrt{\frac{M_p}{M_c}}$ $\delta = \frac{M_u}{M_p}$ $M_p \simeq F_y b_f t(d-t)$ $P_E = \frac{\pi^2 E I_y}{L^2}$

where P_E is elastic bucking load of a section, M_p is the plastic capacity, M_e is the elastic moment, d is the section depth, t_{cp} is the compression flange thickness, b_{cf} is the width of the compression flange, L is the un-braced length and R the girder radius.

Richard *et al.* (1995) derived an alternative equation that gives the ultimate load for a curved beam. The starting equations are based on the theory by Yang and Kuo (1986) while adopting the solution procedure by Fukumoto and Nishida (1981) for the equation development. More terms are included to improve accuracy over a wider curvature range. However, the results in the present study show otherwise. The quartic equation is given below:

$$\begin{aligned}\delta_u^4\lambda^4 - \left[\left(1+\frac{(d-t)P_E L^2}{4M_p Rb} - \frac{(d-t)EI_Z L^2}{2M_p R^3 b} - \frac{2P_E}{M_p^2R^2} + \frac{P_E EI_y}{M_P^2R^2}\left[\frac{L}{\pi}\right]^2\right)\lambda^4 + 1\right. \\ \left. -\frac{2L^2}{\pi^2R^2}\right]\delta_u^2 - \left[\frac{L^2}{2RB} - \frac{P_E L^2\lambda^4}{bM_P^2R^3} - \frac{L^4}{bR^3\pi^2} + \frac{P_E EI_Y}{2M_P^2R^3}\left[\frac{L^4}{\pi^2 b}\right]\lambda^4\right]\delta_u + 1 - \frac{2L^2}{\pi^2R^2} - \\ \frac{2P_E\lambda^4}{R^2M_P^2} + \frac{P_E EI_Y}{M_P^2R^2}\left[\frac{L}{\pi}\right]^2\lambda^4 = 0\end{aligned} \quad (2.67)$$

The above equations are adapted to study both homogeneous and hybrid girders. Reduction factors are used when applying the equations to predict ultimate loads for curved hybrid girders.

2.5 Finite Element Method

The Finite Element Method is a numerical technique that is used to solve differential equation problems. Many practical problems in solid mechanics, fluid mechanics and heat flow do not have closed form solutions save for the simplest of cases. This has prompted the development of numerical techniques to obtain useful approximate solutions. The Finite Element Method is widely used in solving numerical problems owing to the availability of computers.

The Finite element method follows certain steps:

(i) Discretisation: The body under study is divided into an equivalent system of small elements. The elements should be small enough to produce accurate results and big enough to reduce computational effort. Pre-processing packages are used in mesh generation and the analyst makes a decision on element types and mesh density depending on desired accuracy.

(ii) Displacement function: Displacement functions give the displacement field within the element. These functions are defined by nodal values and can be linear, quadratic or higher order polynomials. The step of assigning displacement function is performed by the computer.

(iii) Constitutive relationship: These are material laws giving stress-strain relationships. The most common one is Hooke's law that covers linear elastic behaviour:

$$\sigma_x = E\varepsilon_x$$

where σ_x is the stress in the x-direction, E is the modulus of elasticity and ε_x is the strain in the x-direction.

(iv) Element stiffness matrix: The energy principle and weighted residual are used to derive element equations. The principle of minimum potential is only applicable to elastic materials while the virtual work principle applies to any material. The differential equations are reduced to a system of algebraic equations that can be easily solved by matrix methods. The resulting element equations can be written as follows;

$$[k]\{d\} = \{f\} \tag{2.68}$$

were {k} is the element stiffness, {d} are the nodal degrees of freedom and {f} are the nodal forces.

(v) Assembly: The equations for each element are added up using superposition to form a system of global equations. Therefore continuity and compatibility conditions are ensured.

$$[\mathbf{K}]\{\mathbf{d}\} = \{\mathbf{F}\} \tag{2.69}$$

where [**K**] is the global stiffness, {**d**} are the degrees of freedom and {**F**} and is the global load vector.

(vi) Solution of equation: The equation is solved for the displacements. Here different techniques such as Gauss elimination and Gauss-Seidel can be used.

(vii) Calculation of stress and strains: These are calculated from the resulting displacements and the constitutive laws.

(viii) Post-processing: Post-processing packages give graphical output to help in quick analysis of results.

Theoretical and experimental studies have been done on hybrid girders and curved girders. The review shows that there are guidelines for design of curved hybrid girders. However, background research to these guidelines appears to be limited. The absence of generally accepted set of equations for curved girders has been a hindrance to the study of inelastic curved girder behaviour. The Finite Element Method is used in the next chapter to investigate the combined hybrid and curvature effects on girder stress distribution and load-deflection capacity. The use of Finite Element Method does not require prior knowledge of the governing differential equations.

Chapter 3

Methodology

3.1 Introduction

This chapter presents the details of the model and computational technique used for the investigation. The hybrid and curvature effects on a girder are investigated using the software package ADINA version 8.4 which has a structures analysis module. A brief introduction of the finite element method is given and the specifics relating to analysis software ADINA and the model are outlined.

Computational modeling using finite element analysis is used for this study. The finite element method has been employed by many researchers such as (Davidson *et al.*, 2000*b*,*a*; Jung and W.White, 2006; Richard *et al.*, 1995) in the study of curved girders. It has been shown in the work by Shanmugan *et al.* (2003) to give results close to experimental test values. Finite element method is essentially a numerical technique used to solve differential equations and other boundary value problems. Such problems arise from mathematical idealisations of physical problems such as the of study plates and shells, heat transfer and fluid flow. Problems of this nature can be complex and analytical solutions are generally available only for the simple cases. The complexity can arise from consideration of material nonlinearity, geometric nonlinearity, complex geometry and boundary conditions.

The increase in the computational power available in most computers has led to the finite element method has becoming common compared to other techniques such as finite difference method. In this study, laboratory investigations are not carried out due to time and cost constraints. Furthermore, analytical closed form solutions from the theories are only available only for the much simpler cases covering behaviour in elastic range and it is for this reason that computational modeling is used for the

investigation.

There are several reasons for the finite element method being widely used and these are:

(i) It is generally easy to model body irregularities.

(ii) Complex boundary conditions and loads can be modelled.

(iii) Different materials in a body can be handled through various constitutive relationships.

(iv) It frees up laboratory space and model alterations can be done without extra costs. This allows for large volumes of results to be obtained from parametric studies and thus allows design optimisation.

(v) It can easily handle geometric and material nonlinearity compared to other numerical techniques such as the finite difference method.

While finite element method has its advantages, specialist knowledge and understanding of the approximations is critical because of the volume of data that is often output. The analyst needs background theory to help in model idealisation before putting the model into finite element program. The analyst has to interpret the results from post-processing packages. There is also need for limited physical model testing in order to verify numerical model results and in determine the constitutive models. Alternatively, the finite element analysis results can be verified using known analytical solutions.

A summary of the computational modeling outline adopted for this investigation is given in the flow chart in Figure 3.1.

3.2 Computational model variables

3.2.1 Girder geometry

The investigation focuses on the effects of curvature and hybrid on girder behaviour. Local buckling effects are outside the scope of investigation and for this reason only one girder cross section is used. The 812×300 (8,16) girder cross-section is adopted and arc lengths of 5m and 8m are used. The curvature parameter (R/L) giving the

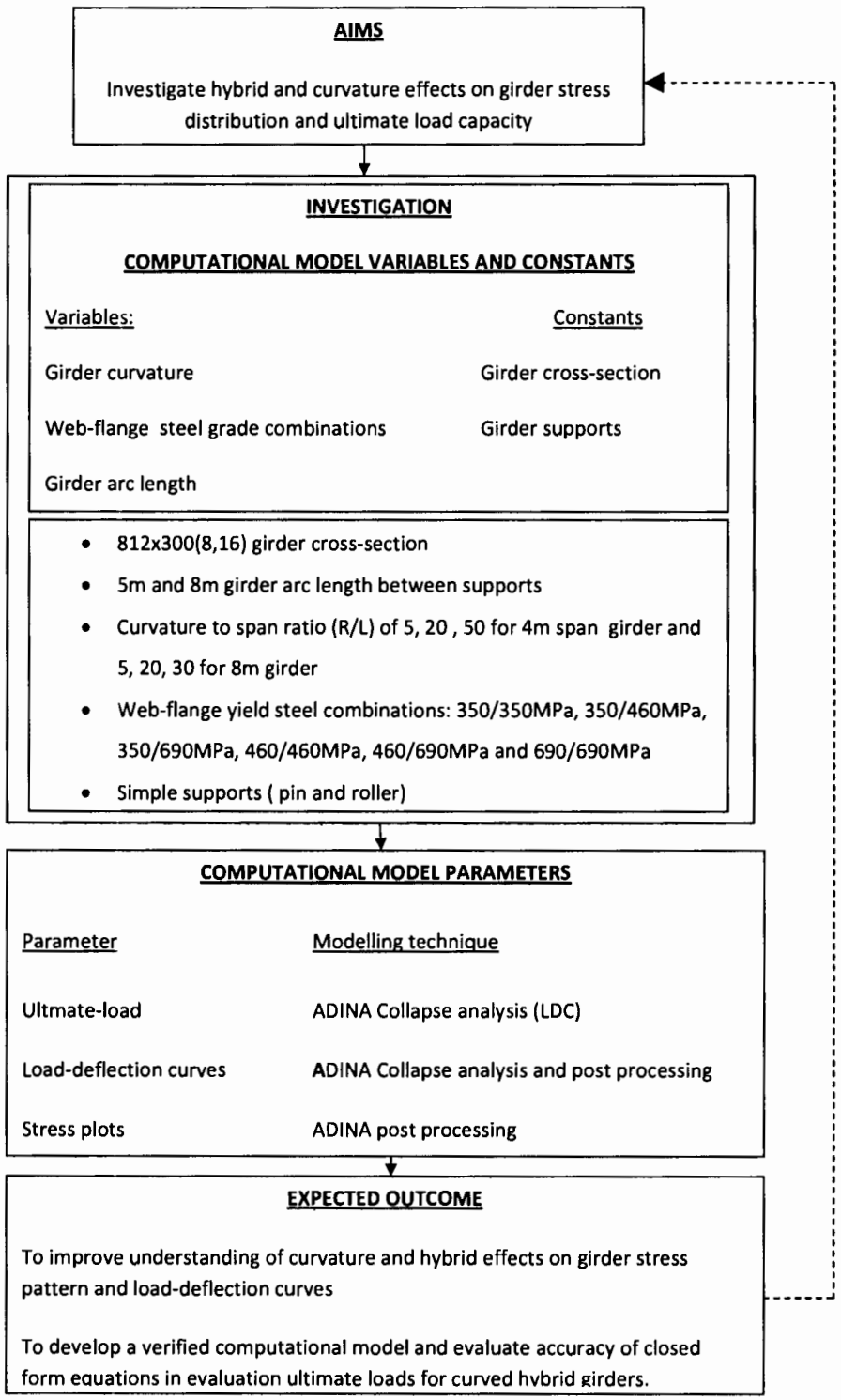

Figure 3.1: Flow chart for computational investigation

ratio of radius to arc length is varied between 5 and 50 is used to help compare girders. For the 5m arc length beams, this gives a radius range from 25m to 250m while the radius range for the 8m beam is between 40m and 240m. A total of 48 models are investigated for effects of curvature and hybrid on girder behaviour. This includes straight girders which are used as reference. A summary of the girder geometries used for the study is given in Table 3.1:

Table 3.1: Girder geometry data

Beam No	h (mm)	b (mm)	t_w (mm)	t_f (mm)	L (mm)	R/L
LU5-ST	812	300	8	16	5000	-
LU5-R25	812	300	8	16	5000	5
LU5-R100	812	300	8	16	5000	20
LU5-R250	812	300	8	16	5000	50
LU8-ST	812	300	8	16	8000	-
LU8-R40	812	300	8	16	8000	5
LU8-R160	812	300	8	16	8000	20
LU8-R240	812	300	8	16	8000	30

Where h is the girder depth, b is the flange width, t_w is the flange thickness, t_w is the web width, $(L/8R)_N$ and $(L/8R)_M$ is the nominal and measured curvature, L is the arc length between supports

3.2.2 Girder support and load input

Boundary conditions are input in the model using the Adina User Interface (AUI). The supports are defined by restricting the degrees of freedom on a given boundary. The boundary can be a point, line, edge or surface. The degrees of freedom which are translational or rotational can be locked globally as master degrees of freedom or locked locally via the application of defined fixities. The current study uses simple supports and these are a hinge on one side and a roller on the other side. The hinge or pin has rotational degrees of freedom free though the twisting degree of freedom about the longitudinal axis is restrained. Translational degrees of freedom are fixed for a pin. The roller is modelled by allowing longitudinal translation free as well as letting the rotation degrees of freedom free.

Loads and displacements can be specified through the AUI. ADINA version 8.4 has load definitions for force, distributed load and pressure loads among others already predefined. The magnitude of these loads is defined using the AUI. In this study, the critical load is not known before hand and thus the automatic algorithm is used

to increment the load until a predefined deflection is reached. More general loading conditions can be written in FORTRAN and inserted in subroutines in ADINA.

3.2.3 Material modeling

Stress-strain measures

Different stress-strain measures are used in ADINA version 8.4 depending on the material model used and the results needed. The common measures are the engineering stress and strain as well as the true stress and strain. Engineering stress is force per unit of original cross-section area:

$$\sigma = \frac{P}{A_0} \tag{3.1}$$

where P is the applied force and A_0 is the original cross-sectional area. Similarly engineering strain is elongation per unit of initial length:

$$\varepsilon = \frac{\Delta l}{l_0} \tag{3.2}$$

where Δl is the change in length and l_0 is the initial length.

When a load is applied to a member, cross sectional dimension can change significantly especially in ductile materials. Thus when large strains are experienced, there are errors in the stress calculation based on engineering stress-strain definition. True stress is defined as the actual stress based on actual area at a given instant:

$$\acute{\sigma} = \frac{P}{A} = \sigma(1 + \varepsilon) \tag{3.3}$$

where A is the instantaneous area.

Similarly, true strain is associated with instantaneous value of gauge length:

$$\delta = ln \frac{l_f}{l_0} = ln\ (1 + \varepsilon) \tag{3.4}$$

where δ is the true strain and l_f is the final length.

Other quantities such as effective stress and effective strain are given as output in the analysis. Effective stress $\bar{\sigma}$ and effective stain $\bar{\varepsilon}$ are defined such that:

(i) $\bar{\sigma}$ and $\bar{\varepsilon}$ reduce to σ_x and ε_x in an x-direction tension test.

(ii) The incremental work per unit volume in deforming a material plastically is $dw = \bar{\sigma}\,\bar{\varepsilon}$

The effective stress determines whether yielding occurs.

ADINA Version 8.4 provides three material models have been widely elastic, elastic-plastic and creep. In this study the material models for steel fall in the classes of elastic and elastic plastic and these models summarised below are used in the current study.

Elastic material model

Elastic deformation is the deformation that is reversed when a load causing it is removed. This can be isotropic or anisotropic. Isotropic refers to a material having same properties in all directions. On the other hand, anisotropic materials have properties that change in different directions. The steel under consideration is considered isotropic. Elastic behaviour can be linear on non linear. In elastic materials the stress is uniquely determined from the strain. The general relationship is given as:

$$^{t}\sigma_{ij} =^{t} C^{t}_{ijrs} e_{rs} \tag{3.5}$$

where $^{t}C_{ijrs}$ is a constant for linear elastic and it is a variable for nonlinear elastic materials. While the concept of elastic behaviour is useful, is is only a starting point in the current analysis; plastic behaviour is of primary interest.

Elastic-plastic material model

This is used to describe material behaviour beyond elastic range. For an elastic plastic model, it is assumed that the strains can be expressed as composed of the elastic and plastic parts:

$$de_{ij} = de^{E}_{ij} + de^{P}_{ij} \tag{3.6}$$

where de^{E}_{ij} and de^{P}_{ij} are the elastic and plastic strains increments respectively. Thus

$$d\sigma_{ij} = C^{E}_{ijrs}\left(de^{E}_{rs} - de^{P}_{rs}\right) \tag{3.7}$$

When using the elastic plastic models, the options include the plastic bilinear and plastic multi-linear models. These are essentially a description of material stress-strain via a combination of linearly varying sections. The bilinear option consists of two linear sections while the multi-linear option has more than two linear sections. In the plastic multi-linear option, a direct data entry is enabled in ADINA version 8.4 through which stress-strain data can be imported from excel spreadsheets. Figure

3.2 shows a sketch of a multi-linear stress-strain model with three linear segments used to model the 350MPa yield steel.

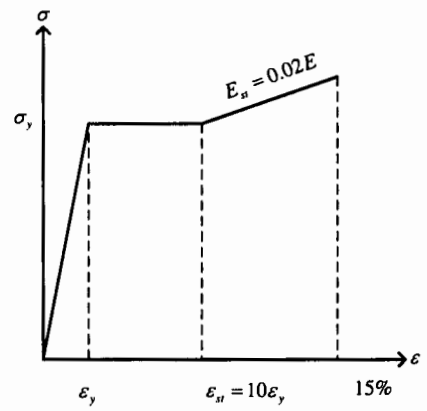

Figure 3.2: 350W Domex steel stress-strain plot

The 350MPa yield steel stress-strain curve is approximated due to lack of data. This approximation is based on the model used by Shanmugan *et al.* (2003). The ADINA multi-linear model does not allow for zero gradient in any given segment. This model of 350MPa yield steel showing a developed yield plateau is typical of mild steel. This yield plateau is necessary because the level of ductility is necessary for plastic hinges to develop in conventional steels. Available steel stress-strain data for 460MPa and 690MPa yield strength steel is used and the plots are given in Figures 3.3 and 3.4. The plots show that the steel in figures 3.3 and 3.4 can develop enough strains greater than 15%. The yield plateau is not fully developed and the ratio of yield strength to ultimate stress is high. These characteristics are common in HPS steels.

In order to calculate plastic strains, other properties have to be specified (Bathe, 1996); namely the yield function, a flow rule and a hardening rule. A yield function gives the yield condition that specifies the state of stress corresponding to the start of plastic flow. The yield condition used is the maximum distortional energy described in the next section. After material yielding, the strains depend on the stress state causing yielding. A flow rule relates the plastic strain increment to the stress increments. A hardening rule specifies how the yield function is modified during plastic flow. Two hardening models are used: isotropic and kinetic hardening. In Isotropic hardening yielding is increased by the same factor along all yielding paths. In kinetic hardening, the yield locus is shifted in the direction of the loading path while the shape and size are kept the same.

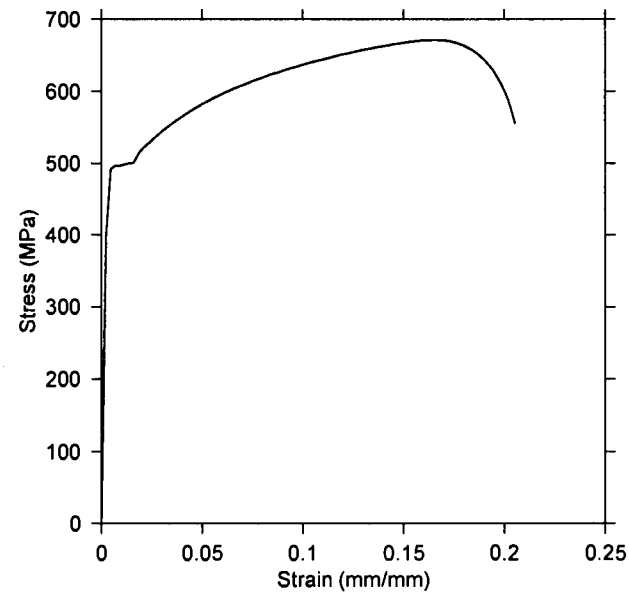

Figure 3.3: 460W Domex steel stress-strain curve

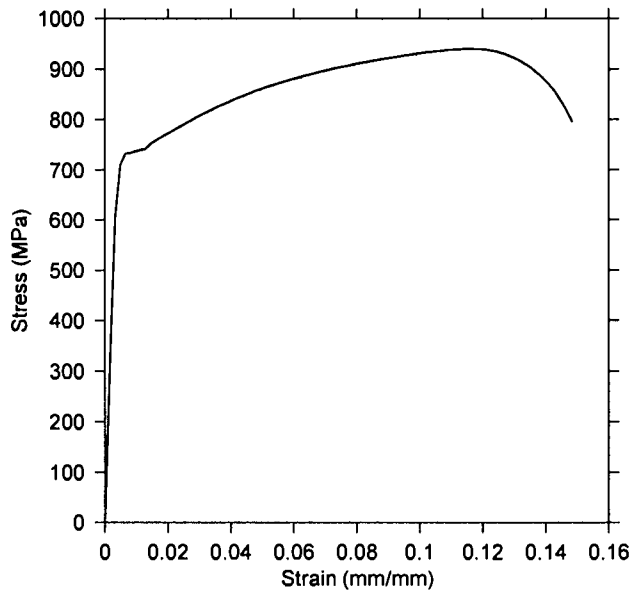

Figure 3.4: 690MC Domex steel stress-strain curve

Residual stresses

Both welded and rolled steel members develop residual stresses because of manufacturing process. The stresses result from the uneven cooling that occurs during the rolling or welding process. A typical stress pattern of residual stress on an I-section used in studies by Shanmugan *et al.* (2003) and Fukumoto and Nishida (1981) is shown in figure 3.5.

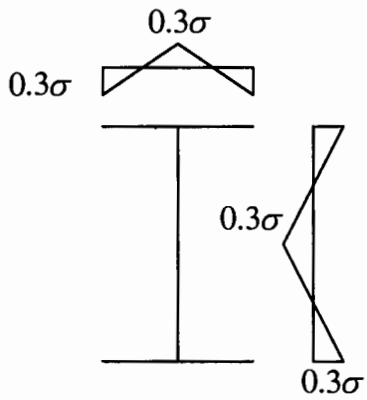

Figure 3.5: Residual stress pattern on I-section

In the case of plate girders, the stresses developed are tensile at junction of the plates because these areas cool at a slower rate. The more exposed areas which have a higher cooling rate experience compression. Trahair and Bradford (1988) have reported that residual stresses can cause premature yielding in fabricated members and also reduce the buckling strength in compressive members.

3.2.4 Material Yielding

A member will respond to applied loads based on the governing constitutive relationship. In general, linear elastic behaviour will occur for small deflections and strains. When unloaded the structure will retain its original dimensions, with all induced strains vanishing. If large deformations are applied beyond the proportional limit a member undergoes large strains part of which remain when it is unloaded. Thus the member will have deformed plastically. If larger strains are applied the member will fracture. Several definitions can be used for structural failure. For many failure theories, failure is related to some measurable quantity in a simple uniaxial stress test using the same material.

Several theories put forward are based on normal stress, shearing stress or strain and strain energy, distortion energy and these are presented in texts such as Boresi

and Chong (1996) and Benham *et al.* (1996). The analysis procedure used in the study uses the Misses yield criterion. A yield criteria is a mathematical expression that gives the stress states necessary for plastic flow Benham *et al.* (1996). Yielding is taken as the transition point where material behaviour changes from elastic to plastic behaviour.

Two theories are generally used to give the yield criteria for ductile materials namely the maximum shear stress criterion and the shear strain energy criterion. The latter is also known as the Misses criterion or Huber-Misses-Henky yield criterion. In the collapse analysis option, ADINA uses the Misses criterion. In formulating the Misses criterion, it is assumed that the total strain energy in a body consists of the energy due to volume change is used to define yield and is given below:

$$U_T = U_V + U_S \tag{3.8}$$

where U_T is the total energy, U_V is the energy due to volume change and U_S is the energy due to shape change.

Similarly, the stresses acting on a body consist of mean stress and deviatoric stress. The mean stress is responsible for the volume change and the deviatoric stress is causes shape change. The energy due to shape change is used to define yield. The energy due to shape change is given below:

$$U_S = \frac{1}{12G}[(\sigma_1 - \sigma_2)^2 + (\sigma_2 - \sigma_3)^2 + (\sigma_3 - \sigma_1)^2] \tag{3.9}$$

where σ_1, σ_2, σ_3 are the principal stresses in a multi-axial stress state.

Yielding occurs when the deviatoric energy equals that in a simple tensile test. In a tensile test, equation 3.9 reduces:

$$U_S = \frac{\sigma_y^2}{6G} \tag{3.10}$$

where $\sigma_2 = \sigma = \sigma_3 = 0$, $\sigma_1 = \sigma_Y$.

From equation 3.9 and 3.10

$$2\sigma_y^2 = [(\sigma_1 - \sigma_2)^2 + (\sigma_2 - \sigma_3)^2 + (\sigma_3 - \sigma_1)^2] \tag{3.11}$$

where $\sigma_1, \sigma_2, \sigma_3$ are the principal tensile or compressive stresses, σ_y is the yield stress.

In most applications one of the stresses is small enough to be neglected. Examples are thin plates where transverse stresses are taken to be negligible or beams where

stress perpendicular to plane of bending are taken to be zero. Thus the equation 3.11 reduces to a plane stress situation:

$$\sigma_y^2 = \sigma_1^2 + \sigma_2^2 - \sigma_1\sigma_2 \tag{3.12}$$

.

The yield locus for Misses criterion is summarised in figure 3.6.

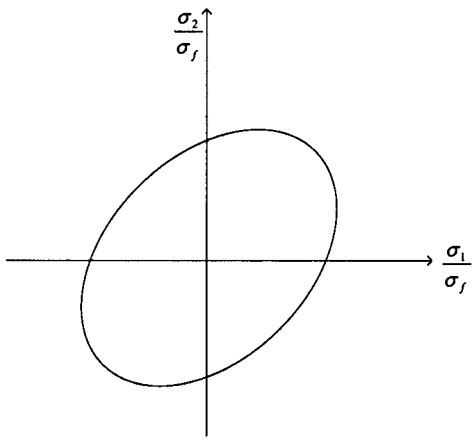

Figure 3.6: Misses yield criterion locus for biaxial stress state

The points along the ellipse represent the transition from elastic to plastic behaviour. The points inside the ellipse represent the elastic stress state while those outside represent plastic stress state. The effective stress already defined is determined for Von Misses criterion:

$$\bar{\sigma} = (1/\sqrt{2})[(\sigma_2 - \sigma_3)^2 + (\sigma_3 - \sigma_1)^2 + (\sigma_1 - \sigma_2)^2]^{1/2} \tag{3.13}$$

3.2.5 Elements

The basis of the finite element method is discretising a body into smaller elements which are then assembled. To facilitate discretisation and accurate modeling, ADINA version 8.4 has a wide range of elements. The choice of the element to use depends on the problem type, geometry, underlying assumptions, level of accuracy desired and the computational effort necessary. A trade off is often made between accuracy and computational effort. Element formulations in ADINA can be used in linear or nonlinear, small and large strain problems.

The present study uses shell elements to discretise the plate girder. Different shell elements with nodes up to 32 can be used. The shell elements can be used with plastic bilinear and plastic multi-linear material models.

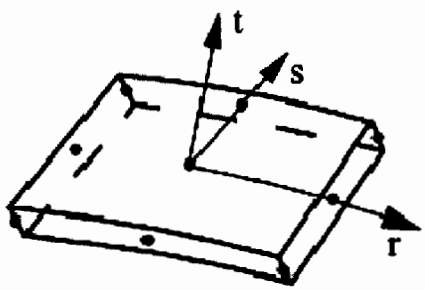

Figure 3.7: Four-node quadrilateral

ADINA element library has a 4 node shell elements referred to as MIT4 and the nine node shell element called MITC 9. The elements are used for thick and thin shell analysis. These elements have good predictive capabilities and are not susceptible to shear locking. The MITC4 is computationally efficient compared to the nine node MITC9 element and is used in this study. Triangular degenerate elements are used as transition elements. The default numerical integration order is used of 2 by 2 for the MITC4 and 3 by 3 for the MITC9 elements is used. Similarly, six degrees of freedom are used because of the presence of stiffening members. In regions of sharp change of curvature and stiffness, this is recommended. Other elements such as the 16 node MITC16 are available for shell analysis, however they come at a higher computational cost. Further, the accuracy provided by the MITC4 is considered adequate.

3.3 Analysis technique

ADINA offers different types of structural analysis and the ones relevant for this study are static and dynamic analysis. In this study only static analysis is considered. Static analysis can be linear or nonlinear. Nonlinearity can arise because of material properties or kinematic assumptions adopted.

In linear static analysis, the equation to be solved is of the form:

$$\mathbf{KU}=\mathbf{R} \tag{3.14}$$

where $\mathbf{K}$ is the stiffness matrix, $\mathbf{U}$ is the displacement vector and $\mathbf{R}$ is the load vector. A direct or iterative method is used to solve the equation. A direct method performs a predetermined number of operations while an iterative method performs

predetermined number of operations while the number of operations is unknown before hand. It is necessary that the stiffness matrix is positive definite and this is ensured through provision of adequate support conditions.

In nonlinear analysis the equation to be solved is:

$$^{t+\Delta t}\mathbf{R} - {}^{t+\Delta t}\mathbf{F} = \mathbf{0} \tag{3.15}$$

where $^{t+\Delta t}\mathbf{R}$ is the external load vector applied at time $t + \Delta t$ and $^{t+\Delta t}\mathbf{F}$ is the nodal point force vector.

Different solution schemes exist for equation 3.15 and are explained in relevant literature such as Bathe (1996). However, two solution schemes deserve mention with regard to ADINA; the Automatic Time Stepping (ATS) and Load Displacement Control (LDC) method.

In the ATS method, the time step is controlled to obtain convergence. The time step is automatically divided by a specified factor to obtain convergence. The solution terminates after many time subdivisions without convergence. The ATS can be used with different analysis techniques with few exceptions.

The LDC is used to study collapse and post collapse behaviour. It can be used to solve nonlinear equilibrium path of a model until collapse. In the current study, the load-deflection behaviour of the girders is investigated until a critical load is obtained.

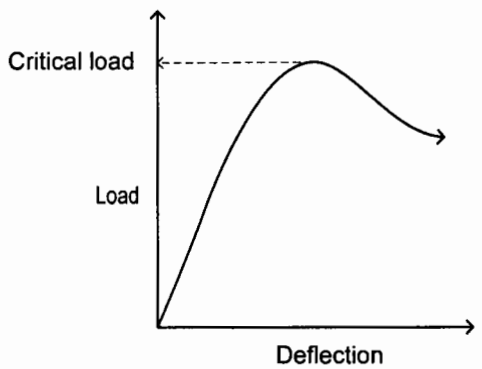

Figure 3.8: Load deflection sketch showing critical load

This critical load which is the peak load is reached when the girder steel yields or when the girder buckles. The post critical load behaviour is also obtained but is not of much interest in this regard. In collapse and buckling analysis, the failure load is not known beforehand. An automatic algorithm (LDC) is used to increase

or decrease the load as required to obtain structural response. The presence of geometric and material nonlinearities can significantly affect the response and thus these effects have to be modeled.

Geometric imperfections arise in structures due to the limitations imposed by fabrication techniques, while material nonlinearity is of concern if the material reserve strength beyond the elastic limits is to be used. This entails the development of significant strains and deflections as is the case of girders under study. Geometric imperfections are effected in ADINA by scaling down the different buckled shapes. Thus a buckling analysis precedes a collapse analysis. Linearised buckling can be used to estimate collapse loads but its accuracy decreases when member behaviour does not approximate a column. In this study, the compression flange has an initial curvature and thus the effects of scaling down buckling modes as imperfections is rather small. However, this procedure is followed for girders with less curvature.

3.4 Post processing

The ADINA version 8.4 post processing capability is used to access and present analysis results. Most of the post processing options produce visuals that can be readily interpreted. The options used in the current study include plotting stress variations and also obtaining load-deflection plots. Stress plots are used to present stress results and also the check the mesh density adequacy in specific regions. An error plot for stresses can also be used to check mesh plot quality. Load-deflection plots can be obtained easily using the ADINA User Interface, however, the data in the study is exported to other software packages for plots.

Chapter 4

Numerical model investigation and results

4.1 Introduction

This chapter presents the results of the finite element analysis, the verification study and the study of different curved hybrid girder configurations. The finite element model is used to study both curvature and hybrid effects on girder ultimate load capacity. Two sets of available experimental data are used for the verification exercise. The experimental and theoretical studies used include the curved laterally unsupported beams studies by Fukumoto and Nishida (1981) and the braced girders studies by Shanmugan *et al.* (2003). Following the model verification, studies are undertaken on simply supported girders with a point load at the centre. The girders are loaded incrementally up to failure.

The literature review shows that research on hybrid girders has been done by Frost and Schilling (1964). However, the study was limited to straight girders. The girders are analysed in this study using ADINA version 8.4 software. The ADINA post processing capabilities are used to provide visuals and load deflection data of respective girders. The data is exported to gri and load-deflection plots are then produced.

Theoretical investigations have been done by Fukumoto and Nishida (1981) and Shanmugan *et al.* (2003, 1995) on curved homogeneous girders and approximate equations have been presented to predict ultimate load behaviour. The approximate ultimate equations are used in the second part of the study to determine the ultimate loads. These are then compared to those obtained from the finite element analysis.

The AASHTO (2007) recommendations regarding hybrid girder load capacity involve using an equivalent homogeneous girder and applying a factor to its load resistance capacity to account for the hybrid effects. The equations given by Fukumoto and Nishida (1981) and Richard *et al.* (1995) are modified using the hybrid factor to give loads for hybrid girders. This is compared with the finite element result.

The adequacy of the model is judged from the ability to predict curved homogeneous girders whose experimental data is available. The non availability of curved hybrid girder experimental data is not considered a major drawback as the design philosophy is based on homogeneous girder behaviour. The ADINA analysis provides both the visuals and the load deflection data which is used to plot graphs and presented in relevant sections.

4.2 Model definition and verification

Fukumoto and Nishida (1981) conducted experiments on two sets of beams to determine their ultimate load. These were denoted as AR and BR to refer to 1700mm and 2800mm span beams respectively and their dimensions are given in Table 4.1.

Table 4.1: Dimensions and curvatures of curved beam

Beam No	h (mm)	b (mm)	t_w (mm)	t_f (mm)	$(L/8R)_N$	$(L/8R)_M$	L (m)
AR-1	251.6	101.6	5.6	8.4	1/100	1/109	1700
AR-2	251.9	101.0	5.7	8.3	1/200	1/238	1700
AR-3	251.9	101.9	5.8	8.3	1/1000	1/798	1700
BR-1	250.1	101.6	5.5	8.4	1/100	1/97	2800
BR-2	251.8	100.6	5.7	8.3	1/200	1/206	2800
BR-3	250.4	100.9	5.6	8.3	1/1000	1/1379	2800

Where h is the girder depth, b is the flange width, t_w is the flange thickness, t_w is the web width, $(L/8R)_N$ and $(L/8R)_M$ is the nominal and measured curvature, L is the arc length between supports.

The curvature term L/(8R) was used to compare ultimate load behaviour for beams with the same span; where R is the radius and L the un braced arc length. Fukumoto and Nishida (1981) considered six beams all simply supported with no lateral supports. The curvature parameter (L/8R) had values from 1/109 and 1/1379. This gives the radius range from 23m to 482m. While the spans for AR

and BR beams were different, the nominal values for the curvature term (L/8R) were the same for both sets of beams. The measured values for the curvature were significantly different especially for beam BR-3. The web slenderness of curved beams or girders depends on the radius as was given by equations 2.56 and 2.57. Based on measured L/(8R), five beams have radius less than 213m and only one has radius 482m. This falls within the maximum radius of 610m imposed by the equation for web slenderness. The relevant equation 2.56 is used:

For $R \leq 213\text{m}$

$$\frac{D}{t_w} \leq 100$$

For $R \geq 213\text{ m}$

$$\frac{D}{t_w} \leq 100 + 0.125\,(R - 213) \leq 150$$

The analysed beams have slenderness much less than 100 and this includes the beam with a radius of 483m. Thus all the beams fall within the limits. The beams are also checked for flange slenderness. It has been pointed out that the modification by Davidson *et al.* (2000*a*) results in a maximum increase of 2% over the straight girder limits. The flanges are thus checked according to equation 2.53:

$$\frac{b_f}{2t_f} \leq 0.38\sqrt{\frac{E}{F_{yc}}}$$

Given $F_{yc} = 314MPa$, and E = 210GPa:

$$\frac{b_f}{2t_f} \leq 9.7$$

For the beams studied by Fukumoto and Nishida (1981), the flange slenderness was within this limit.

Recent studies by Shanmugan *et al.* (2003, 1995) do provide insight into curved homogeneous girder behaviour. The results by Shanmugan *et al.* (2003) are used in this study to further check the adequacy of the model developed. Two groups of beams were tested denoted as CB beams for hot rolled sections cold bent to the required curvature and WB for beams fabricated from flat plates. In total, 10 beams were tested and the curvature ratio R/L was varied from 4.7 to 150. The spans were varied in which eight beams had span of 3.8m, one beam had 4.0m and one had 2.3m span. The significant aspect for these tests was the bracing provided to the beams. The lateral bracing was provided at the point of load application and this

was not at the mid span resulting in two unequal spans of laterally unsupported sections. The support conditions were such that both girder ends fixed (FF) and one end fixed with the other simply supported (SF). The focus of the study was on laterally supported beams and no attempt was made to compute the spacing as given by equation 2.59 and 2.60. For the verification exercise, only three beams were selected with curvature terms covering the lower end so as to have maximum curvature effects and this was only due to time constraints. The geometric properties of the selected beams are summarised in Table 4.2:

Table 4.2: Dimensions and curvatures of laterally supported curved beams

Beam No	b (mm)	h (mm)	t_f (mm)	t_w) (mm)	L (m)	L_1 (m)	R (m)	R/L
CB1	124.3	306.6	12.1	8.0	5.0	3.8	20	4.0
CB2	124.3	306.6	12.1	8.0	5.0	3.8	30	30.0
CB5	124.3	306.6	12.1	8.0	5.0	3.8	30	30.0
CB7	124.3	306.6	12.1	8.0	3.0	2.3	4.7	1.6

Where R is the radius and L_1 is the arc length from one girder support to the brace point

The beams investigated by Fukumoto and Nishida (1981) are modeled first. The boundary conditions are such that twisting at the supports is not permitted but warping is allowed. The models are loaded at mid span till failure. While not clearly stated in the reference Fukumoto and Nishida (1981), transverse and bearing stiffeners are provided at mid span and the beam supports. The models are loaded until collapse which in this case is noted from the significant loss of stiffness. The model definition and verification studies were undertaken first and then the parametric study follows. The rotation was used by Fukumoto and Nishida (1981) as a load effect parameter and this will be undertaken for ease of comparison. Other load effect parameters such as vertical deflection or lateral deflection have been used by Shanmugan *et al.* (2003) to give load deflection behaviour and these will be adopted later.

The beam is loaded at midspan and the load incremented using the collapse analysis option until failure is observed through the significant loss of stiffness. The load is defined as a unit point load acting at the beam mid-span defined using the AUI. The collapse analysis is used to give pre and post critical load behaviour. The behaviour before and after collapse is obtained from the plots of the rotation and translation

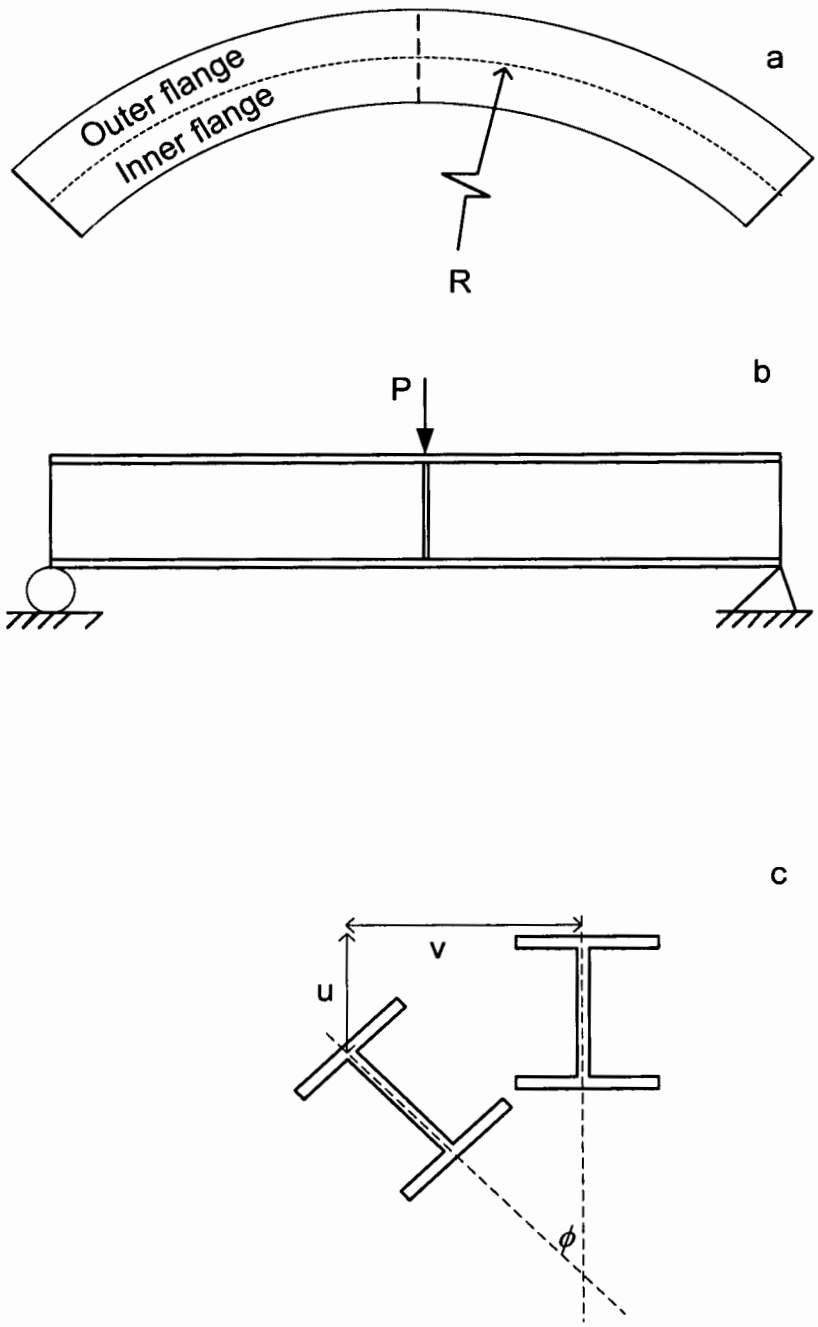

Figure 4.1: Curved beams

of the mid span geometric line and point respectively using ADINA post processing capabilities.

The multi linear material model used by Shanmugan *et al.* (2003) is adopted for this exercise and is shown in Figure 4.2. The material model includes a yield plateau and

a strain hardening zone and fracture occurs at 15% elongation. Due to restrictions placed on gradient values in ADINA and the yield plateau is not entirely horizontal. Isotropic hardening is chosen though model unloading is not of interest in this study. However, this is chosen because of the anticipated large deformations. Material yielding is based on the Misses yield criterion for this kind of analysis. The yield stress and poison ratio for the steel used are given as 314MPa and 0.3 respectively. Bearing stiffeners are placed at load point and at supports. The model description for the experiments by Fukumoto and Nishida (1981) did not provide much detail however, stiffener thickness is chosen equal to flange thickness.

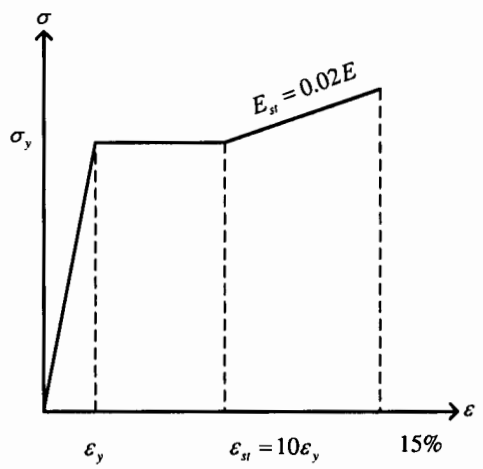

Figure 4.2: Material model for AR and BR curved beams

Residual stresses are approximated as varying linearly from flange centre to the tip. These are modeled as initial strains in ADINA and spatial functions are used for the variation. The stress variation for a typical I-girder has tension at the plate junctions and compression at flange tips.

The beams investigated by Shanmugan *et al.* (2003) are also modeled following the procedure above. The bracing is modeled by fixing the radial movement at the load application section. No attempt is made to model bracing flexibilities and this assumption is adopted from Shanmugan *et al.* (2003). It has been pointed out that in curved beams, cross frames are primary load carrying members thus their stiffness is not only determined by the need to mitigate buckling.

There is a reduction in load resistance capacity as the span is increased from 4m to 8m. When a comparison is made between LU5 and LU8 at a given radius to arc length ratio, there is more than 50% reduction in ultimate load capacity respectively.

The increased span increases the applied moment for a given load and this is the case in both curved and straight girders. The lateral moment is also dependant on both the arc length and curvature. In general, there is a reduction in ultimate load for the LU8 girders as the R/L ratio is reduced.

4.2.1 Mesh convergence

A mesh convergence study is undertaken to assess the optimum mesh for the models. A typical beam is modeled to assess the adequacy of the discretisation. In this particular study, BR-3 is chosen. Studies by Shanmugan *et al.* (2003) used four node quadrilateral elements in ABAQUS and symmetry was used. However, it was pointed out that such elements can be used where stresses are not critical. For this exercise the models are created in ADINA and the four node MITC4 shell element is used to mesh the model. The MITC4 element is used for its computational efficiency and also because it is recommended for thick and thin shells. The default six degrees of freedom are used, three for translation and three for rotations. The six degrees are recommended due to the presence of bearing stiffeners. Two element groups are utilised; one for the flanges and the and the other for the web. While it is not apparent at this stage, this is to facilitate the material differences later imposed in the parametric study. Mesh convergence studies are carried out on beam BR-2. In general, finer meshes produce more accurate results though this comes at the expense of computation time required. Four different meshes are used to study the convergence rate and the results are summarised in the Figure 4.3.

The results summarised in Figure 4.3 show that the ultimate load converges very rapidly even when course meshes are used. There is a small difference in the ultimate load as the mesh is refined. When the number of elements are progressively increased from 2136 to 52780, there is only a reduction of 1.3% in ultimate load. This is rather small considering the 20 fold mesh density increase. However, other parameters such as rotation change significantly, as seen in Figure 4.3. Coarse mesh gives poor rotation and also the post critical behaviour unloads rapidly as compared to finer meshes. Convergence of rotation is rather slow resulting in an increase in rotation of 290% when the model is refined from elements 2136 to 52780. Rotation studies are critical in assessing the ductility of a girder configuration. However, the primary aim of the study is to assess the load resistance capacity. An optimum mesh with maximum length 0.007 is chosen as a trade off between accuracy and efficiency and used for the verification of the other beams.

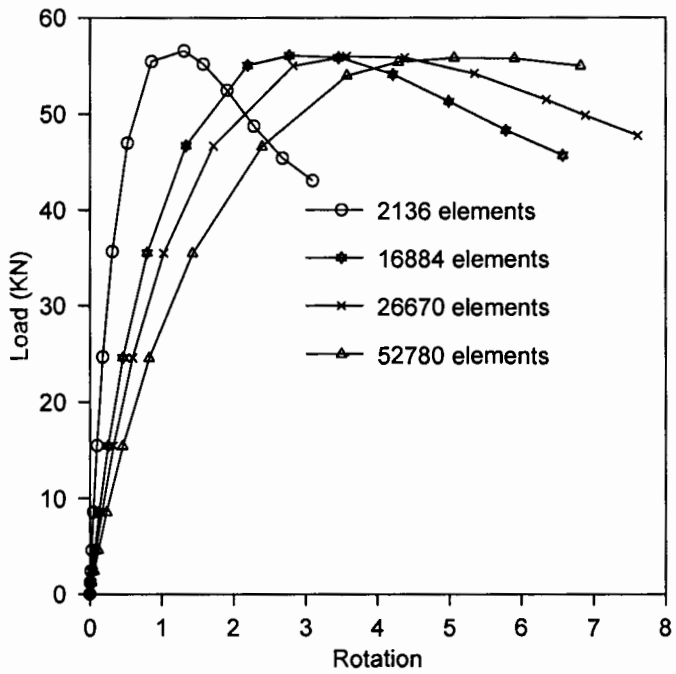

Figure 4.3: Load-deflection curves for different mesh densities

4.2.2 Model verification

The AR and BR beams studied by Fukumoto and Nishida (1981) and already presented in Tables 4.1 are modeled using ADINA for the verification study. The beam spans of 1700m for AR and 2800m for BR beams were utilised. The output from the ADINA post processing is presented below in graphs of load-deection curves. For comparison of the curvature effects when the span is constant, the AR beams are presented in Figure 4.4 and the BR plots are given in Figure 4.4 .

It is observed that the ultimate strength decreases with AR-3 having the highest value and AR-1 having the lowest. This trend is repeated by beam BR-3 having the highest ultimate load and BR-1 with the lowest load. There is a progressive decrease in ultimate strength as R/L decreases with AR-3 having the highest load among the AR beams and BR-3 having the highest load among the BR beams. This curvature-ultimate load pattern is shown in the experimental and theoretical work of Fukumoto and Nishida (1981). A more detailed comparison of ultimate strength prediction with experimental data is presented in the Table 4.3.

Table 4.3 shows the computational model is able to accurately predict the ultimate load for the curved beam. The prediction for the AR beams is within 3% while it

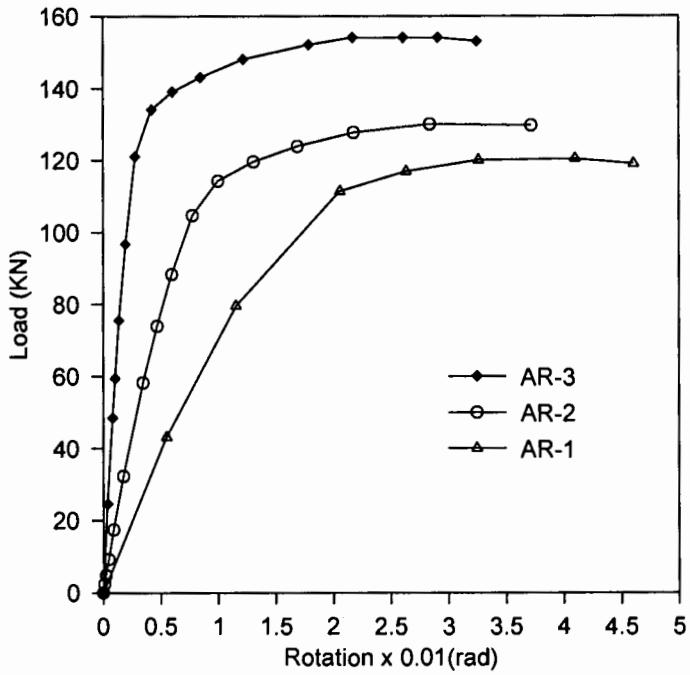

Figure 4.4: Load-deflection curves for AR curved beams

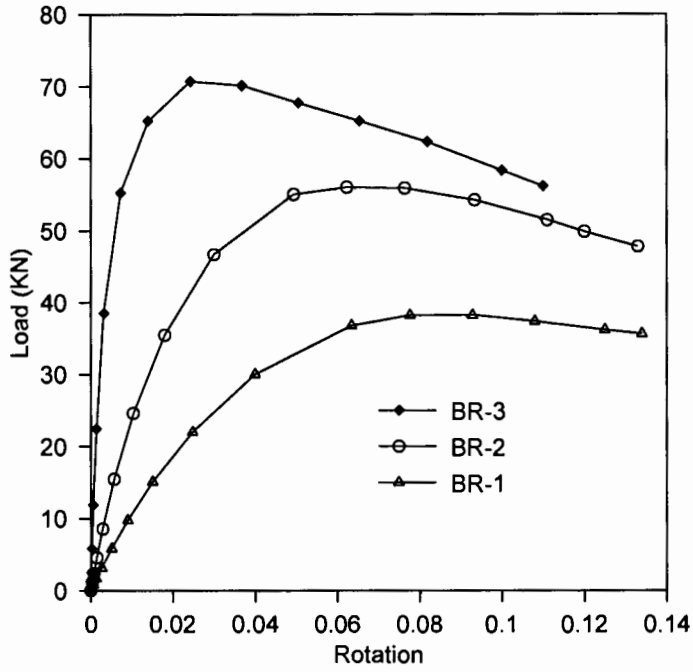

Figure 4.5: Load-deflection curves for BR curved beams

is considerably less accurate for BR beams with maximum of 17% error for BR-1. The study by Shanmugan *et al.* (2003) using ABAQUS generally overestimated

Table 4.3: Comparison of Experimental and FEM results-laterally unsupported

Beam No	L/(8R)	PE (kN)	P(FEM) (kN)	P(E)/P(FEM)
AR-1	1/109	120.1	120	1.00
AR-2	1/238	125.7	130	0.97
AR-3	1/798	149.0	154	0.97
BR-1	1/97	44.6	38	1.17
BR-2	1/206	55.2	56	0.99
BR-3	1/1379	63.9	70.7	0.90

Where PE and P(FEM) are ultimate loads from experiments and Finite Element Model respectively.

the ultimate load by a maximum of 8%. It is observed from Table 4.3 the models this study give values greater than the experimental results. The error is generally under 10% in five of the beams, the exception being BR-1 were the ultimate strength was greatly underestimated. Different idealisation in material modeling in performing a numerical study and these include residual stress pattern and geometric imperfections and this could in part account for the error.

Four laterally supported beams investigated by Shanmugan *et al.* (2003) and given in Table 4.2 are modeled. These beams are chosen to represent the wide curvature range covered in the study. The lateral supports are such that the beam is divided into two segments of 3.8m and 1.2m. The beams are loaded to failure and the results are plotted for comparison in Figure 4.6.

There is a decrease in ultimate strength with a decrease in R/L ratio. The failure pattern shows increased lateral instability in the longer unsupported section. The shorter span does not have large lateral displacement and thus provides some restraint for the longer section of the beam. The ultimate load values are summarised in Table 4.3. The finite element model underestimates the ultimate loads by up to a maximum of 23% compared to the experimental data.

Table 4.4: Comparison of Experimental and FEM results for CB beams

Beam No	R/L	P(E) (kN)	P(FEM) (kN)	P(E)/P(FEM)
CB1	4.0	191.5	155.6	1.23
CB2	6.0	204.5	172.1	1.19
CB5	150	241.5	233.6	1.03
CB7	1.6	196.6	226.0	0.87

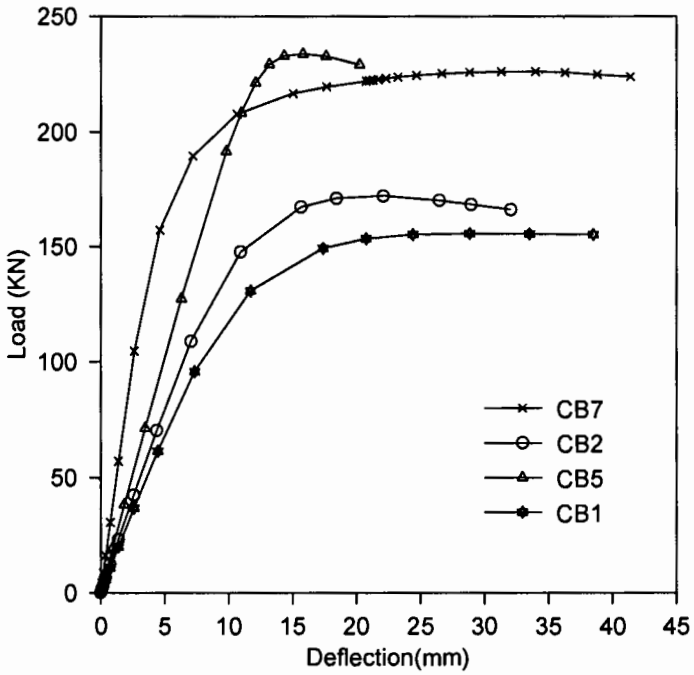

Figure 4.6: Load-deflection curves for CB curved beams

The sources of the error are most likely the assumed constitutive relationship and the simplifications in modeling the supports. Considering the range of beams modeled; six laterally unsupported, four laterally supported and the range of curvature term (R/L) from 1.6 to 150, the computational model developed is considered accurate and robust enough to be used for the subsequent studies.

4.3 Model studies

The primary parameters that are investigated in this study are curvature and hybrid effects. Two sets of girders are investigated with 5m and 8m arc length between supports. The curvature ratio (R/L) is used to help compare similar beams. The curvature ratio is varied from 25 to 250. The steel grades used in the study have yield strengths of 350MPa, 480MPa and 690MPa and the model geometries have are given in the Table 4.5.

Some notation is adopted due to the number of girder analysed. The designation LU shows that the girders are laterally unsupported. The two arc lengths of 5m and 8m are just designated as 5 and 8 respectively. The radius is denoted as R25 to mean 25m radius. The steel combinations are denoted by lowercase letters a, b and

Table 4.5: Curved girder geometry data

Beam No	h (mm)	b (mm)	t_w (mm)	t_f (mm)	L (mm)	R/L
LU5-ST	812	300	8	16	5000	-
LU5-R25	812	300	8	16	5000	5
LU5-R100	812	300	8	16	5000	20
LU5-R250	812	300	8	16	5000	50
LU8-ST	812	300	8	16	8000	-
LU8-R40	812	300	8	16	8000	5
LU8-R160	812	300	8	16	8000	20
LU8-R240	812	300	8	16	8000	30

Where h is the girder depth, b is the flange width, t_w is the flange thickness, t_w is the web width, R/L is the ratio of radius R and arc length between supports.

c for 350 MPa, 480 MPa and 690 MPa respectively. Thus aa denotes a homogeneous girder made of 350MPa steel and ab denotes a hybrid girder with first letter denoting the web steel grade of 350MPa and second letter for flange steel grade of 480MPa. A girder LU5-R25ac is laterally unsupported with a span of 5m, radius 25m, hybrid with 350MPa grade in web and 690MPa in flange. Straight girders are also modelled as a reference. In the notation above, the R letter together with the numerical value of the curvature are simply replaced by ST to denote a straight girder. Thus LU5-STaa is a 5m laterally unsupported straight homogeneous girder with 350MPa yield steel. In total of 48 girders consisting of 36 curved girder variations and 12 straight girder variations are analysed.

4.3.1 Curvature effects

The effects of curvature are investigated first. Simply supported beams are investigated and these are not provided with lateral supports. The hybrid effects are not investigated at this stage and only homogeneous girders with steel yield strength of 350MPa, 460MPa and 690MPa are modeled for each curvature. The automatic algorithm of ADINA version 8.4 collapse analysis is used to obtain the pre and post collapse behaviour. The load-deflection data obtained from the analysis is presented Figures 4.7 and 4.9 for girder LU5-R25.

The plots show that there is an increase in ultimate load when the steel grade is increased. In general, a load-deflection curve for a homogeneous girder has two

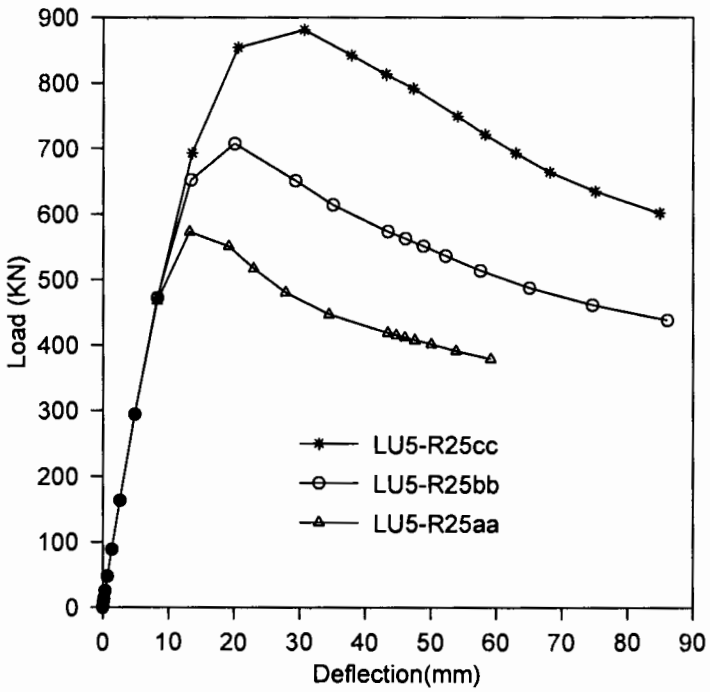

Figure 4.7: Load-deflection curves for LU5-R25 homogeneous girders

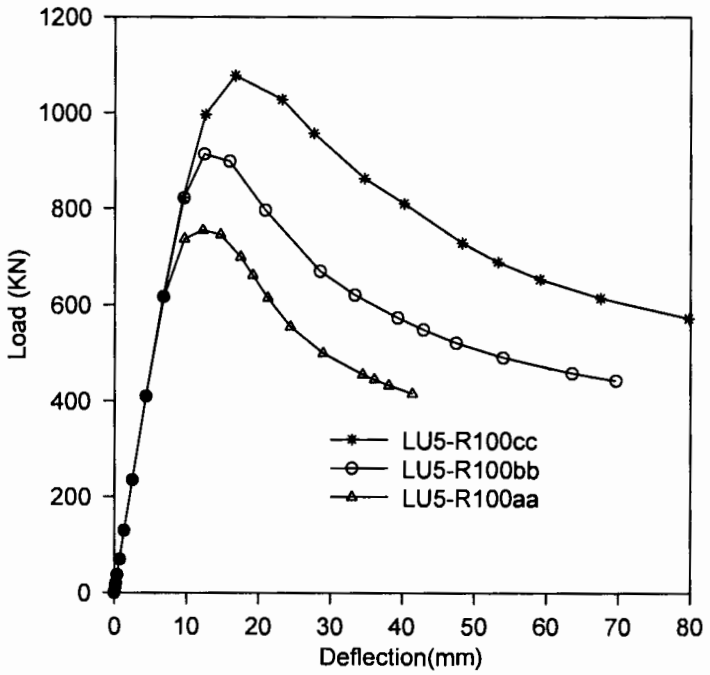

Figure 4.8: Load-deflection curves for LU5-R100 homogeneous girders

parts depending on the magnitude of the load. In the first part of the load-deflection

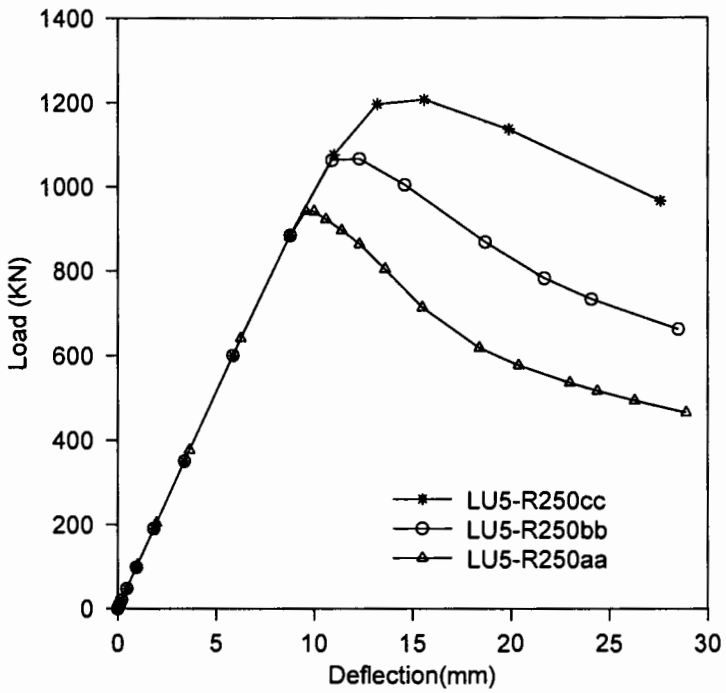

Figure 4.9: Load-deflection curves for LU5-R250 homogeneous girders

curves, the girders are elastic. At a given curvature, there is no difference between the girders made of different steel grades because the elastic modulus is the same for all steel grades. The second part of the curve depict the behaviour when the extreme flange fibres of the flange begin to yield. At this stage, there is a reduction of the tangent modulus in the yielded portion. This reduction of tangent modulus leads to an overall reduction in girder stiffness. The girders with lower yield strength steel reach their yield stress earlier and thus have lower ultimate loads. The load-deflection plots therefore show higher ultimate loads for girders with high yield strength steel. The general unloading pattern of the curves is similar for all the girders.

There is a reduction in load resistance capacity as the span is increased from 5m to 8m. A comparison between LU5 and LU8 at a given curvature to span ratio shows more than 50% reduction in ultimate load. The increased span increases the applied moment for a given load. The lateral moment is also dependant on both the arc length and curvature. In general, there is a reduction in ultimate load for the LU8 girders as the R/L ratio is reduced. This patten is observed in Figure 4.14.

The general nature of the graphs for different steel combinations is similar as seen

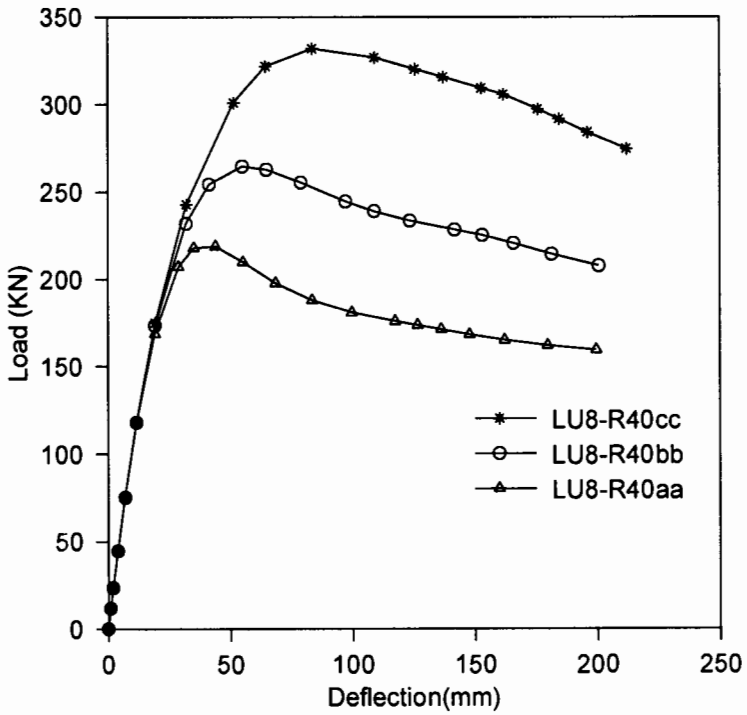

Figure 4.10: Load-deflection curves for LU8-R40 Homogeneous girders

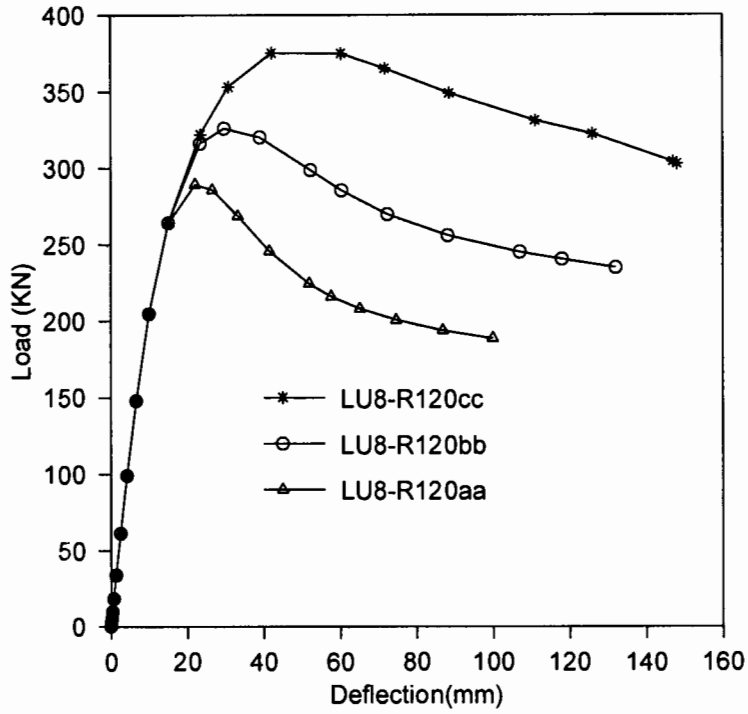

Figure 4.11: Load-deflection curves for LU8-R120 Homogeneous girders

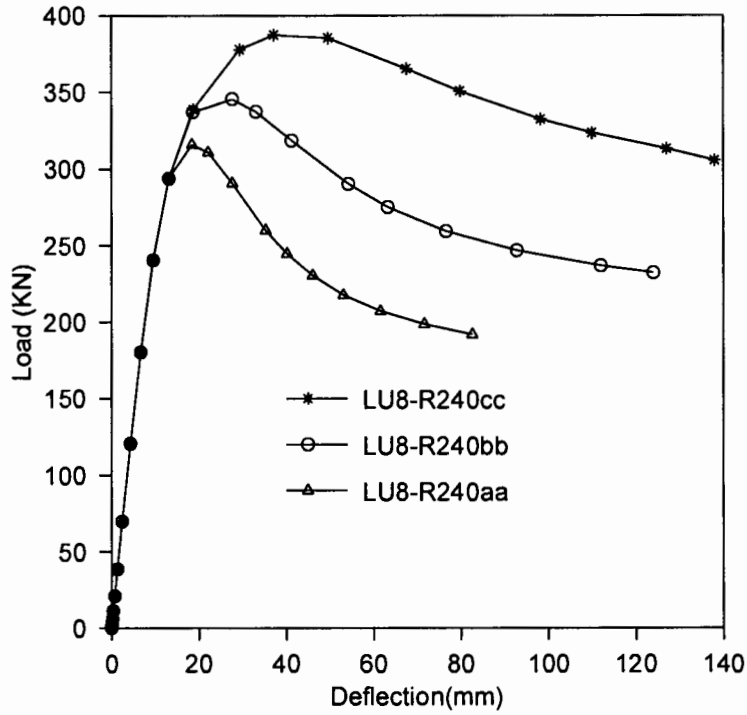

Figure 4.12: Load-deflection curves for LU8-R240 Homogeneous girders

observed in Figures 4.10 to 4.12, thus a comparison of curvature effects is shown only for LU5-R25cc, LU5-R100cc and LU5-R250cc as one set and LU8-40cc, LU8-120cc and LU8-240cc as the other set. Curvature has an effect on load pattern; less curved girders seem to have a larger linear segment of the curve while the linear segment is less for severely curved girders. A comparison of load-deflection made across curvature for each span length shows differences and these are given in Figure 4.13 and 4.14.

To explain the differences in ultimate load, the load carrying mechanism is explained. Curvature results in the presence of lateral moments. The concept of a reduced section introduced by Schilling (1996) imply that part of the flange cross-section is used to support lateral moments. However, the lateral moments increase with curvature and hence the flange area required to support these moments increases. This reduces the available section for vertical moments thus decreasing load resistance capacity. Curvature also has the effects of reducing the elastic critical moment M_{cr} of a girder as seen in equation 1.9. A more curved beam will have a higher modified slenderness already defined as $\lambda = \sqrt{M_p/M_{cr}}$, where M_P is the plastic moment capacity. The failure pattern of a girder involves

an interaction of material yielding and lateral instability. Richard *et al.* (1995) has shown that material yielding is more dominant for low values of slenderness. In

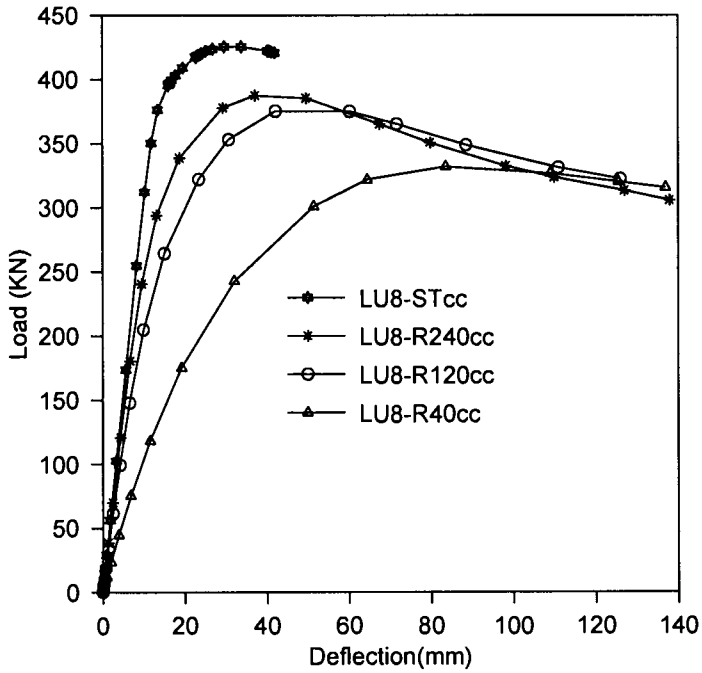

Figure 4.13: Comparison of load-deflection curves for LU8 at various curvatures

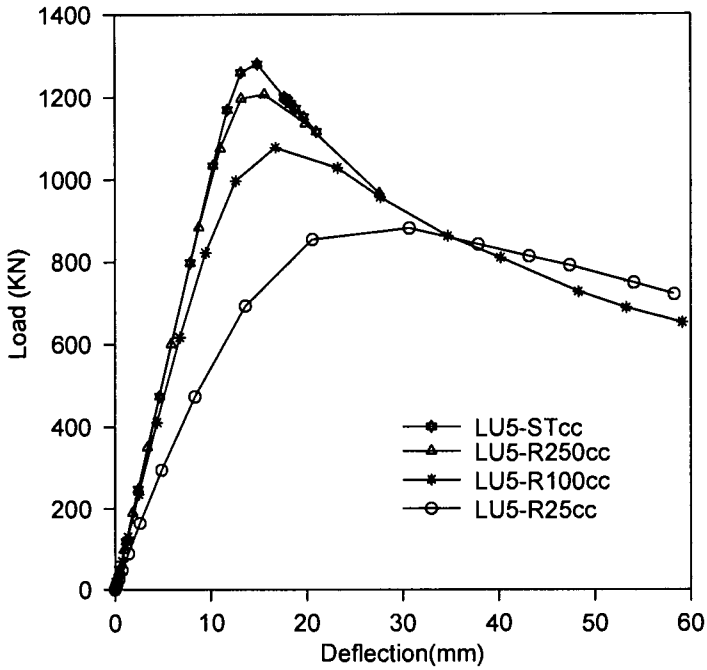

Figure 4.14: Comparison of load-deflection curves for LU5 at various curvatures

girders with greater curvature (R/L), material yielding and lateral instability progress simultaneously. Collapse in this sense is taken as the maximum load reached.

The plots in Figures 4.15, 4.16 and 4.17 show the girder LU5-R25aa. At the mid

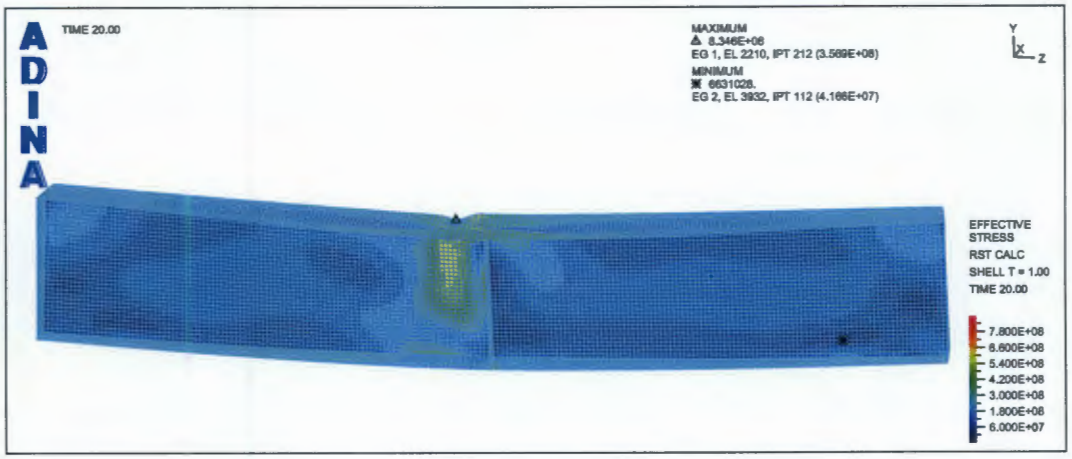

Figure 4.15: Stress plot for LU5-R25aa girder

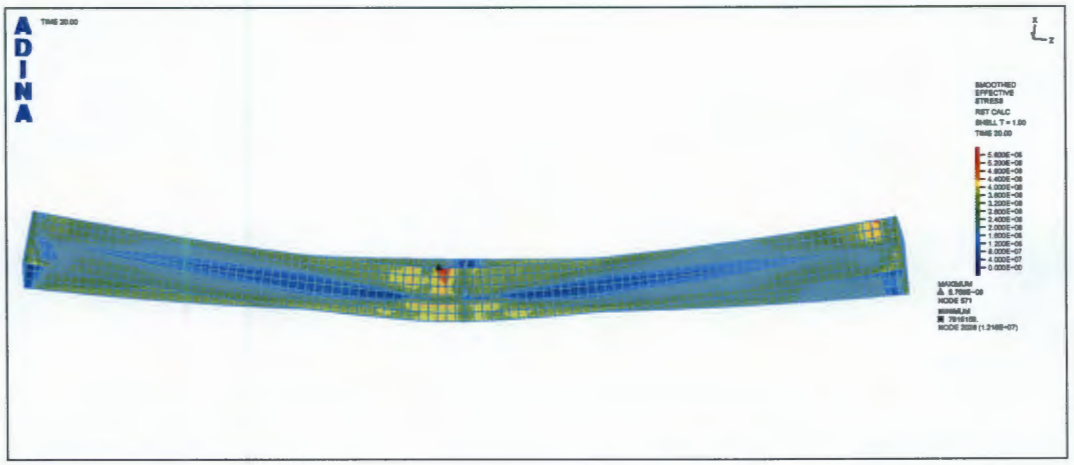

Figure 4.16: LU5-R25aa girder flange lateral movement

span the steel has yielded as seen from the Misses stress exceeding 350MPa. The tension flange does not appear have the same level of stress as the compression flange. There is lateral movement of the compression flange despite the girder being stressed below the buckling load. The effects of curvature are also observed from the stresses in the two halves of the compression flange. Vertical loads produce lateral moments and twist in curved beams. It is these effects together with the secondary effects due to geometric nonlinearity that cause the behaviour observed in curved

beams and girders.

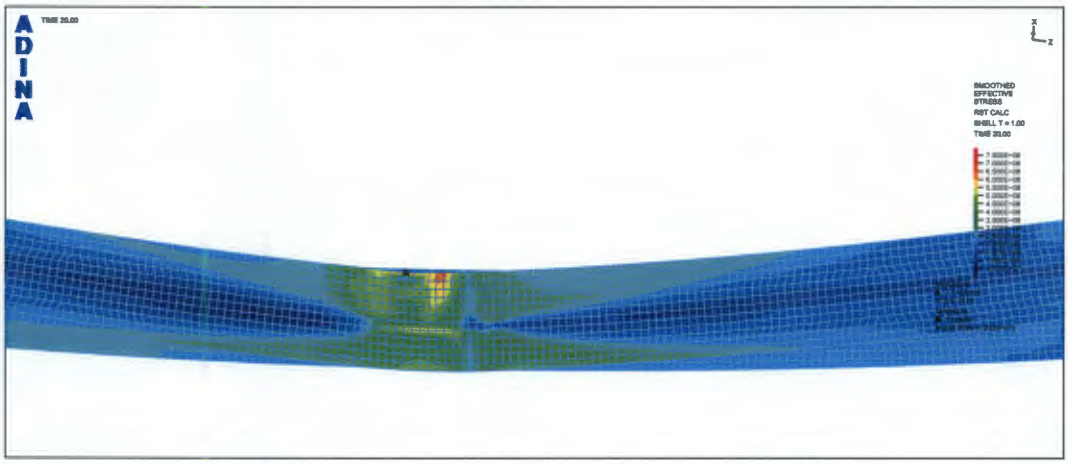

Figure 4.17: Stress plot for LU5-R25aa girder flange

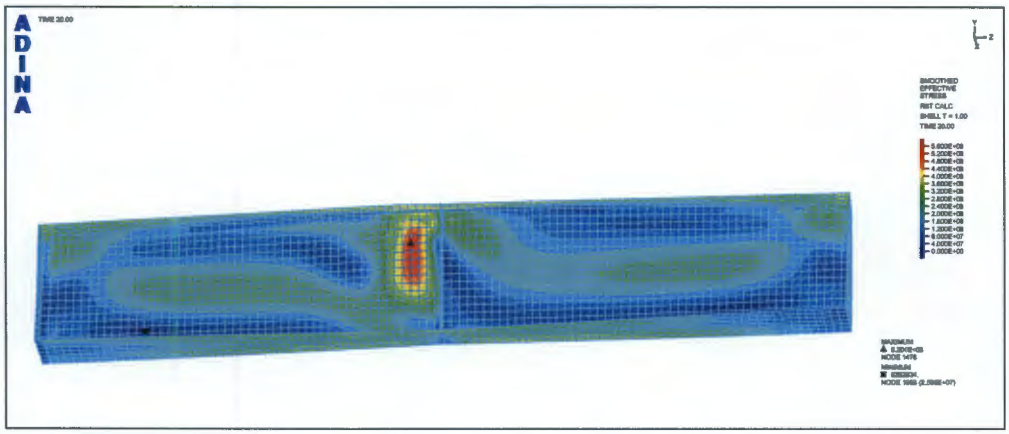

Figure 4.18: Stress plot for LU5-R100aa girder

In Figure 4.17, the lateral moment causes unequal stresses in the flanges. The inner flange with respect to the curvature experiences a higher stress. A small curvature ratio (R/L) results in larger stress differences in the flange tip stresses. The above pattern is observed in the beams LU5-R25bb and LU5-R25cc. The load deflection behaviour for the LU5-R25aa, LU5-R25bb and LU5-R25cc girders is given in the graphs.

Figures 4.18- 4.20 show the girder LU5-R100aa stress plots. As in all simply supported girders with point load at mid span, the moments are highest at the midspan. This is shown in the stress distribution plot. The steel at mid span has yielded, showing Misses stress above 350 MPa. There is lateral movement of the compression flange and this is due to the lateral instability. The reduction in

curvature mean that the lateral moment is smaller compared to LU5-R25 beams. However, it can still be observed from the visual that the inner flange experiences greater stress.

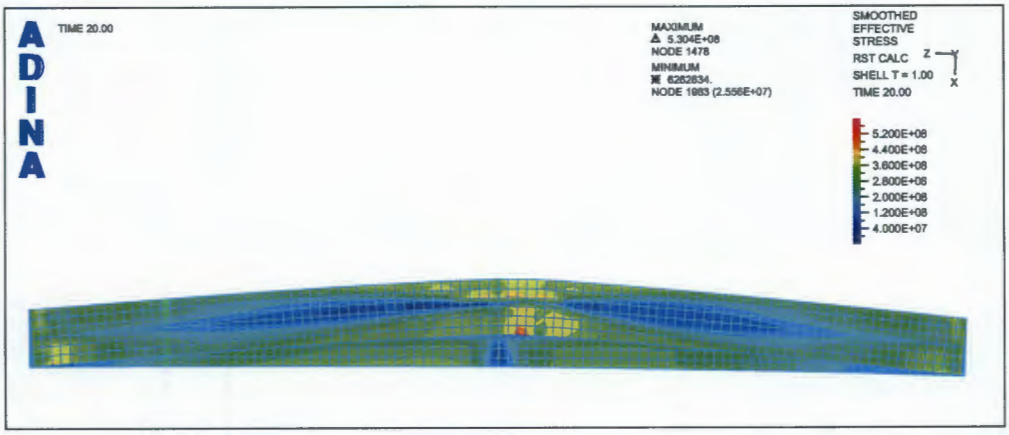

Figure 4.19: LU5-R100aa-Compression flange lateral movement:

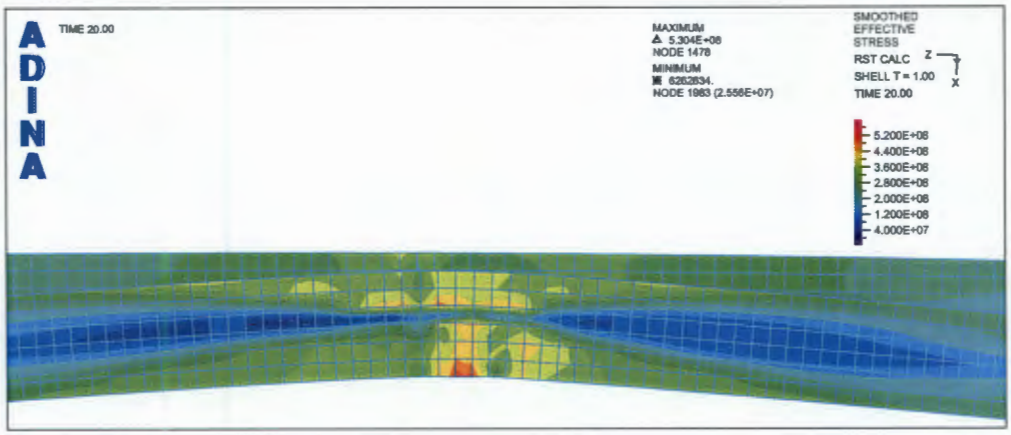

Figure 4.20: Stress plot for LU5-R100aa girder flange

The presence of lateral moment mean that the two halves of the bottom and top flanges are not equally stressed. This is more so significant in the compression zone where buckling is experienced. The inner half of the compression flange has higher stress and can buckle while the outer flange is not buckled. This is to be expected in curved girders. The effects of local flange buckling and lateral movement are less pronounced as the curvature is reduced.

4.3.2 Analytical determination of ultimate strength

Two approximate equations for the ultimate strength of a curved beam have been presented in literature; the one presented first is derived by Fukumoto and Nishida (1981) and the other derived by Richard *et al.* (1995). The approximate equations are not easy to use as a design tool and their accuracy has not been extensively investigated. They are derived for homogeneous girders though it is worth noting that their derivation ignores the girder web contribution. Furthermore, the equations are derived based on plastic moment capacity and not all girders can achieve this. The quartic equations result in four roots and in some of the cases it is necessary to further check graphically to ascertain the correct root. The two equations are both used to predict the ultimate loads for the girders in the present study. The procedure is set out for the first girder LU5-R25aa, where a graphical plot for equation 2.66 is used to illustrate the concept used. The solutions for the other girders are obtained by running a simple script in Matlab and this is given in appendix A and B.

The equation 2.66 by Fukumoto and Nishida (1981) is simpler as it contains fewer terms. For completeness, it is restated below:

$$\lambda^4\delta^4 - \left(\left[\left(1+\frac{p_e(d-t_{cf})}{2M_p}\right)\left(\frac{L^2}{2Rb_{cf}}\right)\lambda^4+1\right]\right)\delta^2 - \left(\frac{L^2}{2Rb_{cf}}\right)\delta + 1 = 0 \quad (4.1)$$

where

$\lambda = \sqrt{\frac{M_p}{M_e}}$ is the slenderness ratio;
$\delta = \frac{M_u}{M_p}$ is the normalised moment capacity
$M_p \simeq F_y b_f t(d-t)$ is the approximate plastic moment capacity
$P_E = \frac{\pi^2 E I_y}{L^2}$ is the elastic buckling load
M_e is the elastic moment, d is the section depth, t_{cp} is the compression flange thickness, b_{cf} is the width of the compression flange, L is the un-braced length and R the girder radius.

The equation 2.67 is also given. The main difference with equation 2.66 is that it contains more terms and is based on the curved beam equations derived by Yang and Kuo (1987).

$$\delta_u^4\lambda^4 - \left[\left(1 + \frac{(d-t)P_E L^2}{4M_p Rb} - \frac{(d-t)EI_Z L^2}{2M_p R^3 b} - \frac{2P_E}{M_p^2 R^2} + \frac{P_E EI_y}{M_p^2 R^2}\left[\frac{L}{\pi}\right]^2\right)\lambda^4 + 1 - \frac{2L^2}{\pi^2 R^2}\right]\delta_u^2 - \left[\frac{L^2}{2RB} - \frac{P_E L^2\lambda^4}{bM_P^2 R^3} - \frac{L^4}{bR^3\pi^2} + \frac{P_E EI_Y}{2M_P^2 R^3}\left[\frac{L^4}{\pi^2 b}\right]\lambda^4\right]\delta_u + 1 - \frac{2L^2}{\pi^2 R^2} - \frac{2P_E\lambda^4}{R^2 M_P^2} + \frac{P_E EI_Y}{M_P^2 R^2}\left[\frac{L}{\pi}\right]^2\lambda^4 = 0 \tag{4.2}$$

The graphical solution for equation 4.1 is obtained from the intersection of two curves: the approximate second order elastic curve and the second order rigid plastic curves. The equations from the curves are derived in the relevant reference and are just restated here.

The second order rigid plastic curve is given below:

$$\frac{U_f}{b} = \frac{1-\delta^2}{4\delta} \tag{4.3}$$

where U_f is defined as the total lateral displacement of the compression flange at midspan,

$$U_0 = \frac{L^2}{8R}$$

The second order elastic curve is given below:

$$\frac{U_f}{b} = \frac{1 + \dfrac{P_E(d-t)}{2M_P}}{1-\lambda^4\delta^2}\frac{U_0}{b} \tag{4.4}$$

All other terms as defined in 4.1 above.

The graphical solution is presented for LU5-25aa:

For the section $812 \times 300 \times (8, 16)$, the following section properties are used:

$A = 15.8 \times 10^3 mm^2$

$I_{yy} = 72 \times 10^6 mm^4$

$J = 937 \times 10^3 mm^4$

$C_W = 11.4 \times 10^{12} mm^6$.

For the simply supported case and a point load at midspan, the ultimate load is given below:

$$P = 4\frac{\delta M_P}{L} \qquad \text{Again all terms as defined above} \tag{4.5}$$

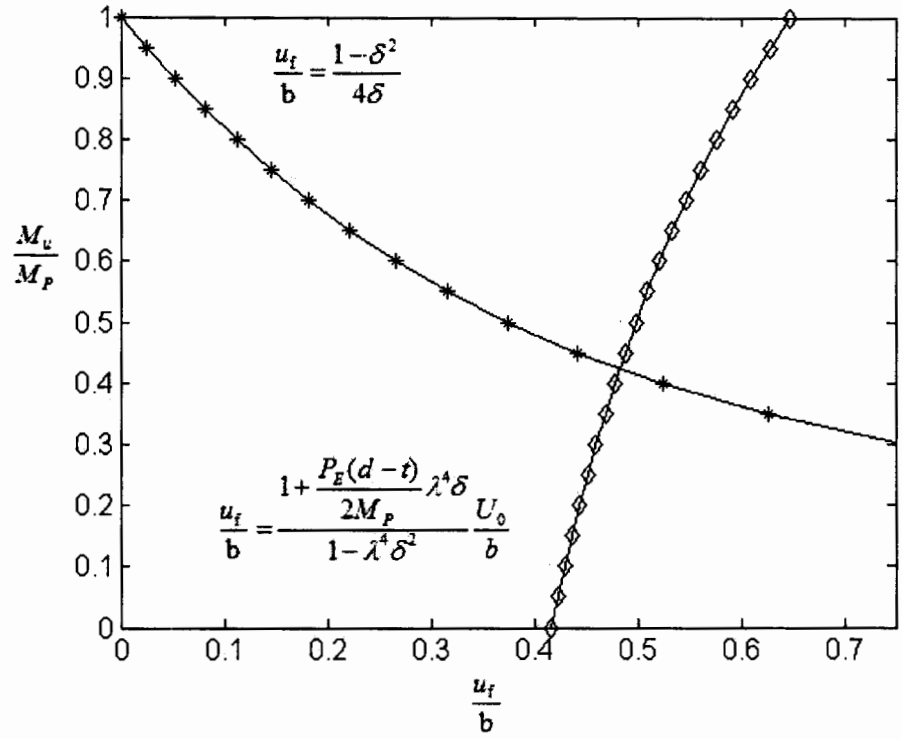

Figure 4.21: LU5-R25aa: Graphical solution for ultimate load

The analytical results are given in a Table 4.6 with the results from finite element analysis. The moment capacities for the homogeneous girders with steel grade shown are given below:
M_P for 350 MPa steel is 1337.28kN.m
M_P for 460 MPa steel is 1757.6kN.m
M_P for 690 MPa steel is 2674.5kN.m. It must be noted that an approximate value of M_P is used in deriving 2.66, neglecting the web contribution.

The results in Table 4.6 show an increase for a given curvature in ultimate load capacity as the steel yield strength increases. The analytical equation 4.1 gives higher load values than 4.2 and this is consistent with the studies by Richard *et al.* (1995) reviewed in Chapter 1. In comparison with the finite element model results, the force values from the two equations are conservative for the LU5-25, LU5-100 and LU8-40 girders. For the rest of the girders, equation 2.67 becomes unconservative resulting in a maximum difference of 85% for LU5-R240aa compared to the finite element result. On the other hand, equation 2.66 predicts values close to finite

Table 4.6: Comparison of analytical and finite element ultimate loads for homogeneous girders

Beam No	$Force_s$ (kN)	$Force_y$ (kN)	$Force_{ADINA}$ (kN)	$\frac{Force_s}{Force_{ADINA}}$	$\frac{Force_y}{Force_{ADINA}}$
LU5-R25aa	371.7	341.7	571.4	0.65	0.60
LU5-R25bb	482.6	430.7	706.9	0.68	0.61
LU5-R25cc	706.5	591.6	881.0	0.80	0.67
LU5-R100aa	738.6	696.2	754.3	0.98	0.92
LU5-R100bb	946.6	861.2	913.1	1.04	0.94
LU5-R100cc	1363.3	1118.4	1077.2	1.27	1.04
LU5-R250aa	910.0	871.9	943.7	0.96	0.92
LU5-R250bb	1180.2	1086.9	1065.7	1.11	1.02
LU5-R250cc	1721.6	1391.8	1206.3	1.43	1.15
LU8-R40aa	157.3	131.5	218.7	0.72	0.60
LU8-R40bb	204.2	161.2	264.5	0.77	0.61
LU8-R40cc	299.0	210.6	331.8	0.90	0.63
LU8-R120aa	311.5	248.3	289.2	1.08	0.86
LU8-R120bb	392.5	286.8	320.1	1.23	0.90
LU8-R120cc	543.2	338.1	375.2	1.45	0.90
LU8-R240aa	415.0	319.0	315.8	1.31	1.01
LU8-R240aa	521.2	355.9	345.3	1.51	1.03
LU8-R240aa	715.1	397.3	387.2	1.85	1.03

Where $Force_s$, $Force_y$ and $Force_{ADINA}$ are the ultimate girder forces obtained from equation 4.1, 4.2 and Finite Element Model respectively

element model with a maximum difference of 15% for LU5-250cc.

For comparison across curvature, the ultimate loads for straight girders are presented and used as reference for curved girders. The ultimate loads obtained are summarised in Table 4.7 and 4.8. The non-dimensionalised load referred to here is normalised load obtained by dividing the girder load with the load from the reference girder. There is an increase in normalised load as yield steel strengths are increased and this is observed across all spans and curvatures. For girder LU5-R25, the normalised load increases from 0.57 to 0.69 when yield strength increases from 350MPa to 690MPa. The steel grade does have a direct effect on the normalised girder slenderness and thus has an influence on which failure mode becomes dominant.

The girders LU5-R250 and LU8-R240 had the least curvature (R/L) and also had the highest normalised loads. This pattern is expected because such girders closely

Table 4.7: Analytical and finite element ultimate loads for straight homogeneous girders

Beam No	$Force_{SANS10162}$ (kN)	$Force_{ADINA}$ (kN)	$\frac{Force_R}{Force_{ADINA}}$
LU5-STaa	1069	1002	1.07
LU5-STbb	1243	1173	1.06
LU5-STcc	1328	1280	1.04
LU8-STaa	349	380	0.91
LU8-STbb	349	399	0.87
LU8-STcc	349	425	0.82

Where $Force_S$, and $Force_{ADINA}$ are the ultimate girder forces obtained from equation SANS 10162 (Appendix D) and Finite Element Model respectively.

Table 4.8: Comparison of normalised ultimate loads for different curvatures

Beam No	$Force_{ADINA}$ (kN)	Reference Girder	Normalised load
LU5-R25aa	571.4	LU5-STaa	0.57
LU5-R100aa	754.3	LU5-STaa	0.75
LU5-R250aa	943.7	LU5-STaa	0.94
LU5-R25bb	706.9	LU5-STbb	0.60
LU5-R100bb	913.1	LU5-STbb	0.78
LU5-R250bb	1065.7	LU5-STbb	0.91
LU5-R25cc	881	LU5-STcc	0.69
LU5-R100cc	1077.2	LU5-STcc	0.84
LU5-R250cc	1206.3	LU5-STcc	0.94
LU8-R40aa	218.7	LU8-STaa	0.58
LU8-R120aa	289.2	LU8-STaa	0.76
LU8-R240aa	315.8	LU8-STaa	0.83
LU8-R40bb	264.5	LU8-STbb	0.66
LU8-R120bb	320.1	LU8-STbb	0.80
LU8-R240bb	345.3	LU8-STbb	0.87
LU8R40cc	331.8	LU8-STcc	0.78
LU8R120cc	375.2	LU8-STcc	0.88
LU8-R240cc	387.2	LU8-STcc	0.91

approximate straight girders. Girders LU5-25 and LU8-R40 have a curvature (R/L) of 5. The normalised load for the homogeneous configurations LU5-R25aa and LU8-R40 is close. However as the steel yield strength is increased, there is a marked difference largely because lateral instability and not yielding controls the ultimate load of reference girder LU8-STbb and LU8-STcc.

4.3.3 Investigation of hybrid effects on curved girders

The study of hybrid effects is first done using finite element analysis. The procedure is similar to that followed for curvature effects only in this case the material in the web and flange is varied at a given curvature to obtain a hybrid configuration. Girders and beams are primarily bending moment resisting members and thus the configurations considered have higher grade steel in flange. The girders are all simply supported and twist is not permitted at the two ends. The girders are loaded with a point load at mid span. The automatic algorithm of collapse analysis is performed for each steel combination in web and flange. Load-deflection data is obtained after collapse analysis using the ADINA version 8.4 post processing capability. This is compared with the analytical results as given by equation 2.66 and 2.67. The quantitative results from the model are supplemented by visuals showing stress distributions, lateral flange movement and local buckling of the girders.

The first principles approach to curved girder behaviour is not directly useful because of the lack of general equations that relate the bending moment to the load. Furthermore, the stress distribution in a curved girder is more complex, varying through girder depth and also across flange width. The approach outlined for the EN3 to design hybrid girders is also not flexible enough to accommodate the curvature effects as it is formulated for straight girder stress state. The recommendation by ASCE-AASHO (1968) that hybrid beams be treated as homogeneous of flange steel is adopted here and hybrid factors used for correction. Two approximate equations have been put forward for analytical determination of ultimate load and these are compared with the finite element result.

Finite element results

Several girders are loaded to collapse and the load-deflection data obtained. In straight hybrid girders, ultimate load is defined as the load reached when the extreme flange fibres begin to yield. This definition is suited to straight girders with adequate bracing. In curved girders, the flange is not stressed equally across the flange width

and depth. The collapse analysis option is used to trace the load beyond a critical load which is taken as maximum load attained. The critical load is used as a reference for comparison with other hybrid girder configurations. The overall beam notation is used here. The stress distribution of hybrid girders is also observed because the web is of low yield strength steel. Bearing stiffeners are used at midspan and at the supports due to the high concentrated load. It has been stated from theory that flange vertical buckling is not a problem in hybrid girders as they can support the flange after yielding. The visuals of selected girders are shown below and observations made regarding stress distribution.

The Figures 4.22- 4.25 show the LU5-R25 girder and this has high curvature.

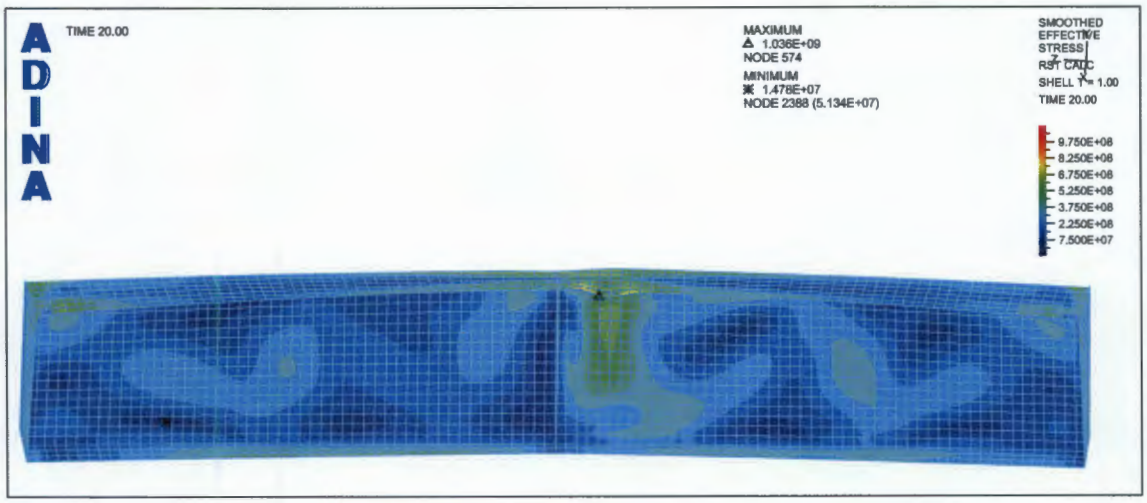

Figure 4.22: Stress plot for LU5-R25ab girder

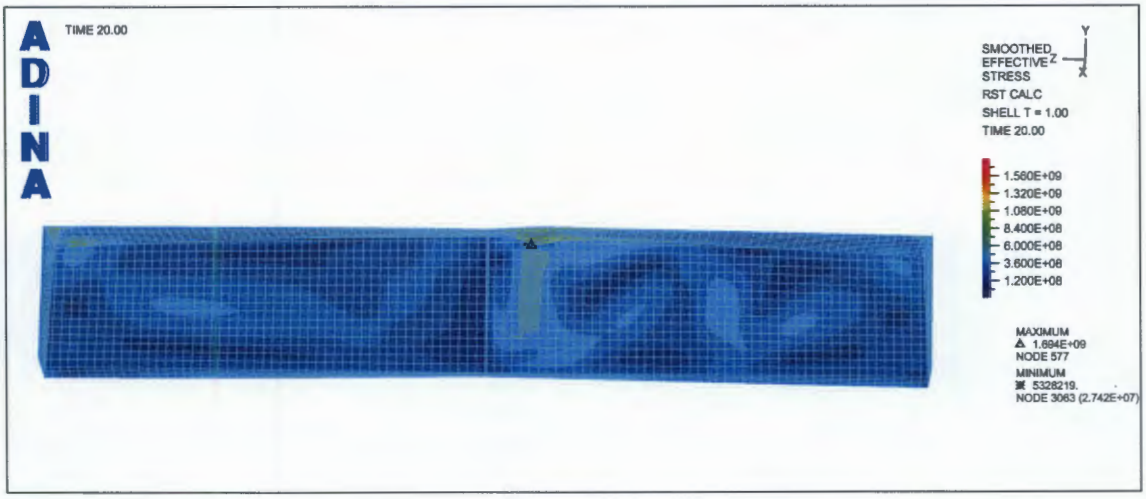

Figure 4.23: Stress plot for LU5-R25ac girder

The stress plots show that portions of the web have yielded and that the yield zone penetrates down from the compression half. Figure 4.22 shows zones of high stress and this depicts tension field action. In these zones the effective stress is higher than 350MPa showing that web steel has yielded. Figure 4.23 also shows zones of higher stress where the web steel has yielded. However, in Figure 4.23 the zones are not fully developed in one half and have a horizontal orientation. This girder has web steel yield stress of 350MPa and flange yield stress of 690MPa; such a ratio is outside the recommendation by AASHTO (2007). The visuals are taken after analysis is complete and thus shows the flanges having yielded as well.

Figures 4.24 and 4.25 show the compression flange stress distribution and flange local buckling.

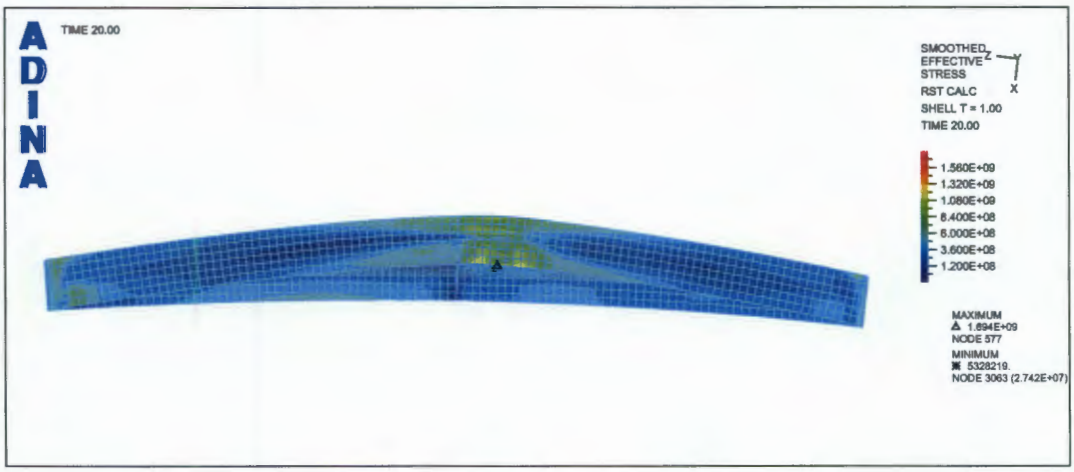

Figure 4.24: Stress plot for LU5-R25ac girder flange

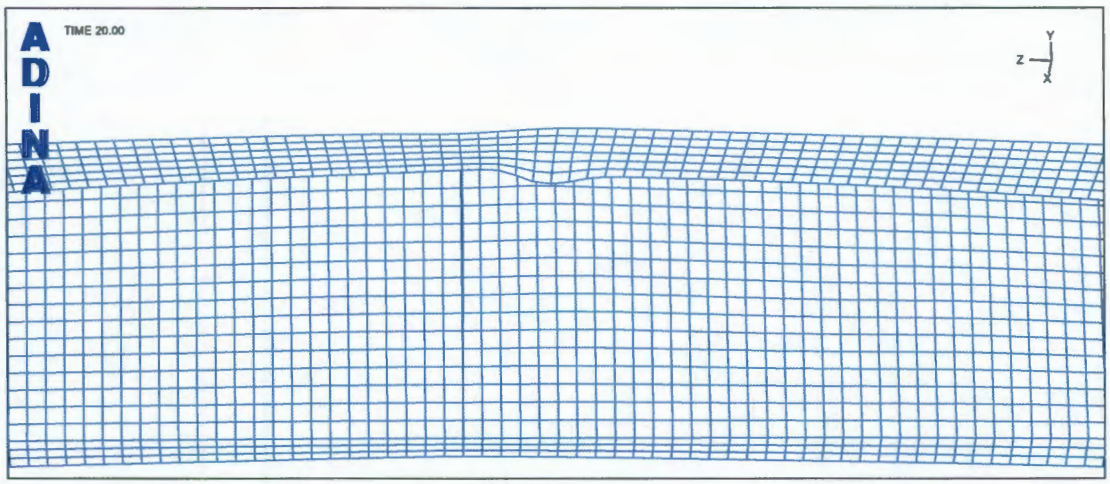

Figure 4.25: Mesh plot of LU5-R25ab girder showing local buckling

The two flanges are not equally stressed with the inner half having higher stress at the tip. The stress pattern shown is similar to that observed in curved homogeneous girders studied earlier. This stress pattern across flange width is due to the lateral moment caused by the presence of curvature. The visual also shows the relative compression flange movement with respect to the tension flange. The direction of lateral movement is not arbitrary, rather it is in the direction of initial curvature. The mesh plot in Figure 4.25 shows local flange buckling of the inner half of the compression flange tip. This local buckling is observed at loads beyond peak load.

The girders with same curvature and span are compared and homogeneous girders representing lower and upper bounds are also plotted. The load-deflection plot for a hybrid girder has three phases. In the first phase the girder is elastic and no distinction can be made between the hybrid girder configurations. The second phase is where the web starts yielding and this does not lead to significant loss of girder stiffness because the flanges carry most of the moment. The third phase is where the flange starts yielding. In curved girders, this initial flange yielding happens at the flange tips because of the stress variation across flange width. It is flange yielding that results in loss of stiffness.

The plots of the girders analysed show that the ultimate load is largely determined by the flange steel grade. In girders such as LU5-R25ac, LU5-R100ac, LU5-R250ac, LU8-R40ac, LU8-R120ac and LU8-240ac the web steel yield strength is 51% of the flange steel and this is less than the 70% required by AASHTO (2007). The ultimate loads obtained are very close to the ultimate load for the corresponding homogeneous girder with flange grade steel. The girders with web-flange yield steel combinations of 350/460MPa give load-deflection pattern close to a similar homogeneous girder with flange steel 460MPa. Girders with web-flange yield steel combinations of 350/690MPa or those with 460/690MPa give load deflection curves close to a similar homogeneous girder with 690MPa yield steel. Load deflection plots obtained for the different hybrid girder configurations investigated are plotted in Figures 4.26-4.37.

Figure 4.26 shows the load deflection plot for LU5-R25ab shown alongside those of homogeneous girders. Girder LU5-R25ab behaves almost like LU5-R25bb. Girders LU5-R25ac and LU5-R25bc are also shown plotted with homogeneous girders LU5-R25bb and LU5-R25cc in Figure 4.27. It is observed that both hybrid girders have plots similar to homogeneous girder LU5-R25cc.

The pattern established in Figures 4.26 to 4.27 is repeated in all the LU5 hybrid girders. It is clear that for the spans considered, the hybrid girders closely

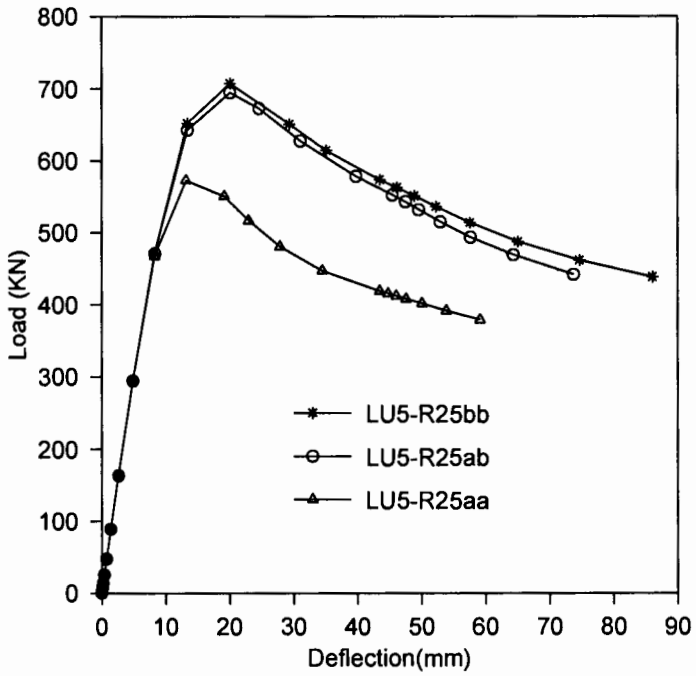

Figure 4.26: Load-deflection plot comparison for LU5-R25ab

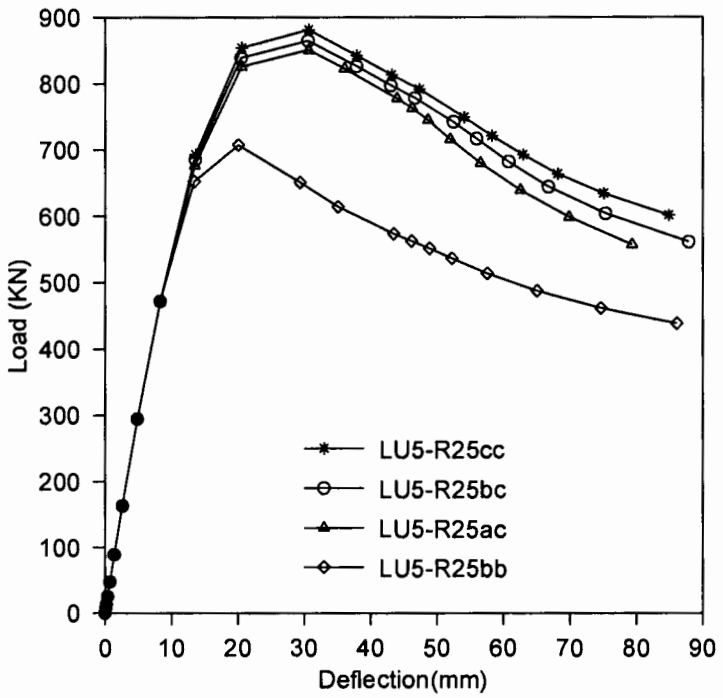

Figure 4.27: Load-deflection plot comparison for LU5-R25ab and LU5-R25ac

approximate the load deflection behaviour of the corresponding homogeneous girder with flange steel grade. Even more significant is the fact that this is true for girders with a lower ratio of web to flange steel yield outside AASHTO (2007) limits. The girders with higher ratios of web to flange steel yield strength are the closest to the corresponding homogeneous girders.

The results for hybrid girders LU5-R100 and LU5-250 are shown in Figures 4.28 to 4.31.

The observations for LU5-R25 still apply to LU5-R100 and LU5-R250 showing that the load-deflection plot of the hybrid girder is close to the homogeneous girder made of flange yield steel. The ultimate load increases with an increase in curvature ratio (R/L) and this is similar to what has already been established for homogenous girders. The graphs also show that as the R/L ratio increases, the hybrid curve is almost identical to the homogeneous girder and this is investigated later. A reduction in curvature leads to a reduction in modified slenderness λ and this shifts the collapse mechanism towards material yielding. The modified slenderness is close to that for homogeneous girder because the web contribution to moment resistance is small. The curvature effects are thus of primary concern. The load deflection pattern for the LU8 girders is presented in Figures 4.32 to 4.37.

As before, hybrid girders are plotted with corresponding homogeneous girders that are used to show lower and upperbound limits. It is clear from Figures 4.32 to 4.37 the behaviour of hybrid girders is closer the homogeneous girder with flange steel. While the graphs for hybrid girders approximate those for corresponding hybrid girders in Figures 4.32 and 4.33, the plots for each girder can be clearly distinguished from each other. For higher R/L ratio such as LU8-R120 and LU8-R240 the curves are so close that the differences between hybrid and homogeneous girders are negligible. Both the elastic range, peak load and post collapse load patterns given in Figures 4.32 to 4.37 show that the load-deflection behaviour and the ultimate load attained by a hybrid girder are close to the corresponding homogeneous girder. The girder yield strength increases with increasing flange steel yield stress. The increasing strength is expected because flanges carry most of the moments in beams and girders while webs primarily carry shear. There is also an increase in ultimate load capacity as R/L ratio is increased as established before in the study of curved homogeneous girders. The curvature effects are thus of primary concern compared to hybrid effects in these girders.

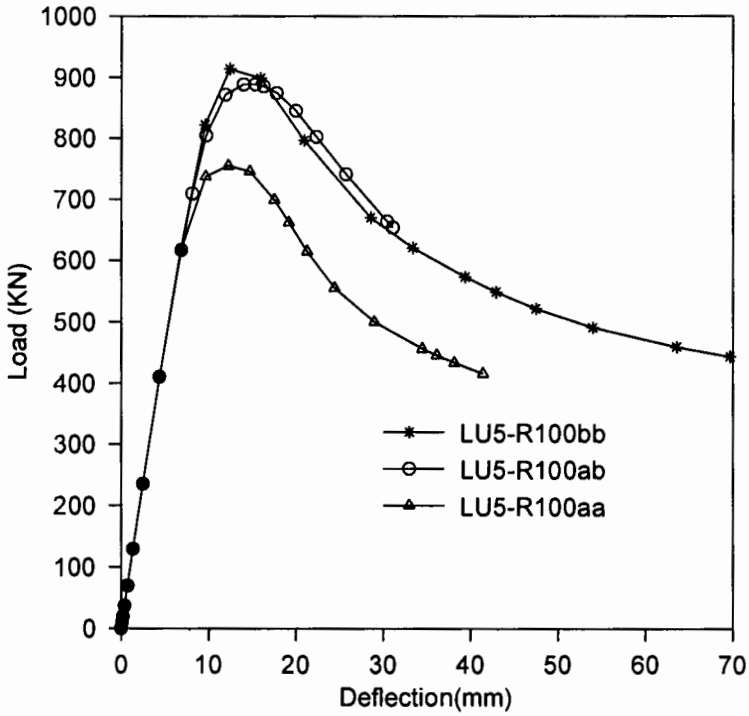

Figure 4.28: Load-deflection plot comparison for LU5-R100ab

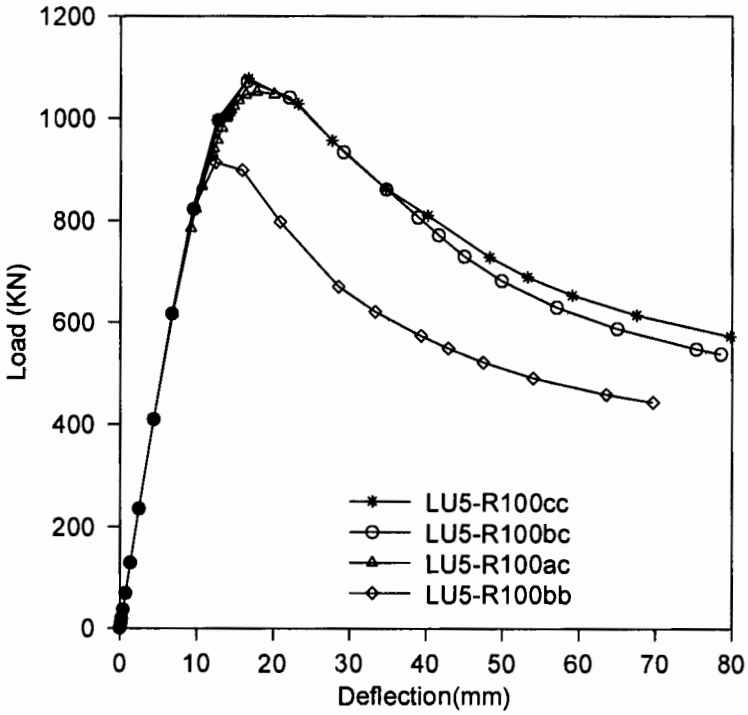

Figure 4.29: Load-deflection plot comparison for LU5-R100ac and LU5-R100bc

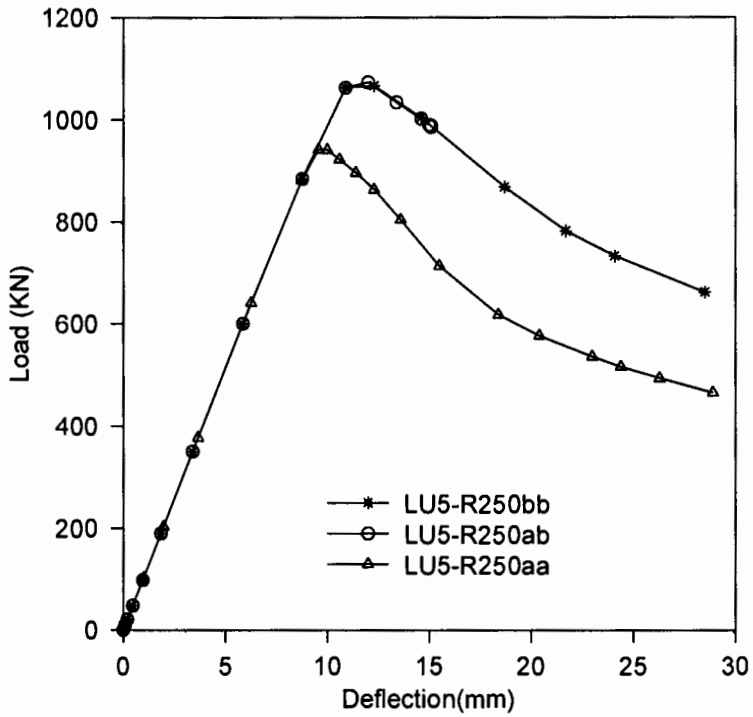

Figure 4.30: Load-deflection plot comparison for LU5-R250ab

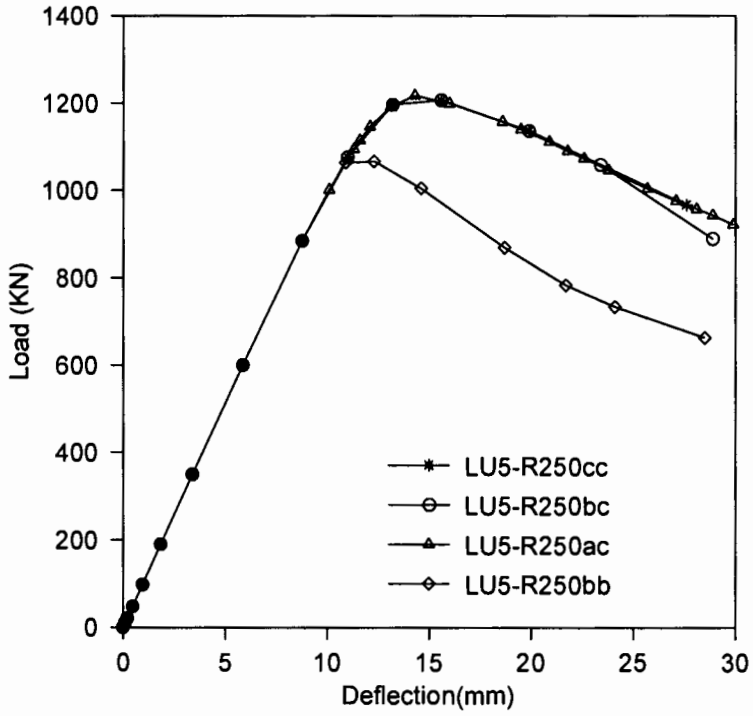

Figure 4.31: Load-deflection plot comparison for LU5-R250ac and LU5-R250bc

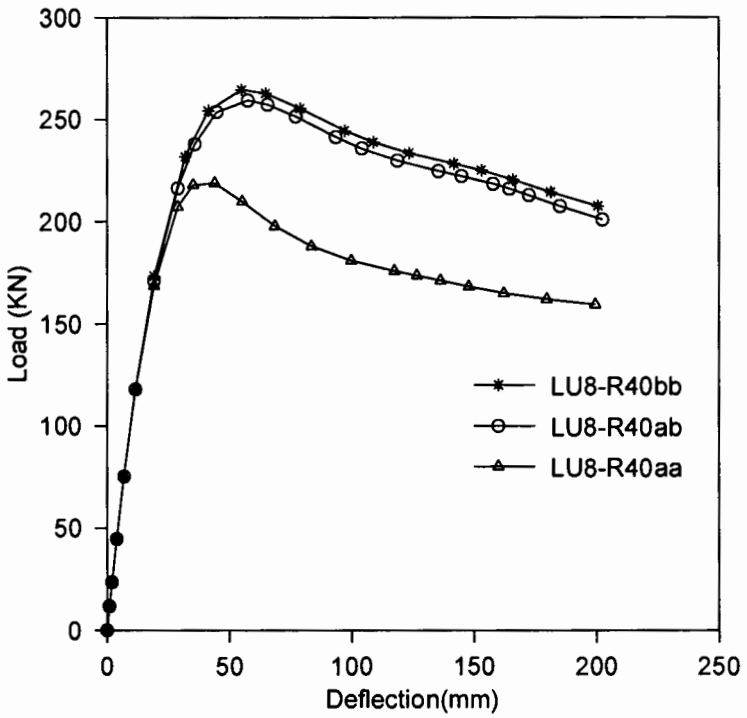

Figure 4.32: Load-deflection plot comparison for LU8-R40ab

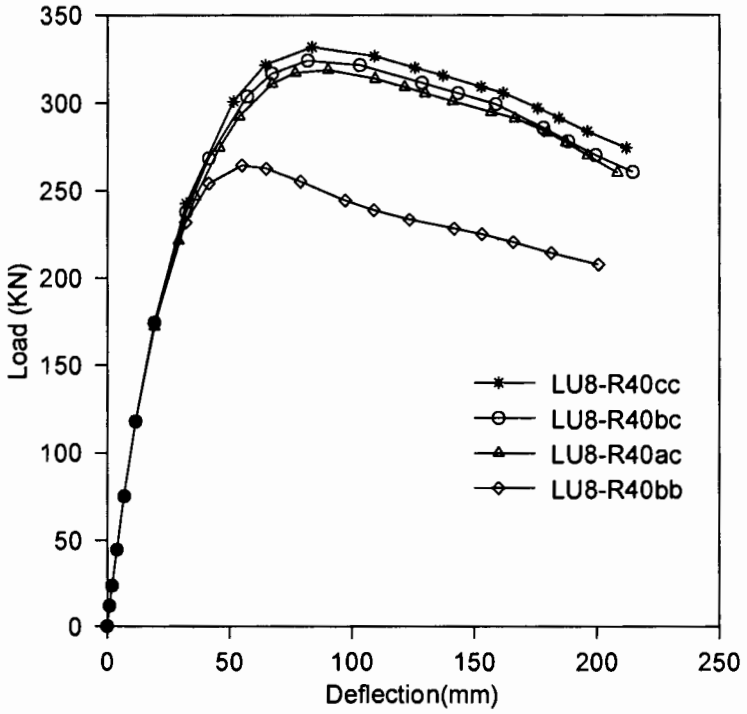

Figure 4.33: Load-deflection plot comparison for LU8-R40ac and LU8-R40bc

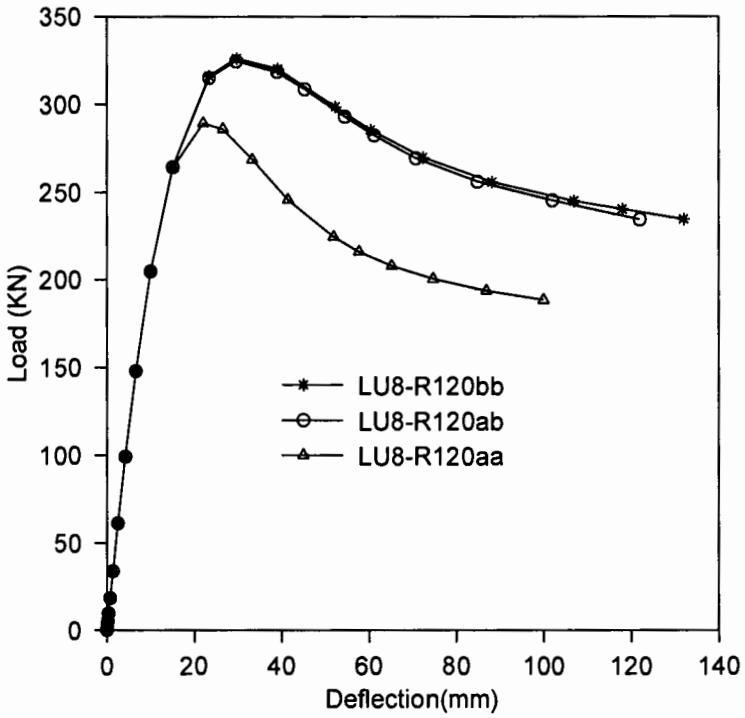

Figure 4.34: Load-deflection plot comparison for LU8-R120ab

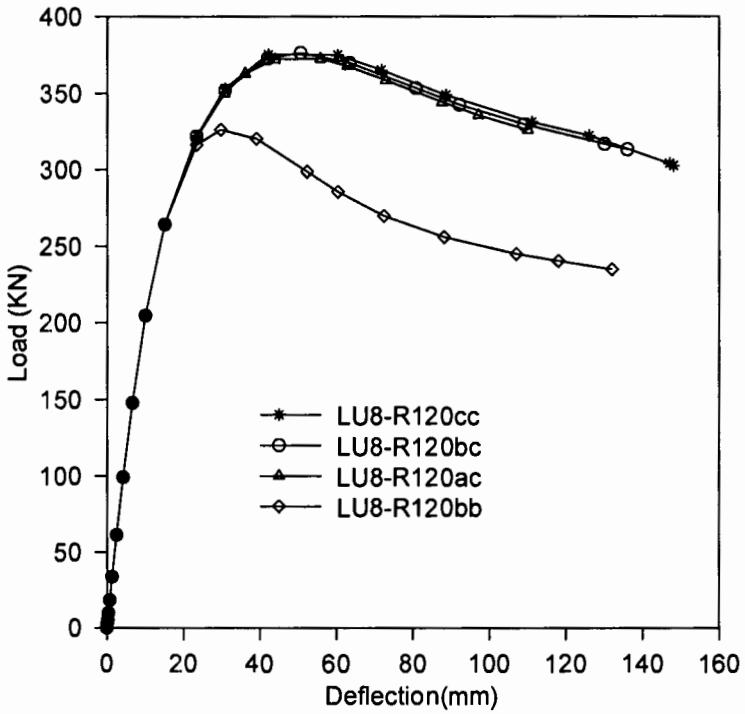

Figure 4.35: Load-deflection plot comparison for LU8-R120ac and LU8-R120bc

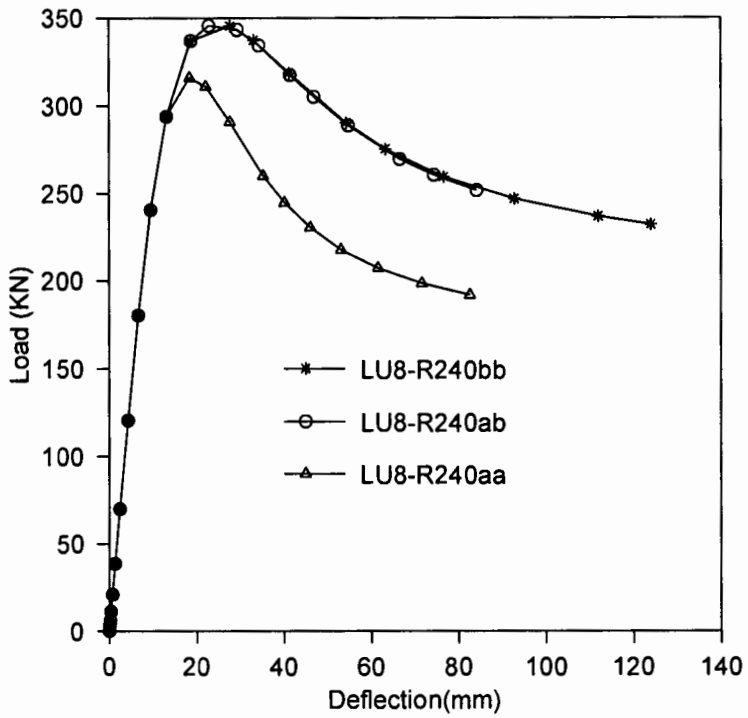

Figure 4.36: Load-deflection plot comparison for LU8-R240ab

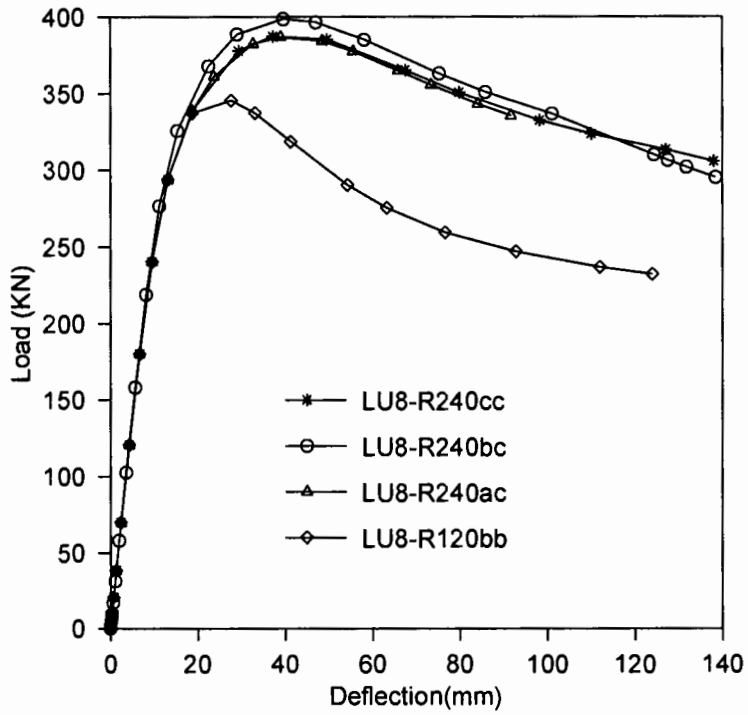

Figure 4.37: Load-deflection plot comparison for LU8-R240ac and LU8-R240bc

4.3.4 Analytical determination of ultimate strength

The analytical approach for hybrid girders closely follows the homogeneous girder approach. This is justified because as seen from load deflection plots, a hybrid girder behaves almost like a homogeneous girder with flange steel. It is expected that the deflections for a hybrid girder are greater at ultimate load, however this is not evident in the study. Frost and Schilling (1964) assume a perfectly elastic-plastic material behaviour and this too had an effect on the analytical curve provided.

The quartic equations used in this study were derived for homogeneous girders and the approximation used for the reference moment M_p ignores the web steel. This was done to obtain a simpler equation. In the LU8 girder, lateral instability is significant especially when higher yield steel is used. The moment resistance capacity is reduced from yield moment M_y to M_r which is bound by the elastic critical moment. The analytical ultimate loads obtained before in the analysis of homogeneous girders are utilised with reduction factors. The reduction factors are based on the steel combinations in the web and flange and are determined from the relevant equation 2.18 restated below:

$$R_h = \frac{12 + \beta(3\rho - \rho^3)}{12 + 2\beta} \tag{4.6}$$

where
$\beta = \dfrac{2D_n t_n}{A_{fn}}$ and ρ = smaller of $\dfrac{F_{yw}}{f_n}$ and 1.0
A_{fn} = sum of the flange area and the area of any cover plates on the side of the neutral axis corresponding to D_n (mm^2)
D_n = the distance from neutral axis to the inside face of the flange on the side of the neutral axis where yielding occurs first.
f_n = the largest of the specified minimum yield strengths of each component included in calculation of A_{fn}.

It is stated in the commentary AASHTO (2007) that in most cases R_h is equal to one. Though the conditions in the AASHTO (2007) regarding ratio of flange steel grade to web steel are clearly violated for the hybrid girders with 350MPa yield steel in web and 690MPa yield steel in flange, the reduction factor is used nevertheless. This is also justified by the fact that this particular steel combination also gave results that are close to homogenous girders in the load-deflection plots. The results from the ADINA finite element study show that the ratio of the ultimate load of a hybrid girder to that of the corresponding homogeneous girder with flange grade steel is close to one.

The analytical study gives values of ultimate load for a homogeneous girder scaled down to the corresponding hybrid girder using R_h. In general, the analytical approach is rather conservative when a curvature ratio (R/L) of 5 is used for a the given span lengths. As the ratio R/L increases, there is a shift showing increasingly unconservative predictions by equation 2.66 as compared to the finite element model. The equation 2.67 is also unconservative especially when the ratio R/L increases. The difference with finite element model results increase as R/L increases, thus it is seen that the proposed equations do not converge to the straight girder case. As R/L increases, the curvature effects become less pronounced and the lateral moment reduces. The mode of failure is also dependant on curvature as it shifts from lateral instability to material yielding depending on beam slenderness λ. The results from analytical and computational methods are summarised in Table 4.9 for comparison.

Table 4.9: Comparison of analytical and finite element ultimate loads for hybrid girders

Beam No	$Force_s$ (kN)	$Force_y$ (kN)	$Force_{ADINA}$ (kN)	$\frac{Force_s}{Force_{ADINA}}$	$\frac{Force_y}{Force_{ADINA}}$
LU5-R25ab	475.8	442.8	694.2	0.69	0.64
LU5-R25ac	668.4	611	850.7	0.79	0.72
LU5-R25bc	688.2	576.2	864.3	0.80	0.67
LU5-R100ab	936.4	902.2	888.0	1.05	1.02
LU5-R100ac	1289.7	1222.1	1051.5	1.23	1.16
LU5-R100bc	1327.9	1089.4	1071.8	1.24	1.02
LU5-R250ab	1163.7	1129.9	1072.5	1.09	1.05
LU5-R250ac	1628.7	1542.3	1216.7	1.34	1.27
LU5-R250bc	1676.9	1355.6	1206.2	1.39	1.12
LU8-R40ab	201.4	17.4	259.2	0.78	0.66
LU8-R40ac	282.8	228.7	318.7	0.89	0.72
LU8-R40bc	291.2	205.2	324.1	0.90	0.63
LU8-R160ab	387.0	321.8	324.4	1.19	0.99
LU8-R160ac	513.9	407.0	372.5	1.38	1.09
LU8-R160bc	529.1	329.3	376.2	1.41	0.88
LU8-R240ab	513.9	413.4	354.9	1.45	1.16
LU8-R240ac	676.5	505.0	397.2	1.70	1.27
LU8-R240bc	696.5	387	398.5	1.75	0.97

Where $Force_s$, $Force_y$ and $Force_{ADINA}$ are the ultimate girder forces obtained from equation 2.66, 2.67 and Finite Element Model respectively

The analytical procedure gives results lower than the finite element method for

girders LU5-R25 and LU8-R40 which have curvature ratio of 5. Equation 2.67 gives higher values than equation 2.66 for all the girders and also predicts higher values than the finite element method in all girders except the two given above. At higher R/L ratio, the analytical equations overestimate the ultimate load and this is despite the fact that their derivation ignores the small contribution of the web. The equation by Fukumoto and Nishida (1981) gives the smallest load difference compared to the finite element method and the equation by Richard *et al.* (1995) is generally unconservative.

Results from the computational models from homogeneous and hybrid girders are compared. The normalised loads for hybrid girders are given with reference to corresponding homogenous girders. These are shown in Table 4.10 below:

Table 4.10: Comparison of normalised ultimate loads for hybrid girders

Beam No	$Force_{ADINA}$ (kN)	Reference Girder	Normalised load
LU5R25ab	694.2	LU5R25bb	0.98
LU5R25ac	850.7	LU5R25cc	0.97
LU5R25bc	864.3	LU5R25cc	0.98
LU5R100ab	888.0	LU5R100bb	0.97
LU5R100ac	1051.5	LU5R100cc	0.98
LU5R100bc	1071.8	LU5R100cc	0.99
LU5R250ab	1072.5	LU5R250bb	1.01
LU5R250ac	1216.7	LU5R250cc	1.01
LU5R250bc	1206.2	LU5R250cc	1.00
LU8R40ab	259.2	LU8R40bb	0.98
LU8R40ac	318.7	LU8R40cc	0.96
LU8R40bc	324.1	LU8R40cc	0.98
LU8R120ab	324.4	LU8R120bb	1.01
LU8R120ac	372.5	LU8R120cc	0.99
LU8R120bc	376.2	LU8R120cc	1.00
LU8R240ab	354.9	LU8R240bb	1.03
LU8R240ac	397.2	LU8R240cc	1.03
LU8R240bc	398.5	LU8R240cc	1.03

It is seen from above table that hybrid girders give ultimate loads atleast 97% of the corresponding homogeneous girders. Such a ratio is consistent with the hybrid factor R_h previously used in the analytical procedure. This behaviour is expected since the flanges are the primary load carrying members in girders.

Chapter 5

Conclusion and recommendations

5.1 Conclusion

1. **Effect of curvature on ultimate load**
   Curved hybrid girders have been studied using a verified finite element procedure. The study covered both hybrid and curvature effects. The presence of curvature radically modifies a girder's load pattern by causing additional lateral bending moments. The presence of lateral bending moments reduces the vertical load carrying capacity of a girder. For the girder and spans investigated, there is a reduction of 57% in ultimate load for radius to span ratio (R/L) of 5 compared to a straight girder of similar proportions and span.The effects of curvature reduce as the arc length to radius of curvature ratio of a girder is increased.

2. **Stress configuration in curved girder**
   When curvature is introduced, the stress pattern especially in the flange is altered. This is because the lateral causes the flanges to be unequally stressed. The inner part of the flange with respect to centre of curvature experiences higher stresses. Where such stresses are compressive, the inner part will buckle locally before the outer half.

3. **Hybrid configuration**
   The hybrid configuration considered here had higher strength steel in the flange and lower strength steel in the web. For all the cases investigated, the hybrid girders had load deflection plots close to corresponding homogeneous girders with flange steel grade. The hybrid girders attained at least 97% of the ultimate load capacity of reference homogeneous girders. The steel

combinations used such as 350MPa in web and 690MPa in flange clearly lie outside the AASHTO (2007) imposed limits.

4. **Analysis techniques**
   From literature, two equations are presented to determine the ultimate load of homogeneous curved girders. The range of application of these equations is not known. In the present study, the equation proposed by Fukumoto and Nishida (1981) generally produces conservative results compared to finite element model results. The equation proposed by Richard *et al.* (1995) predicts loads lower than finite element method for R/L of 5, it is unconservative for other girders modelled. The finite element model developed was robust enough as it produced results in agreement with both braced and unbrace girders previously investigated by Fukumoto and Nishida (1981) and Richard *et al.* (1995). In the absence of generally agreed curved beam equations, it remains the main tool to analyse complex curved beam behaviour.

5.2 Recommendations

1. **Range of application for available equations**
   The ultimate load has been determined using available closed form equations and finite element analysis. The range of application for the two available equations should be investigated further. While a wide range for the arc length to span ratio was investigated, only two spans of 5m and 8m were considered.

2. **Hybrid girder moment capacity**
   The hybrid girders investigated had load-defection behaviour closely matching that of homogeneous girders. The hybrid girders attained at least 98% of the ultimate load for the reference girders and thus the hybrid factors predicted are on the safe side.The hybrid factor as proposed by AASHTO (2007) produces good results and its should be used for the simplified procedure of approximating hybrid girder loads from homogeneous girder loads.

3. **Curved hybrid girder design**
   The simpler equation proposed by Fukumoto and Nishida (1981) produces conservative results and can be used for preliminary design, however other techniques such as the finite element method should still be used to assess buckling effects. It is recommended that restrictions on moment redistribution

due to use of high performance steels with yield strength greater that 490MPa should be investigated further as new HPS are introduced.

Appendices

Appendix A

Solution of quartic equation

A.1 Quartic equation derived by Fukumoto and Nishida (1981)

The solution for ultimate load of a curved girder was implemented using Matlab. The equation below is solved and the program given.

$$\lambda^4\delta^4 - \left(\left[\left(1 + \frac{p_e(d - t_{cf})}{2M_p}\right)\left(\frac{L^2}{2Rb_{cf}}\right)\lambda^4 + 1\right]\right)\delta^2 - \left(\frac{L^2}{2Rb_{cf}}\right)\delta + 1 = 0 \quad \text{(A.1)}$$

where $\lambda = \sqrt{\frac{M_p}{M_c}}$ $\delta = \frac{M_u}{M_p}$ $M_p \simeq F_y b_f t(d - t)$ $P_E = \frac{\pi^2 E I_y}{L^2}$

A.2 Matlab program

```
% Section and material constants
b=300;
t=16;
d=812;
L=1.2*5000;   % Distabilising load condition factor considered.
F=350;   % Steel yield stress. Values considered include 460MPa and 690MPa.
R=25000;   % The radius is varied according to R/L ratio.
E=206000;
I=72000000;
G=77000;
J=937000; C=11400000000000;
%Calculation of plastic moment capacity.
```

MR=F*b*t*(d-t)

%Calculation of critical buckling moment.

MC = 1.35*sqrt((1-L^2/($pi^2 * R^2$)) * ($pi^2 * E * I/L^2$) * ($G * J + pi^2 * E * C/L^2$))

$\%Nondimensionalisedslenderness.$

$lm = sqrt(MR/MC);$

PE=pi$^2 * E * I/L^2$; $\%Eulercriticalload.$

$\%Polynomialcoefficients.$

$A1 = lm^4;$

$A2 = 0;$

$A3 = (1 + PE * (d - t)/(2 * MR) * (L^2)/(2 * R * b)) * A1 + 1;$

$A4 = L^2/(2 * R * b);$

$A5 = 1;$

$A6 = PE * (d - t)/(2 * MR) * A1;$

$A7 = L^2/(8 * R * b);$

$\%AA = (1 + PE * (d - t) * A1 * 0.4091/(2 * MP)) * A7/(1 - A1 * 0.4091^2);$

$\%AB = (1 - 0.4091^2)/(4 * 0.4091);$

$p = [A1 - A2 - A3 - A4A5];$

$rp = roots(p);$

$RM = min(abs(rp));$

$\%plotequation$

$\%y = 0 : 0.000005 : 1;$

$\%x = (1 - y.^2)./(4 * y);$

$\%x = x. * (abs(x) < 1e10);$

$\%x1 = (1 + A6. * y) * A7./(1 - A1. * y.^2);$

$\%x1 = x1. * (abs(x) < 1e10);$

$\%plot(x, y, x1, y)$

Appendix B

Solution of quartic equation

B.1 Quartic equation presented by Shanmugan *et al.* (2003)

The solution for ultimate load of a curved girder was implemented using Matlab. The equation below is solved and the program given.

$$\delta_u^4\lambda^4 - \left[\left(1 + \frac{(d-t)P_E L^2}{4M_p Rb} - \frac{(d-t)EI_Z L^2}{2M_p R^3 b} - \frac{2P_E}{M_p^2 R^2} + \frac{P_E EI_y}{M_P^2 R^2}\left[\frac{L}{\pi}\right]^2\right)\lambda^4 + 1 - \frac{2L^2}{\pi^2 R^2}\right]\delta_u^2 - \left[\frac{L^2}{2RB} - \frac{P_E L^2\lambda^4}{bM_P^2 R^3} - \frac{L^4}{bR^3\pi^2} + \frac{P_E EI_Y}{2M_P^2 R^3}\left[\frac{L^4}{\pi^2 b}\right]\lambda^4\right]\delta_u + 1 - \frac{2L^2}{\pi^2 R^2} - \frac{2P_E\lambda^4}{R^2 M_P^2} + \frac{P_E EI_Y}{M_P^2 R^2}\left[\frac{L}{\pi}\right]^2\lambda^4 = 0$$

$$\lambda = \sqrt{\frac{M_p}{M_c}} \quad \delta = \frac{M_u}{M_p} \quad M_p \simeq F_y b_f t(d-t) \quad P_E = \frac{\pi^2 EI_y}{L^2}$$

B.2 Matlab program

```
%Section and material constants b=300;
t=16;
d=812;
L=1.2*8000;
% Arc length of 5000 and 8000 used
F=690;
```

% Yield strength of 350, 460 and 690 used

R=240000;

Radius varies in line with R/L ratio

E=206000;

I=1840000000;

% Major axis IZ=72000000;

% Minor axis G=77000;

J=937000;

C=11400000000000;

%Calculation of plastic moment capacity

M=F*b*t*(d-t);

% Calculation of critical elastic moment capacity

MC=1.35*sqrt((1-L^2/($pi^2 * R^2$)) * ($pi^2 * E * I/L^2$) * ($G * J + pi^2 * E * C/L^2$));

$lm = sqrt(M/MC)$;%$nondimensionalisedslenderness$

$P = pi^2 * E * I/L^2$;%$Eulercriticalload$

%$Coefficientsofpolynomial$

$A1 = lm^4$;

$A2 = 0$;

$A3 = (1 + P * L^2 * (d - t)/(4 * M * b * R) - (d - t) * E * IZ * L^2/(2 * M * R^3 * b) -$
$2 * P/(M^2 * R^2) + (P * E * I * L^2)/(M^2 * R^2 * pi^2)) * A1 + 1 + 2 * L^2/(pi^2 * R^2)$;

$A4 = L^2/(2 * R * b) - P * L^2 * A1/(b * M^2 * R^3) - L^4/(b * R^3 * pi^2) + P * E * I *$
$L^4 * A1/(2 * M^2 * R^3 * pi^2 * b)$;

$A5$ =
$1 - 2 * L^2/(pi^2 * R^2) - 2 * P * A1/(R^2 * M^2) + P * E * I * L^2 * A1/(M^2 * R^2 * pi^2)$;

%$Solution$

$p = [A1 - A2 - A3 - A4A5]$;

$rp = roots(p)$

$RM = min(abs(rp))$

Appendix C

Hybrid factor AASHTO (2007)

C.1 Hybrid factor

The hybrid factor is used to determine ultimate strength of a hybrid beam by scaling that of a corresponding homogeneous beam with flange steel grade.

$$R_h = \frac{12 + \beta(3\rho - \rho^3)}{12 + 2\beta} \tag{C.1}$$

where $\beta = \frac{2D_n t_n}{A_{fn}}$, and ρ = smaller of $\frac{F_{yw}}{f_n}$ and 1.0,
A_{fn} = sum of the flange area and the area of any cover plates on the side of the neutral axis corresponding to D_n (mm^2)
D_n = the distance from neutral axis to the inside face of the flange on the side of the neutral axis where yielding occurs first.
f_n = the largest of the specified minimum yield strengths of each component included in calculation of A_{fn}.

Section and material constants
b=300mm;
t=16mm;
d=812mm;
Thus D = 780mm

Case 1: 460MPa steel in flange 350MPa steel in the web.

$$\rho = \frac{350}{460} = 0.76087$$
$$\beta = \frac{2 \times 390 \times 8}{300 \times 16} = 1.3$$

$$R_h = \frac{12 + 1.3(3 \times 0.76087 - 0.76087^3)}{12 + 2 \times 1.3} = 0.986 \tag{C.2}$$

Case 2: 690MPa steel in flange 350MPa steel in the web.

$$\rho = \frac{350}{690} = 0.5072$$
$$\beta = \frac{2 \times 390 \times 8}{300 \times 16} = 1.3$$

$$R_h = \frac{12 + 1.3(3 \times 0.5072 - 0.5072^3)}{12 + 2 \times 1.3} = 0.946 \tag{C.3}$$

Case 2: 690MPa steel in flange 460MPa steel in the web.

$$\rho = \frac{460}{690} = 0.667$$
$$\beta = \frac{2 \times 390 \times 8}{300 \times 16} = 1.3$$

$$R_h = \frac{12 + 1.3(3 \times 0.667 - 0.667^3)}{12 + 2 \times 1.3} = 0.974 \tag{C.4}$$

The commentary to the AASHTO (2007) state that R_h is always close to 1.0

Appendix D

Girder moment capacity: SANS 10162-1

D.1 Yield moment

For section 812*300(8,16), $Z_e = 4530 \times 10^3 mm^2$ The unfactored capacity for web-flange steel combinations:
aa: $Z_e f_y = 1585.5kNm$
bb: $Z_e f_y = 2083.8kNm$
cc: $Z_e f_y = 3125.7kNm$

For the 5m and 8 m simply supported straight girders with a distabilising load the critical moment is obtained SAISC (2008):
5m girder: $M_{cr} = 1660kNm$
8m girder: $M_{cr} = 613kNm$

Moment capacity is given as before:

(i) when $M_{cr} > 0.67M_y$

$$M_r = 1.15\phi M_y \left(1 - \frac{0.28M_y}{M_{cr}}\right) \text{ but not greater than } \phi M_y$$

(ii) when $M_{cr} \leq 0.67M_y$

$$M_r = \phi M_{cr}$$

where:
M_{cr} is elastic buckling moment given in equation 2.3

M_y is the moment resistance capacity given as $M_y = \phi Z_y f_y$

Z_e is elastic section modulus

f_y is the steel yield strength.
$\phi = 1$, no factors applied.

Thus for 5m girder, the moment resistance is given:
aa: $M_r = 1335.7kNm$
bb: $M_r = 1554.1kNm$
cc: $M_r = 1660kNm$

Thus for 8m girder $M_cr \leq 0.67M_p$, thus moment resistance is given:
aa: $M_r = 613.3kNm$
bb: $M_r = 613.3kNm$
cc: $M_r = 613.3kNm$

The load at the mid span is obtained: $P = \frac{4M_r}{L}$ where L is the span: 5m girder:
aa: $M_r = 1068.6kNm$
bb: $M_r = 1243.3kNm$
cc: $M_r = 1328.0kNm$

8m girder:
aa: $M_r = 349kNm$
bb: $M_r = 349kNm$
cc: $M_r = 349kNm$

References

AASHTO, *LRFD Bridge Design Specifications*, American Association of State Highway and Transportation Officials, Washington, D.C, 2007.

Abdel-Sayed G., "Curved webs under combined shear and normal stresses," *Journal of the Structural Division ASCE*, Vol 99 No.ST3; 511–525, March 1973.

ASCE, "Curved I-Girder bridge Design Recommendations," *Journal of Structural Engineering ASCE*, Vol 103 ST5; 1137–1396, May 1977.

ASCE W.R.C., *Plastic design in Steel, a guide and commentary, 2Ed*, ASCE, New York, (1971).

ASCE-AASHO, "Design of Hybrid Steel Beams," *Journal of Structural Engineering ASCE*, ST6; 1397–1426, 1968.

Azizinamini A., Barth K., Dexter R. and Reubeiz C., "High Performance Steel: Research Front-Historical Account of Research Activities," *Journal of Bridge Engineering ASCE*, Vol 9 No3; 212–217, May 2004.

Barth K.E., Righman J.E. and Freeman L.B., "Assessment of AASHTO LRFD Specification for Hybrid HPS 690W Steel I-Girders," *Journal of Bridge Engineering*, Vol 12; 380–388, 2007.

Basler K. and Thurlimann B., "Strength of plate girders in bending," *Journal of the Structural Division ASCE*, Vol 87 No.ST6; 153–181, August 1961.

Bathe K.J., *Finite Element Procedures 1 Ed*, Prentice-Hall, Inc. New Jersey, (1996).

Benham P., Crawford R.J. and Armstrong C., *Mechanics of Engineering Materials 2nd ed*, Pearsod Ed Limited Harlow, England, (1996).

Bjorhivde R., "Development and use of high performance steel," *Journal of Construction Steel Research*, Vol 60; 393–400, 2004.

Boresi A.P. and Chong K.P., *Elasticity in Engineering Mechanics 2nd ed*, John Wiley & Sons inc, New York, (1996).

Carskaddan P.S., "Shear buckling of unstiffened hybrid beams," *Journal of Structural Engineering ASCE*, Vol 94 ST8; 1965–1991, August 1968.

Chung W. and Sotelino E.D., "Three-dimensional finite element modeling of composite girder bridges," *Engineering Structures*, Vol 28; 63–71, 2006.

Culver C.G. and Frampton R.E., "Local instability of horizontally curved members," *Journal of Structural Division, ASCE*, Vol 96 No ST2; 245–265, Feb 1970.

Davidson J., Ballance S.R. and Yoo C.H., "Evaluation of Strength formulations for horizontally curved flexural members," *Journal of Bridge Engineering ASCE*, Vol5 No3; 200–207, August 2000*b*.

Davidson J., Ballance S.R. and Yoo C.H., "Behaviour of curved I-girder webs subjected to combined bending and shear," *Journal of Bridge Engineering ASCE*, Vol5 No2; 165–178, May 2000*a*.

Davidson J.S., Ballance S.R. and Yoo C.H., "Finite displacement behaviour of curved I-girder webs subject to bending," *Journal of Bridge Engineering ASCE*, Vol 4 No3; 213–220, August 1999.

Davidson J.S., Keller M.A. and Yoo C.H., "Cross-frame spacing and parametric effects in horizontally curved I-girder bridges," *Journal of Structural Engineering ASCE*, Vol 122, No9; 1089–1096, 1996.

Davidson J.S. and Yoo C.H., "Local buckling of curved I-girders," *Journal of Structural Engineering ASCE*, Vol 122, No8; 938–948, 1996.

Earls C., "On the inelastic failure of high strength steel I-shaped beams," *Journal of Construction Steel Research*, Vol 49; 1–24, 1999.

EN1993-1-1 E., "Eurocode EN 1993-1-1," .

Frost R.W. and Schilling C.G., "Behaviour of hybrid beams subjected to static loads," *Journal of Structural Division, ASCE*, Vol 90 No ST3; 55–87, June 1964.

Fukumoto Y. and Nishida S., "Ultimate Load Behaviour of Curved I-Beams," *Journal of Engineering Mechanics ASCE*, Vol 107 No.EM2; 367–385, April 1981.

Galambos T.V. (ed.), *Guide to Stability Design Criteria for Metal Structures 5Ed*, John Wiley and Sons Inc, New York, (1998).

Gunther H.P. (ed.), *Use and Application of High-Performance Steels for Steel Structures*, IABSE-AIPC-IVBH, Zirich, (2005).

Haaijer G., "Economy of high strength steel structural members," *Journal of the Structural Division Proc of ASCE*, ST 8; 1–23, 1961.

Hall D.H., "Curved girders are special," *Engineering Structures*, 18-10; 769–777, 1996.

Heins C., *Bending and Torsional Design in Structural Members*, D.C. Heath and Company, Massachusetts, (1975).

Ito M., Nozaka K., Shirosaki T. and Yamasaki K., "Experimental Study on Moment-Plastic Rotation Capacity of Hybrid Beams," *Journal of Bridge Engineering ASCE*, Vol 10 No 4; 490–496, 2005.

Jung S.K. and W.White D., "Shear strength of horizontally curved steel I-girders-finite element analysis studies," *Journal of Construction Steel Research*, Vol 62; 329–342, 2006.

Kang Y.J. and Yoo C.H., "Thin-walled curved beams I: Analytical solution for buckling of arches," *Journal of the Structural Engineering ASCE*, Vol 120 No.10; 2072–2099, October 1994*a*.

Kang Y.J. and Yoo C.H., "Thin-walled curved beams II: Analytical solution for buckling of arches," *Journal of the Structural Engineering ASCE*, Vol 120 No.10; 2102–2125, October 1994*b*.

Lee S., Davidson J. and Yoo C., "Shear buckling coefficients of plate girder web panels," *Computers and structures*, Vol 59 No.5; 789–795, 1996.

Lee S.C. and Yoo C.H., "Strength of plate girder web panels under pure shear," *Journal of Structural Engineering ASCE*, Vol 124 No2; 184–194, 1998.

Lee S.C. and Yoo C.H., "Experimental study on ultimate shear strength of web panels," *Journal of Structural Engineering ASCE*, Vol 125 No.8; 838–846, 1999*a*.

Lee S.C. and Yoo C.H., "Strength of curved I- girder web panels under pure shear," *Journal of Structural Engineering ASCE*, Vol 125 No.8; 847–853, 1999*b*.

Linzell D., Hall D. and White D., "Historical Perspective on Horizontal Curved I Girder Bridge Design in the United States," *Journal of Bridge Engineering ASCE*, Vol 9 No 3; 218–229, May 2004.

Miki C., Homma K. and Tominaga T., "High strength and high performance steels and their use in bridge structures," *Journal of Construction Steel Research*, Vol 58; 3–20, 2002.

Murray D.W. and Rajasekaran S., "Technique for formulating beam equations," *Journal of Engineering Mechanics ASCE*, Vol 101 EMC5; 561–572, 1975.

NCHRP-Report-563, *Development of LRFD Specifications for Horizontally Curved Steel Girder Bridges*, 2006.

Paik J.K. and Thayamballi A.K., *Ultimate Limit State Design of Steel-Plated Structures, 1st Ed*, John Wiley & Sons Ltd, England, (2003).

Papangelis J. and Trahair N., "Flexural-Torsional Buckling of Arches," *Journal of the Structural Engineering ASCE*, Vol 113 No.4; 889–906, April 1987.

Pi Y.L. and Bradford M.A., "Strength design of steel I-section beams curved in plan," *Journal of Structural Engineering ASCE*, Vol 127 No6; 639–646, June 2001.

Rajasekaran and Ramm E., "Flexural-Torsional Stability of Curved Beams-Discussion," *Journal of Structural Engineering ASCE*, Vol No; 144–149, December 1982.

Richard J.Y., Thevendran L.V., Shanmugan N.E. and Tan L., "Behaviour and Design of Horizontally Curved Steel Beams," *Journal of Construction Steel Research*, Vol 37; 37–67, 1995.

SAISC, *Southern African Steel Construction Handbook, 6Ed*, SAISC, Johannesburg, (2008).

Saje M., Turk G., Kalagasidu A. and Vratanar B., "A Kinematically exact finite element formulation of elastic-plastic curved beams," *Computers and Structures*, Vol 67; 197–214, 1998.

Salmon C.G. and Johnson J.E., *Steel Structures-Design and Behaviour, 4th Ed*, Prentice Hall,Inc. New Jersey, (1996).

Sause R. and Fahnestock L., "Strength and ductility of HPS-100W I-Girders in negative flexure," *Journal of Bridge Engineering ASCE*, Vol 6 No5; 316–323, October 2001.

Schilling C.G., "Yield-Interaction Relationships for Curved I-Girders," *Journal of Bridge Engineering*, Vol 1; 26–33, 1996.

Schilling C.G., "Web cripling tests on hybrid beams," *Journal of Structural Engineering*, Vol 93 ST1; 59–71, Feb 1967.

Schilling C.G., "Moment Rotation Tests of Steel Bridge Girders," *Journal of Structural Engineering*, Vol 114 No.1; 134–149, January 1988.

Shanmugan N.E., Mahendrakumar M. and Thevendran V., "Ultimate load behaviour of horizontally curved plate girders," *Journal of Construction Steel Research*, Vol 59; 510–529, 2003.

Shanmugan N.E., Thevendran V., Liew J.R. and Tan L., "Experimental study on steel beams curved in plan," *Journal of Structural Engineering*, Vol 121 No2; 249–259, Feb 1995.

Tall L., *Structural steel design 2nd Ed*, The Ronald Press Company, New York, (1974).

Timoshenko G., *Theory of Elastic Stability 2nd Ed*, McGraw-Hill Book Company, Inc, (1961).

Trahair N. and Bradford M., *The Behaviour and Design of Steel Structures*, Chapman and Hall, London, (1988).

Ugural A. and Fenster S.K., *Advanced Strength and applied Elasticity, 1st Ed*, Edward Anold Publisher, London, (1981).

Vacharajittiphan P. and Trahair N., "Flexural-Torsional Buckling of Curved Members," *Journal of the Structural Division ASCE*, Vol 101 No.ST6; 1223–1238, June 1975.

Veljkovic M. and Johansson B., "Design of hybrid steel girders," *Journal of Construction Steel Research*, Vol 60; 535–547, 2004.

Vlasov V., *Thin Walled Elastic Beams, 2nd Ed*, Israel Program for Scientific Translations, Jerusalem, (1961).

White D.W. and Barth K., "Strength and Ductility of Compact-Flange I-Girders in Negative Bending," *Journal of Construction Steel Research*, Vol 45 No 3; 241–280, 1998.

Wollman G.P., "Steel Girder Design per AASHTO LRFD Specifications (Part 1)," *Journal of Bridge Engineering*, Vol 9; 364–374, 2004.

Yang Y.B. and Kuo S.R., "Static Stability of Curved Thin-Walled Beams," *Journal of Engineering Mechanics ASCE*, Vol 112 No8; 821–841, August 1986.

Yang Y.B. and Kuo S.R., "Effect of Curvature on Stability of Curved Beams," *Journal of Structural Engineering ASCE*, Vol 113 No6; 1185–1202, June 1987.

Yoo C.H., "Flexural Torsional Stability of Curved Beams," *Journal of Engineering Mechanics Division ASCE*, Vol 108 No.EM6; 1351–1369, Dec 1982.

Yoo C.H. and Davidson J.S., "Yield-interaction relationships for nominal bending strength of curved I-girders," *Journal of bridge engineering ASCE*, Vol 2 No.2; 37–44, 1997.

Yoo C.H. and Heins C.P., "Plastic Collapse of Horizontally Curved Bridge Girders," *Journal of Structural Division ASCE*, Vol 98 No.ST4; 899–914, April 1972.

Zureick A., Linzel D. and R. T Leon J.B., "Curved steel I-girder bridges: experimental and analytical studies," *Engineering Structures*, Vol 22; 180–190, 2000.